THESIS FOR THE DEGREE OF DOCTOR OF PHILOSOPHY

in

Thermo and Fluid Dynamics

Gasoline Engine HCCI Combustion

Extending the high load limit

by

DANIEL DAHL

Department of Applied Mechanics
CHALMERS UNIVERSITY OF TECHNOLOGY
Göteborg, Sweden, 2012

Gasoline Engine HCCI Combustion
Extending the high load limit
DANIEL DAHL
ISBN 978-91-7385-686-7

Doktorsavhandlingar vid Chalmers tekniska hgskola
Ny serie nr 3367
ISSN: 0346-718X

Department of Applied Mechanics
Chalmers University of Technology
SE-412 96 Göteborg
Sweden
Telephone +46 (0)31 7721000

This document was typeset using LaTeX.

Chalmers Reproservice
Göteborg, Sweden 2012

The best time to plan an experiment is after you've done it.
R. A. Fisher

Abstract

There is an increasing global focus on reducing emissions of greenhouse gases. For the automotive industry this means reducing CO_2 emissions of the vehicles manufactured, which is synonymous with reducing their fuel consumption or adapting them for using renewable fuels.

This thesis is based on a project aimed at improving the efficiency of gasoline engines in the lower load/speed region. The focus was mainly on a combustion strategy called homogeneous charge compression ignition (HCCI), but also on homogeneous lean and stratified lean spark-ignited combustion. In contrast to traditional stoichiometric spark-ignited combustion, HCCI can operate with diluted mixtures, which leads to better cycle efficiency, smaller pumping losses and smaller heat losses. However, at relatively high loads, HCCI combustion becomes excessively rapid, generating in-cylinder pressure oscillations (ringing), which are perceived as noise by the human ear. The main objective of the project was to identify ways to avoid this ringing behaviour in order to increase the upper load limit of HCCI. This is vital to avoid the need for mode switches to spark-ignited combustion at higher loads and to operate the engine as much as possible in the more effective HCCI mode.

The strategy for reducing ringing investigated most extensively in the project was charge stratification, achieved by injecting part of the fuel late in the compression stroke. Available literature on effects of this strategy gave conflicting indications, both positive and negative effects have been reported, depending on the type of fuel and engine used. It was soon found that the strategy is effective for reducing ringing, but with resulting increases of NO_X emissions. Further, in order for the strategy to be effective, global air/fuel ratios must not be much leaner than stoichiometric. The increases in NO_X emissions were countered by shifting the ratio towards stoichiometric using exhaust gas recirculation (EGR), allowing a three-way catalyst to reduce the excess NO_X. Intake air boosting was also experimented on and is discussed as an alternative method or as a method to use in combination with charge stratification.

During the project, experiments have been conducted with a production-like multi-cylinder engine and a single-cylinder research engine to investigate the potential of various strategies for raising the high load limit of HCCI when using gasoline or gasoline-like fuels. To explain observed phenomena, optical

experiments were conducted in which high-speed video was used to capture light from the combustion and the residuals. A method was developed to extract pressure oscillations from these measurements and to correlate them to the combustion. Laser-based experiments were further used to analyse fuel and temperature distributions before the combustion to investigate their effects on combustion and pressure oscillations.

Based on the acquired data, plausible reasons why charge stratification can reduce ringing, and the circumstances in which it can do so, are presented. The thesis also shows the extent to which the load can be increased using the strategy, and the resulting efficiency penalties, observed in both the production-like gasoline engine and single-cylinder research engine.

Finally, the various strategies for load extension using combinations of charge stratification, EGR and boosting were compared to operating the engine in two-stroke HCCI mode. Although two-stroke operation was investigated very briefly, in an engine not designed for it, indications were obtained that this might be a much better alternative, since it provided higher loads, more stable combustion, less ringing, low NO_X levels and higher efficiency than any of the other tested load extension strategies.

Keywords: HCCI, SCCI, CAI, NVO, gasoline engine, high load, stratified charge, stoichiometric, ringing, knock.

List of papers

This thesis is based on the work contained in the following papers.

I D. Dahl, I. Denbratt, and L. Koopmans. An Evaluation of Different Combustion Strategies for SI Engines in a Multi-Mode Combustion Engine. *SAE International Journal of Engines*, 1(1):324-335, 2009.

II D. Dahl, M. Andersson, A. Berntsson, I. Denbratt, and L. Koopmans. Reducing Pressure Fluctuations at High Loads by Means of Charge Stratification in HCCI Combustion with Negative Valve Overlap. *SAE Technical Paper 2009-01-1785*, 2009.

III D. Dahl and I. Denbratt. HCCI/SCCI Load Limits and Stoichiometric Operation in a Multicylinder Naturally Aspirated Spark Ignition Engine Operated on Gasoline and E85. *International Journal of Engine Research*, 12(1):58-68, 2011.

IV D. Dahl, M. Andersson, and I. Denbratt. The Origin of Pressure Waves in High Load HCCI Combustion: A High-Speed Video Analysis. *Combustion Science and Technology*, 183(11):1266-1281, 2011.

V D. Dahl and I. Denbratt. Valve Profile Adaptation, Stratification, Boosting and 2-stroke Strategies for Raising Loads of Gasoline HCCI Engines. *SAE International Journal of Engines*, 5(3), 2012.

VI D. Dahl, M. Andersson, and I. Denbratt. The Role of Charge Stratification for Reducing Ringing in Gasoline Engine HCCI Combustion. *Submitted for publication.*

Other papers (not included in the thesis).

VII A. Berntsson, M. Andersson, D. Dahl, and I. Denbratt. LIF imaging of OH during the Negative Valve Overlap of a HCCI Combustion Engine. *SIA Technical Paper R-2007-01-22*, 2007.

VIII A. Berntsson, M. Andersson, D. Dahl, and I. Denbratt. A LIF-Study of OH in the Negative Valve Overlap of a Spark-assisted HCCI Combustion Engine. *SAE Technical Paper 2008-01-0037*, 2008.

Acknowledgements

First of all, I would like to express my gratitude to my supervisor, Professor Ingemar Denbratt, for giving me the opportunity to work in this exciting field and for believing in me as a PhD student. To have a person with his experience and knowledge as a supervisor is a great benefit.

I would further like to thank my co-supervisor, Mats Andersson, who I have spent many hours with conducting optical experiments. His patience is endless and his expertise invaluable. Without him, performing the optical experiments would have been impossible.

I am also grateful to the other senior researchers at the department for always being willing to answer questions, especially Sven Andersson who deepened my interest in internal combustion engines through his excellent lectures, but also Petter Dahlander, Mark Linne and Valeri Golovitchev.

This project was a continuation of the work performed by Lucien Koopmans at Volvo Car Corporation. During the first two and a half years he was also my industrial advisor, for which I am truly grateful. His enthusiasm and keenness gave the project a kick-start and kept me alert. Hopefully, I will have the opportunity to work with him again in the future.

Working as a PhD student can often be rather solitary. Fortunately, I have had the privilege of working close to other PhD students, with whom I have exchanged many ideas and had many discussions. Andreas Berntsson was a great support during the first years of my studies as he had been working in the same field for several years. I have also enjoyed many discussions with Martin Eriksson, my friend from undergraduate studies and my office room-mate during the first years. This beneficial relationship continued with my second room-mate, Markus Grahn. In addition to our discussions on various engine-related matters, he has always been very helpful, especially in making Matlab codes run faster (saving me a lot of time). Without mentioning any more names, I would like to thank all the other PhD students at the Combustion Division for their friendship and collaboration.

Of course, I am also grateful to the administrative and technical personnel for all their help through the years. In particular, I would like to thank Elenor Norberg, Ulla Lindberg-Thieme, Rolf Berg, Alf Magnusson, Allan Sognell, Lars Jernqvist, Morgan Svensson and Daniel Härensten.

Hopefully, the future might bring possibilities for me to collaborate with the Combustion Division at Chalmers in some way, which I a would truly value.

This project has been conducted in collaboration with Volvo Car Corporation, and I am grateful for both their financial support and supply of experimental equipment. Roy Ekdahl deserves special thanks for his help through the years and his fantastic sense of humour, but I would also like to thank Göran Josefsson, Börje Grandin, and Patrik Johansson. During the last year I was also working part-time at Volvo Cars on other, but related, R&D areas to HCCI. This provided very good experience and a different perspective on engine development, for which I am also grateful. The Green Car Project 2 and Swedish Energy Agency also provided financial support for the project.

I would also like to take this opportunity to thank Professor Gautam Kalghatgi for taking on the role as opponent of this thesis.

Finally, I would like to express my gratitude to my family and fiancée Hanna, who have all been unconditionally supportive through the years, even during the most intense periods.

Abbreviations and symbols

Abbreviations

AFR	Air to Fuel Ratio (m_{air}/m_{fuel})
AFR_s	Stoichiometric Air to Fuel Ratio
aTDC	after Top Dead Centre
a.u.	arbitrary unit
bTDC	before Top Dead Centre
BMEP	Brake Mean Effective Pressure
CAD	Crank Angle Degree
CA50	Crank Angle degree of 50% heat release
CO	Carbon monoxide
CO_2	Carbon dioxide
CPS	Cam Profile Switching
CUHR	Cumulative Heat Release Rate
CV	Coefficient of Variation
DI	Direct Injection
EGR	Exhaust Gas Recirculation
EOI	End Of Injection
E85	Mixture of 85% ethanol & 15% gasoline
EVC	Exhaust Valve Closing
FSN	Filter Smoke Number
HC	HydroCarbon
HCCI	Homogeneous Charge Compression Ignition
HPF	High-Pass Filtered
HSV	High-Speed Video
H_2O	Water
H_2O_2	Hydrogen Peroxide
IMEP	Indicated Mean Effective Pressure
$IMEP_n$	net Indicated Mean Effective Pressure
$IMEP_g$	gross Indicated Mean Effective Pressure
ISSoot	net Indicated Specific Soot
LCE	Light Collection Efficiency

LIF	Laser induced Fluorescence
LI10	crank angle degree of 10% Light Intensity
LPF	Low-Pass Filtered
LI_{MaxDer}	Maximum Light Intensity Derivative
N_2	Nitrogen
NA	Naturally Aspirated
NEDC	New European Drive Cycle
NO_X	Nitrogen oxides
NVO	Negative Valve Overlap
O_2	Oxygen
PLIF	Planar Laser Induced Fluorescence
PRF	Primary Reference Fuel
PRR	Pressure-Rise Rate
RI	Ringing Intensity
RFC	Relative Fuel Concentration
ROHR	Rate Of Heat Release
SCCI	Stratified Charge Compression Ignition
SCR	Selective Catalytic Reduction
SCSI	Stratified Charge Spark Ignition
SGDI	Spray-Guided Direct Injection
SI	Spark-Ignited
SSI	Stoichiometric Spark Ignition
SOI	Start Of Injection
TDC	piston Top Dead Centre
VCT	Variable Cam Timing

Symbols

η	Efficiency
h_c	Heat transfer coefficient
γ	Ratio of specific heats
κ	Polytropic coefficient
λ	Relative air to fuel ratio (AFR/AFR_s)
r_c	Compression ratio
σ	Standard deviation
θ	Crank angle

Contents

Preface

This project started five years ago, with general investigations of alternative combustion strategies for gasoline engines to reduce fuel consumption while facilitating emission after-treatment. However, the focus was soon narrowed to homogeneous charge compression ignition (HCCI) combustion, especially the high load limit of HCCI combustion and (more specifically) how and why charge stratification can be used to increase it. There are several ways of running HCCI combustion in both gasoline and Diesel engines, however this thesis focuses on gasoline engine HCCI combustion controlled with negative valve overlap and direct injection operated using gasoline or gasoline-like fuels. For a broader perspective of the field, the reader can consult the book edited by Zhao (2007).

The project this thesis is based upon was of solely experimental nature (except for some use of one-dimensional engine codes). Experiments were conducted using production-like multi-cylinder engines and a single-cylinder metal engine to investigate the potential of various strategies for reducing the fuel consumption in the lower load/speed range. However, most investigations concerned charge stratification and ways in which it could be used to extend the high load limit of HCCI. To help explain observed phenomena, the experiments were complemented with laser-based measuring techniques and high-speed video measurements in an optical engine.

HCCI is a contradictory name to use for the combustion when charge stratification is applied since the mixture is far from homogeneous and thus a more appropriate name, stratified charge compression ignition (SCCI), is used in this thesis when a stratified charge is deliberately created by using a late fuel injection. When injection is early with the intention of creating a homogeneous mixture, HCCI is used to denote the combustion even though the mixture is not perfectly homogeneous.

In Chapter 1, the motivation and objectives of the project are presented. Chapter 2 provides a brief, literature-based introduction to HCCI and other lean combustion strategies, and compares them to traditional stoichiometric spark-ignited combustion. These strategies were experimentally compared, and the results are described in the first appended paper (Paper I), but they are not presented in the result section of this thesis. The chapter contin-

ues with a description of basic aspects of combustion and ignition, then the high load phenomenon ringing is described. The chapter ends by describing ways of extending the high load limit for HCCI operation. Chapter 3 provides a description of the engines, measuring equipment and methods used in the project. Chapter 4 presents a selection of the main findings from the experiments. It starts by describing the ringing phenomenon in more depth, and then how charge stratification was used to reduce ringing (and thus increase the loads of both naturally aspirated and boosted operation). After this, results from optical experiments designed to elucidate the ringing inhibiting effect of charge stratification are provided, then observations on the phenomenon are summarised to provide a hypothesis on the ringing inhibiting effect of charge stratification in these types of engines. Finally, the tested four-stroke strategies are compared with two-stroke operation as an alternative approach for load extension. The work is summarized in a discussion of the results and how they can be used, and suggestions for extended future investigations are made, in Chapter 5. The papers appended to the thesis are summarised in Chapter 6, and the thesis finishes with three appendices: one describing the procedure used to evaluate the data acquired from temperature measurements, another to describe evaluation of the high-speed video data and a final one describing the heat release calculations.

Daniel Dahl
Göteborg
2012

Chapter 1

Introduction

1.1 Motivation

Reducing CO_2 emissions, and thus fuel consumption, is a key challenge for all car manufacturers today, in order to meet emission legislation (mainly) and customers' increasing concerns about rising fuel prices and the environment. The main focus has thus shifted from reducing the more traditionally targeted emissions, such as carbon monoxide (CO), hydrocarbons (HC) and nitrogen oxides (NO_X) towards decreasing CO_2 emissions. However, while much attention is being paid to CO_2 emissions, legislation on the other emissions is also getting stricter.

In 2007, the European Commission proposed legislation to limit CO_2 emissions from passenger cars that was subsequently adopted by the European Parliament in 2009. The legislation stipulates that the fleet average limit for new cars sold in the EU shall be reduced to 130 g CO_2/km by 2015, and sets a target of 95 g/km for 2020, both to be met by improvements in vehicle motor technology. A further 10 g/km reduction should be accomplished by other measures, such as use of alternative fuels. There will be an allowance for heavier cars to emit more CO_2 according to Eq. 1.1.

$$\text{Specific emissions of } CO_2 = 130 + a \times (M - M_0) \tag{1.1}$$

where $a = 0.0457$, M is the mass of the vehicle and $M_0 = 1372$ kg (until 2015) (EU, 2009). Similarly, in the USA, the current legislation stipulates that the Corporate Average Fuel Economy (CAFE) shall be 35.5 miles per gallon by 2016, corresponding to 155.3 g CO_2/km if all reductions are due to improvements in fuel economy (NHTSA, 2010). Further, a joint proposal by the U.S. Environmental Protection Agency (EPA) and the Department of Transportation's National Highway Traffic Safety Administration (NHTSA) has recently been issued. In their proposal, the average CO_2 emission limit for new vehicles will be 101 g/km by 2025, corresponding to 54.5 mpg if all

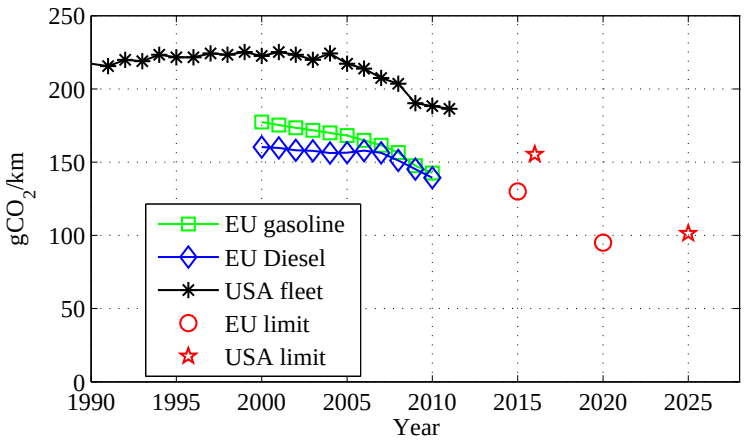

Figure 1.1 – Changes in actual CO_2 emission levels and future limits for the EU and USA from 1990 to 2025 (EEA, 2011; NHTSA, 2010, 2011).

reductions are due to improvements in fuel economy. As in the EU, heavier vehicles will be allowed to emit more than smaller vehicles (EPA, 2011). Figure 1.1 shows these limits and trends in recent years. From these data we can conclude that a 46% reduction will be required in the USA from 2011 to 2025, and a 32% reduction in the EU from 2010 to 2020, corresponding to 3.3 and 3.2% reductions per year (from the original values), respectively.

One way to reduce the fuel consumption of gasoline engines is to utilize an alternative combustion strategy, such as homogeneous charge compression ignition (HCCI). Section 2.2.3 describes the strategy more fully, but for now it can be simply stated that it is a combustion strategy for reducing fuel consumption. Figure 1.2a shows a fictional but representative speed/load map for a quite large gasoline engine, of 3 litre displaced volume in a normal-sized passenger car. The engine speed and load are shown on the x and y axes, respectively. The absolute load is measured in torque [Nm] and the load relative to the engine's displaced volume in brake mean effective pressure (BMEP [bar]). The contour lines show the fuel consumption using traditional spark-ignited (SI) combustion, in which fuel consumption is minimal at relatively low speeds and high loads, and increases rapidly at low loads. The area indicated by green lines shows where the engine is most frequently used, in both real operation and test cycles used to measure CO_2 emissions of the vehicle. As now apparent, during much of the driving an ineffective operating region of the engine is used. Fortunately, this is the region where we can utilize HCCI combustion (or other alternative strategies). However, during driving, the engine would have to switch back and forth between the two combustion modes, which would cause driveability and emission after-treatment problems. Hence, it is essential to increase the upper load limit of HCCI (as explained further in

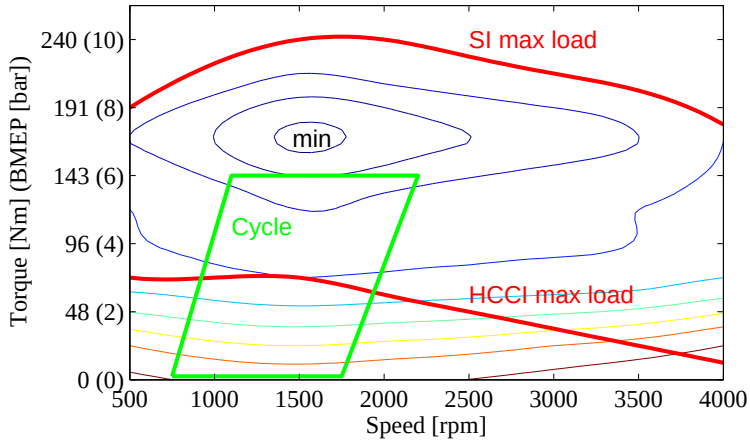

(a) 3 L naturally aspirated engine.

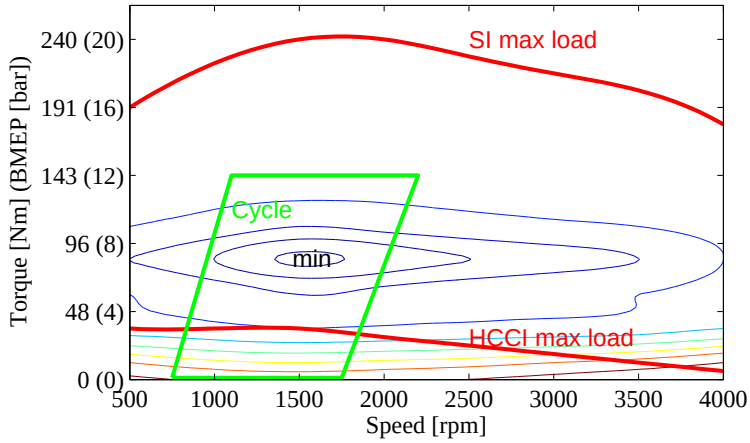

(b) 1.5 L engine turbocharged to reach the same torque as for the 3 L engine.

Figure 1.2 – Speed/load maps of 3 and 1.5 L gasoline engines. Contour lines indicate fuel consumption for SI combustion (increasing from the zones of minimum consumption). The thick red lines indicate the maximum possible loads for SI and HCCI combustion. The green lines indicate zones where most time is spent under normal driving conditions. All information is fictional but representative.

Section 2.4), to avoid mode switches, but also to reduce the fuel consumption a little further buy operating the engine more in HCCI.

An increasingly popular method to reduce fuel consumption today is to downsize engines. This is illustrated in Figure 1.2b. The (fictional) data shown are for an engine of 1.5 litre displaced volume. To compensate for the smaller volume it can be turbocharged to maintain the maximum load in terms of torque. However, this doubles the maximum load in terms of BMEP, and since the fuel consumption is more strongly related to the specific load the contour lines are pushed downwards. Thus, more time will be spent in regions of good efficiency. Unfortunately for HCCI, in which the maximum load curve is more closely linked to the normalized load, less time will be spent using this strategy and there will be more mode switches. Hence, for downsized engines, it is even more important to increase the HCCI load limit for the strategy to be competitive.

1.2 Objectives

The overall objective of the project this thesis is based upon was to investigate and improve alternative combustion strategies to traditional homogeneous stoichiometric SI combustion capable of reducing CO_2 emissions while facilitating emission after-treatment. The focus was on combustion strategies that can be applied in the lower load regime of gasoline engines that would use SI combustion at higher loads. Thus, the engines would have moderate compression ratios and should be operated on gasoline (or similar fuels, such as E85). Early in the project, the objectives were focused on HCCI combustion controlled with negative valve overlap, more specifically on ways to increase the maximum load limit of HCCI operation, preferably using existing components such as direct injection. Therefore, much of the attention was focused on charge stratification as a means to extend the load limit. A further goal was to avoid the need to use any other emission after-treatment systems in addition to three-way catalysts.

Chapter 2

Background

2.1 Traditional combustion and its limitations

In the first four-stroke gasoline engine, run by Nicolaus Otto in 1876, combustion was initiated using the spark-ignition strategy, in which a mixture of air and fuel is compressed and then ignited by a spark. Around this spark a small flame kernel is created, which propagates outwards toward the combustion chamber walls, see Figure 2.1a. Ahead of the flame front there is fresh charge and behind it there are products from the combustion, apart from nitrogen (N_2), which consist mainly of carbon dioxide (CO_2) and water (H_2O), but also include harmful species, such as unburned hydrocarbons (HC), carbon monoxide (CO) and nitrogen oxides (NO_X). In order to obtain a stable propagating flame, the mixture must fulfil certain criteria. Notably, the amount of air cannot be either much more or much less than that required to oxidise the fuel. More specifically, the air to fuel ratio (AFR=m_a/m_f) must be between ca. 8 and 20 (around the stoichiometric air to fuel ratio, $AFR_s \approx 14.5$) under normal conditions (Stone, 1999). Moreover, in the last ca. 25 years cars with gasoline engines have been equipped with a three-way catalyst that simultaneously oxidises CO and HC emissions while reducing NO_X emissions. However, in order for the catalyst to simultaneously oxidise and reduce the emissions the engine must run stoichiometrically, i.e. with precisely (or oscillating around) the required amounts of air needed to oxidise all the fuel (λ=1 where λ=AFR/AFR_s), eliminating possibilities of using steady-state excess air. When the spark-ignition strategy is applied in a stoichiometric manner it is here referred to as SSI (stoichiometric spark ignition).

In order to run the engine at part load and keep within the required air/fuel ratio range the airflow must be constrained, usually using a throttle, which increases the so-called "pumping losses" because more power is required during the intake stroke to pull the piston downwards when the pressure is reduced in the intake manifold. This is one of the major reasons for the low part load

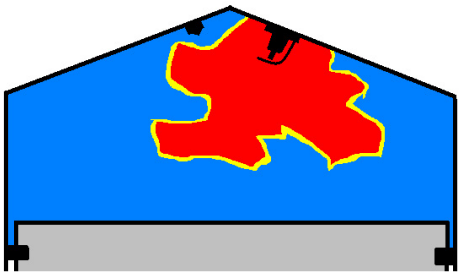

(a) Homogeneous spark-ignited (SI) combustion showing the unburnt air-fuel mixture (blue), combustion residuals (red) and the flame front (yellow) moving from the residuals towards the unburnt charge.

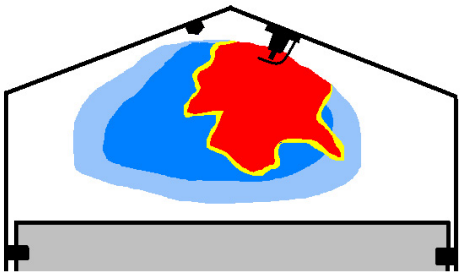

(b) Stratified charge spark-ignited (SCSI) combustion showing the air only zones (white), the unburnt air-fuel mixture (blue), the combustion residuals (red) and the flame front (yellow) moving from the residuals towards the unburnt charge.

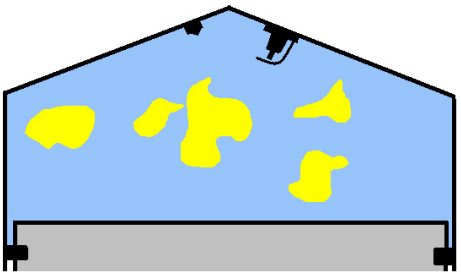

(c) Homogeneous charge compression ignition (HCCI) combustion showing the unburnt air-fuel mixture (blue) and zones where the combustion has started (yellow).

Figure 2.1 – Schematic diagrams of three different combustion strategies.

efficiency of SI combustion engines.

Because of the undiluted charge used in SSI combustion, the combustion and combustion products are very hot, with peak temperatures typically around 2500 K (Heywood, 1988). This results in large wall heat losses and is a second major reason for low SI engine efficiency.

In the ideal Otto cycle, heat is added at constant volume, meaning that the fuel should burn instantaneously and the main heat release should occur at piston top dead center (TDC) in order to fully exploit the energy released. When heat transfer is taken into account, heat release should occur slightly after TDC since the volume changes slowly around TDC, which provides an unnecessarily long time for heat losses. On the other hand, if combustion is too late, less energy is exploited in the exhaust stroke as work and more is

wasted in the form of hotter exhaust gases (sometimes deliberately to heat the catalyst). Real combustion cycles are more complex, since the combustion is actually quite slow, with typical burn durations (CA10-90; i.e. the crank angle interval at which 10-90% of the heat has been released) of 20-40 crank angle degrees (CAD) and a non-linear heat release profile. This means that some of the heat is released too early and some too late, which further reduces the efficiency. Normally, the optimal combustion phasing, measured as the CAD of 50% heat release (CA50), in real SI engines is around 5-10 CAD aTDC.

Despite the low efficiency of SSI combustion it is still used in most gasoline (Otto) engines today, because it allows easy control of both load (using a throttle) and combustion timing (using a spark) together with successful emission after-treatment (using a three-way catalyst). Furthermore, it is robust, having low sensitivity to engine wear and external parameters (such as air density and temperature) and it allows the engine to run smoothly and quietly. However, due to the increasing pressures to reduce CO_2 emissions, car manufacturers will probably soon have to partly abandon this convenient strategy for more efficient alternatives.

2.2 Alternative combustion strategies

2.2.1 Lean combustion

The purpose of lean combustion is to overcome, or at least reduce, some of the shortcomings of the SSI combustion strategy. In this context, lean means that there is an excess of air compared to the stoichiometric air to fuel ratio. The most obvious benefit is the reduction of pumping losses, due to the increased intake manifold pressure required to deliver more air.

A less intuitive benefit of lean combustion is the thermodynamically more beneficial gas composition. The ideal Otto cycle efficiency can be simply expressed using the engine compression ratio, r_c, and the ratio of specific heats, γ, of the gas according to:

$$\eta = 1 - \frac{1}{r_c^{\gamma-1}}$$

Not only does the cycle efficiency increase with the compression ratio (which is also true for Diesel engines and is one of their major advantages over gasoline engines since they have higher r_c), it also increases with increases in γ. Figure 2.2 shows how η and γ vary with λ for a mixture of iso-octane and air at 1000 K and $r_c = 11$. Normally, γ changes with temperature and composition during the cycle, however the example shows the impact of γ (and thus λ) on the cycle efficiency.

When the charge is diluted with air the temperature inside the combustion chamber is reduced, thereby reducing not only wall heat losses but also

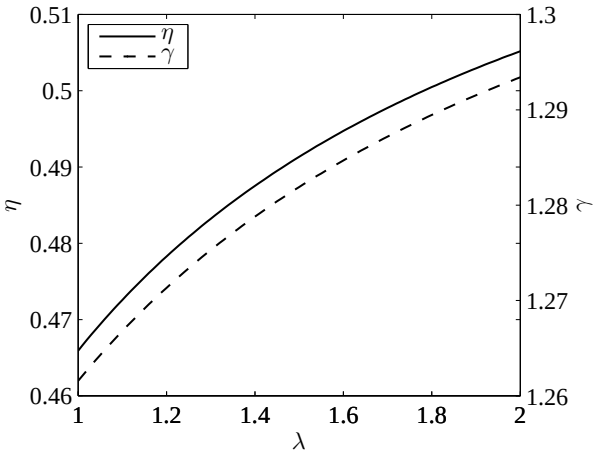

Figure 2.2 – Ratio of specific heats γ (right axis and dashed line) and resulting Otto cycle efficiency (left axis and solid line) as a function of the relative air to fuel ratio λ for $r_c = 11$ and T=1000 K.

the dissociation of CO_2 and H_2O, which increases the combustion efficiency (Heywood, 1988). Combustion efficiency also increases because excess oxygen pushes the equilibrium of the reactions into more complete residuals (Stone, 1999).

Unfortunately, for SI combustion there is a limit to how much the charge can be diluted with air, called the lean limit. If the mixture is too lean, cycle-to-cycle variations in the work produced in each engine cycle makes the engine behave unsteadily. This is caused by slow initial flame development. Beyond a certain point, with excessively lean mixtures the flame is extinguished (Heywood, 1988). This is related to the flammability limit, at which the rate of heat loss from the flame begins to exceed the rate of heat generation by the reactions (Glassman and Yetter, 2008).

The major drawbacks of utilizing lean combustion are the associated exhaust emission after-treatment problems. Since the mixture is lean, it is not sufficient to use a standard three-way catalyst, which will only effectively oxidise HC's and CO under lean conditions. In order to reduce NO_X as well, a lean NO_X after-treatment system must be used, such as a lean NO_X trap or an SCR (selective catalytic reduction) catalyst, which will increase costs of the vehicle and penalize the CO_2 gain.

2.2.2 Stratified SI combustion

One way to overcome the lean limit of homogeneous spark-ignited combustion is to use stratified charge spark ignition (SCSI). As the name implies, in this strategy the mixture is no longer homogeneous. The fuel is injected late,

directly into the cylinder, creating a local cloud of fuel-air mixture, in near-stoichiometric conditions, located in the vicinity of the spark plug. The gases in the rest of the combustion chamber consist (ideally) only of air, which does not participate in the chemical reactions, see Figure 2.1b. In this way the global λ can be much higher, while the local λ where combustion occurs is kept low.

The strategy has many advantages. Notably, the system can run with wide open throttle, thereby minimizing pumping losses. The ratio of specific heats is increased further, giving an even higher cycle efficiency, and the global temperature is lower, further reducing heat losses. Directly injecting the fuel brings an additional benefit of charge cooling, due to the fuel evaporating. This effect inhibits knock when running homogeneous operation at higher loads and makes it possible to increase the compression ratio, which further increases the cycle efficiency compared to that of a port fuel injected engine. Spicher et al. (1999) argue that for such reasons the fuel consumption can be reduced by up to 50% at the lowest loads and speeds, with smaller reductions at higher loads and speeds.

Unfortunately, creating a perfect enclosed fuel-air mixture at the spark plug is not straightforward, therefore much of the effort in SCSI research concerns mixture formation. There are three main configurations for a stratified charge ignition system, two of which (narrow spacing and wide spacing, or spray-guided and wall-guided, respectively) are discussed by Spicher et al. (1999). In a narrow spacing arrangement, also called spray-guided direct injection (SGDI), the injector is located close to the spark plug and the fuel spray should never hit the combustion chamber walls, as illustrated in Figure 2.1b. In a wide spacing, or wall-guided, arrangement the injector is further away from the spark plug, with the spray directed towards and impinging on the piston, which directs it towards the spark-plug. The latter was the first production gasoline stratified charge system, introduced by Mitsubishi in the mid-1990's (Iwamoto et al., 1997), but it never yielded substantial fuel consumption reductions and suffered from soot and excess hydrocarbon emissions (Spicher et al., 1999). A variant of the wide spacing arrangement was used in the Hesselman engine, which was developed in about 1930 and can be regarded as the first SCSI engine (Lumley, 1999). It could run on many types of fuels, such as gasoline (for starting), alcohol, kerosene and crude oil, and was seen as a rival to the upcoming Diesel engine (Olsson, 1990). The third system is the air-guided system, in which the gas motion within the cylinder is responsible for both air-fuel mixing and deflecting the spray towards the spark plug. FEV Motorentechnik developed such a system with variable tumble in the late 1990's and reported fuel consumption reductions of 20% compared to the SSI strategy in stationary operation at 2000 rpm and 2.8 bar IMEP (Geiger et al., 1999).

Today, the focus is mostly on the SGDI system. BMW has obtained fuel consumption reductions of 20% in the NEDC drive cycle using this system, although it is not clear how much of the reduction was solely due to the combustion system (Schwartz et al., 2006).

In addition to the required lean NO_X after-treatment required to run SCSI, there is a risk of fuel-rich zones forming, which can cause soot production, especially at higher loads, and hence requires use of a soot-treating device, e.g. a particulate filter. Also, further effort is needed to improve the stability and robustness of the system.

2.2.3 HCCI combustion

Homogeneous charge compression ignition (HCCI) differs substantially from SI and SCSI combustion in that there is no propagating flame initiated by a spark. In HCCI combustion the charge is auto-ignited, much like in the Diesel engine but with the important difference that the charge is premixed and auto-ignited almost simultaneously throughout the combustion chamber, see Figure 2.1c.

HCCI is not an entirely new combustion strategy (although it has not been used in any four-stroke gasoline production engines to date). Indeed, Erlandsson (2002) has speculated whether the combustion in the "hot-bulb engine" patented in 1897 used HCCI combustion alone, or auto-ignition in combination with subsequent flame propagation, or diffusion burning. In a definite early application, a 2-stroke Diesel model airplane engine emerged on the market in the 1940s that used HCCI combustion (Zhao, 2007), and in an issue of TFA (1952) there is an article about a new motorcycle engine of just 18 cc called the "Lohman engine". This was a premixed two-stroke HCCI engine, fuelled with Diesel fuels, which used a variable compression ratio to control the combustion. However, it was not until 1979 that systematic investigations of this combustion strategy were published. Both Onishi et al. (1979) and Noguchi et al. (1979) managed to stabilize and control the "abnormal" combustion that was usually encountered in two-stroke gasoline engines and they reported improvements in both fuel consumption and emissions. Onishi and colleagues called the new combustion strategy "Active Thermo-Atmosphere Combustion" (ATAC) while Noguchi and colleagues called it "Toyota Soken" (TS). The name "Homogeneous Charge Compression Ignition" with the acronym "HCCI" was first introduced by Thring (1989) and today HCCI and "Controlled Auto Ignition" (CAI) are the most common names for this type of combustion strategy in gasoline engines.

In HCCI, the charge is always diluted in some way, by excess air, residuals or a combination of air and residuals. This dilution reduces the combustion rate, which would be excessively fast in a stoichiometric mixture of just air

and fuel and has the further benefits of reducing both pumping losses and temperatures, which leads to less wall-heat losses. Normally, temperatures are sufficiently low so that only a few ppm of NO_X are produced. Also, in comparison to SI combustion the temperature in HCCI is nearly homogeneous, thus avoiding compression of the residuals from the first burnt charge, which would otherwise cause high temperatures and large NO_X production. Finally, the fast combustion makes HCCI resemble the ideal Otto cycle better which further improves the efficiency.

The auto-ignition is governed by temperature, pressure, composition and the time-history of the charge, which can be controlled by adjusting the following parameters, listed by Zhao (2007):

- EGR or amount of residuals.
- Timing of a direct injection.
- Air/fuel ratio.
- Compression ratio.
- Inlet mixture temperature.
- Inlet manifold pressure.
- Properties of the fuel or fuel blend.
- Coolant temperature.

The first and second of these parameters were used in the project this thesis is based upon to control combustion timing, following the work by Koopmans (2005). A negative valve overlap (NVO) was used, in which the exhaust valve closes early in order to trap hot residuals (Willand et al., 1998; Denbratt, 1998; Koopmans and Denbratt, 2001). This requires compression work in the exhaust stroke, but the work will be returned if the intake valve is opened late so that the compressed gas is allowed to expand. However, the temperature increase due to compression leads to some heat losses and thus not all the work is returned. By controlling the valve timings, especially the exhaust valve closing (EVC), the amount of residuals can be controlled and hence the temperature in the combustion chamber, which affects the auto-ignition timing. In this way, the residuals serve two purposes: initiating the combustion while at the same time restraining the reaction rates. Koopmans et al. (2003) and Urushihara et al. (2003) found that a small pilot direct injection prior to the NVO was an effective tool to further control the combustion through a combination of exothermic reactions and production of radicals during the NVO.

At low loads and speeds, HCCI combustion with NVO is limited by misfires since there is insufficient heat in the residuals to initiate combustion. This

might be solved using a SI stratified charge to initiate the combustion, as shown by Berntsson and Denbratt (2007a). At high loads, HCCI combustion is limited by rapid combustion causing pressure oscillations and audible noise which is described in more detail in Section 2.4 since this is what the project focused on overcoming. HCCI combustion is not directly controlled, by a spark for example, thus some sort of feedback control will have to be used, in which the combustion is monitored and some of the parameters listed above are adjusted to deliver the desired behaviour. As in the SCSI strategy, there will be NO_X after-treatment problems if the combustion is lean, but since the levels of NO_X emissions are very low (except at relatively high loads where they might become a problem), lean NO_X after-treatment may not be needed, or at least less complex and cheaper systems may suffice. On the other hand, HCCI will incur extra costs for combustion control since there is a need for additional systems to control the combustion, e.g. variable cam timing (VCT), cam profile switching (CPS) and direct injection, and sensors to monitor the combustion, e.g. ion current sensors or pressure transducers. However, VCT/CPS systems (or other complex valve train systems) and direct injection are becoming increasingly common in gasoline engines for other reasons and thus soon only combustion sensors may need to be added for the HCCI technique to be implemented in production engines.

A comparison of homogeneous stoichiometric SI, homogeneous lean SI, stratified lean SI and lean HCCI was performed in the appended Paper I but will not be further discussed in this thesis.

2.3 Combustion fundamentals

This section provides a short but deeper explanation of some combustion phenomena, mainly focusing on ignition. It will probably be too brief for a layman to understand, but can help for better understanding of later discussions on knock, ringing, dilution and the influence of two-stage ignition.

An excellent categorization of practical combustion phenomena is given by Kanury (1982), who states that combustion is primarily controlled by:

(1) Chemical kinetics,
(2) Diffusion, flow and other physical mixing processes,
(3) Or a combination of (1) & (2)

Ignition and explosion are said to be of the first type, and spray-combustion of the second type. The main combustion event in a classic Diesel engine is said to be diffusion-controlled (or sometimes mixing-controlled). Here, reactants (oxygen and fuel) are not mixed before combustion, but diffuse into the flame while products and heat diffuse away from it. Flames in gasoline en-

gines are said to be of the third type, since they are governed by chemical kinetics and flows of heat and mass. Such flames, where the ignitable mixture of air and fuel is separated from the combustion residuals by a moving flame front, are called *deflagration* waves. Perhaps a better description than "flow of heat and mass" is heat conduction and diffusion of radicals (Glassman and Yetter, 2008). Since HCCI combustion occurs more or less uniformly in the entire combustion chamber and it is premixed, it is best described as being controlled by chemical kinetics.

Chain reactions are of great importance for combustion. This can be most easily illustrated by the following four reactions (of more than 40 that may occur) in the combustion of hydrogen with oxygen (the bullets indicate highly reactive radicals).

(1)	$H_2 + O_2 \rightarrow 2OH\bullet$	*chain initiation*
(2)	$OH\bullet + H_2 \rightarrow H_2O + H\bullet$	*chain propagation*
(3)	$H\bullet + O_2 \rightarrow OH\bullet + O\bullet$	*chain branching*
(4)	$H\bullet + O_2 + M \rightarrow HO_2 + M$	*chain termination*

In the first reaction, *chain initiation*, radicals are formed from stable species. In the second reaction, *chain propagation*, the same numbers of radicals are formed and consumed. In the third step, *chain branching*, more radicals are formed than consumed and in the last stage, *chain termination*, radicals react to form stable species. At a certain temperature and pressure ignition occurs. This is illustrated by the explosion limits in Figure 2.3 for hydrogen (left) and hydrocarbon fuels (right). To the left of the limits slow reactions can occur, but they will never accelerate to become explosive (very fast), as they do to the right of the limit. Below the first explosion limit, formed radicals diffuse to the walls because of the low pressure, where they recombine to form stable species. Above this limit radicals form more rapidly than they diffuse and ignition occurs. Reaction (4) accelerates more rapidly with pressure increases than reaction (3) and dominates above the second limit, thus ignition is not possible. Located between the second and third limits, the rate of reaction (3) increases with temperature while the rate of reaction (4) decreases. Thus at sufficiently high temperatures reaction (3) dominates and ignition occurs. At the third limit (*thermal explosion limit*) another reaction breaks the stability of HO_2:

(5) $HO_2 + H_2 \rightarrow H_2O_2 + H\bullet$

where

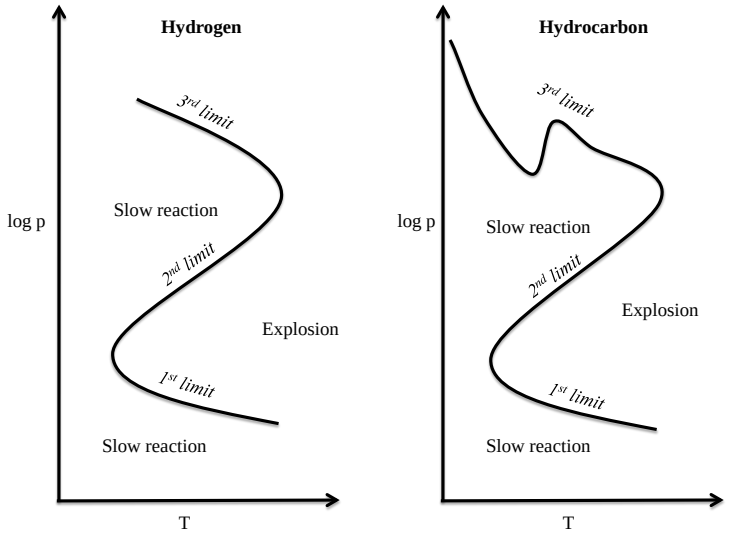

Figure 2.3 – Schematic illustration of explosion limits for hydrogen (left) and hydrocarbon (right) (Warnatz et al., 2010; Glassman and Yetter, 2008).

(6) $H_2O_2 \rightarrow 2OH\bullet$

and ignition occurs (Glassman and Yetter, 2008; Warnatz et al., 2010).

In a review by Westbrook (2000) reaction (6) is identified as the governing reaction for auto-ignition in HCCI combustion, auto-ignition in Diesel combustion and knock in SI combustion. The decomposition of H_2O_2 occurs at around 1000 K and any factor that affects the timing of its decomposition also affects the auto-ignition timing.

In section 2.2.3 the role of dilution in slowing reaction speeds was mentioned. The cause of this can be understood by considering reaction (4). The third-body M can be a wall or in the case of dilution another molecule, but it is required for conversion of the radicals into less active species by removing energy (Kanury, 1982; Heywood, 1988).

In engines, pressures are normally high, so only the third explosion limit is of interest. This limit can also be much more complex for hydrocarbon fuels, see Figure 2.3. At this limit, combustion can occur at several stages (multi-stage ignition). Warnatz et al. (2010) gives a good example of one such reason for methane-oxygen mixtures:

(7) $CH_3\bullet + O_2 \rightleftharpoons CH_3O_2\bullet$
(8) $CH_3O_2\bullet + CH_4 \rightarrow CH_3OOH + CH_3\bullet$
(9) $CH_3OOH \rightarrow CH_3O\bullet + OH\bullet$

At high temperatures, the equilibrium of reaction (7) is shifted to the left

and the chain-branching step (9) is no longer fed by reactions (7) and (8), a phenomenon called *degenerate branching*. This short discussion suffices to show that the chemical reactions can cause ignition at several stages. In HCCI combustion, *two-stage ignition* is often encountered, which is relevant for later discussions of charge stratification. Such ignition often occurs when using primary reference fuels (PRF) that include N-heptane, but seldom when using fuels such as iso-octane or gasoline, where *single-stage ignition* is more common. Whether there is single-stage or two-stage ignition is not only dependent on the fuel, but also under what conditions the engine is run. Kalghatgi et al. (2003) exemplifies this with two different fuels that both show significant low temperature chemistry at high pressure / low temperature conditions but very little low temperature chemistry at low pressure / high temperature conditions.

The ignition can be classified as a pure *thermal explosion* or a *chain explosion*. According to Warnatz et al. (2010) in a pure thermal explosion temperature rises at once (even though the initial rise is slow) and there is no ignition-delay and Kanury (1982) adds that the reaction rate is only influenced by the concentrations of the initial reactants and the heat released elevates the temperature, thereby accelerating the reaction rate. If a chain-branching mechanism is important for the chemical reactions ignition can be classified as a chain explosion. There is then a certain ignition-delay, during which a radical pool accumulates while the temperature is almost constant (Warnatz et al., 2010). Kanury (1982) points out that in reality both mechanisms are important.

2.4 High load HCCI limitation, ringing

As already touched upon in Section 1.1 & 2.2.3, HCCI combustion is limited to low loads and speeds. While the last 20 years of HCCI research has mainly focused on ways to control the combustion, increasing attention is now being paid to other aspects, such as expansion of the operational area.

At high loads the dilution ratio is not sufficient to restrain the reaction speeds (see Section 2.3), causing in-cylinder pressure fluctuations which appear as audible noise emitted from the engine. This is illustrated in Figure 2.4, where phenomena at two loads are considered: a "low" load of 2.2 bar $\mathrm{IMEP_n}$ and a "high" load of 3.5 bar $\mathrm{IMEP_n}$, both at an engine speed of 2000 rpm. In Figure 2.4a, the original in-cylinder pressures (at which there are fluctuations) and the low-pass filtered (LPF) pressures are displayed. Figure 2.4b shows the rate of heat release calculated from the LPF pressures and it is evident that the heat release rate is greater at the higher load, in other words, combustion is more intense. By applying a high-pass filter (HPF) to the pressure signal, as shown in 2.4c, one can extract the pressure oscillations and it becomes evident

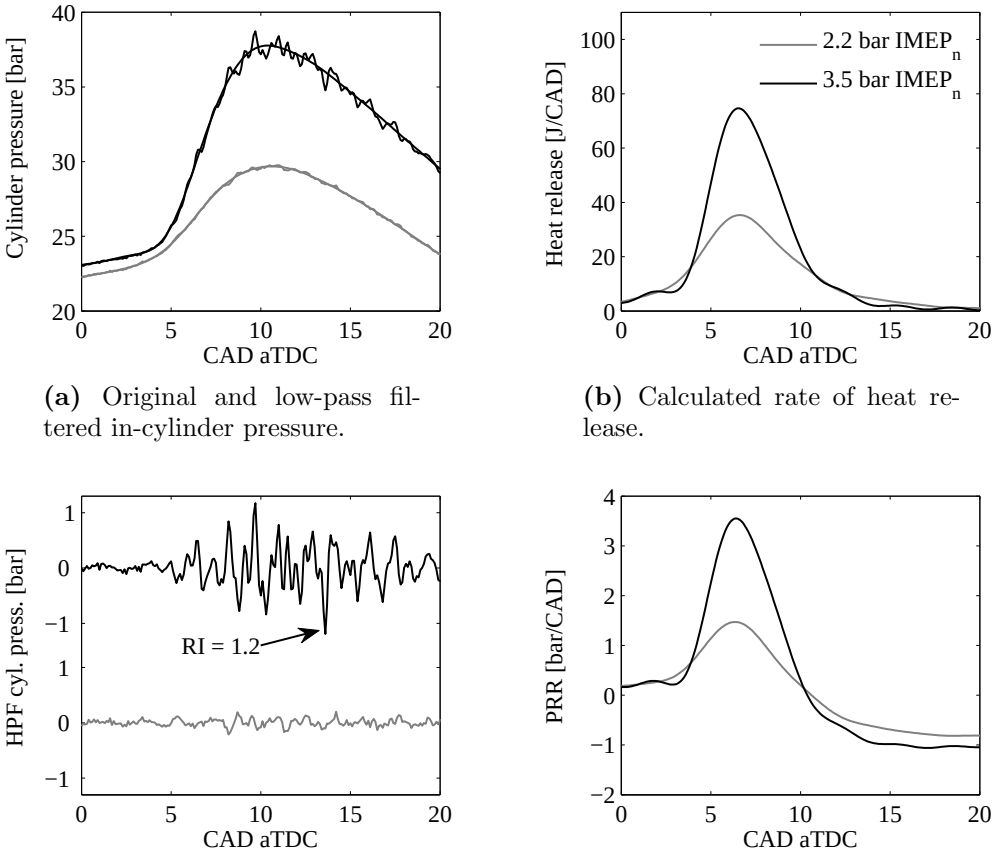

(a) Original and low-pass filtered in-cylinder pressure.

(b) Calculated rate of heat release.

(c) High-pass filtered in-cylinder pressure.

(d) Pressure-rise rate.

Figure 2.4 – Comparison of low load (grey curves) and high load (black curves) cases at the same combustion phasing and engine speed (2000 rpm).

that these oscillations are much greater in the higher load case. Another consequence of the intense combustion is a higher global pressure-rise rate (PRR), which is the derivative of pressure with respect to CAD ($dP/dCAD$).

The pressure oscillations that appear at high loads and the resulting engine noise are very similar to the phenomenon of knock in SI engines. However, most people think of knock as the noise resulting from auto-ignition of the unburnt gas ahead of the flame front (called end-gas) in SI combustion, thus a term introduced by Eng (2002), *ringing*, is used here to describe the pressure oscillations in HCCI combustion.

There are several ways in which ringing in an engine can be identified and classified by analysing pressure traces, some of which are described by Burgdorf and Denbratt (1997) but for knock. A simple way that was found to be very appropriate in the project underlying this thesis is to define the ringing inten-

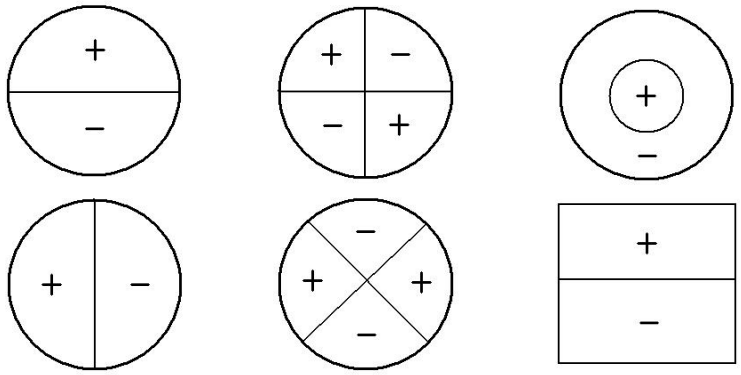

(a) First circumferential modes

(b) Second circumferential modes

(c) First radial and axial modes

Figure 2.5 – Schematic diagram of some low frequency acoustic resonance modes of a simple cylinder (Draper, 1935; Hickling et al., 1983; Scholl et al., 1998).

sity (RI) as the maximum amplitude of the high-pass filtered pressure signal. This is normally done over many cycles (300 in this project) and the average value for RI is used to classify the ringing intensity. In Figure 2.4c the pressure peak used to classify the RI for the illustrative cycle is pointed out. The definition of ringing intensity used here should not be confused with the correlation for ringing intensity developed by Eng (2002) which can be used when information about the actual pressure fluctuations is not available (for example in zero-dimensional chemical kinetic models).

The in-cylinder pressure waves, or ringing, that can be detected with pressure transducers are standing waves or acoustic resonance modes. Calculations based on wave equations and measurements of such modes were performed by Draper (1935); Hickling et al. (1983); Scholl et al. (1998). In Figure 2.5, some of the lowest frequency acoustic modes that they identified for a simple cylinder are displayed. The nodes (where pressure is constant) are represented by lines and the antinodes (where pressure oscillates) by plus and minus signs. The first circumferential modes (Figure 2.5a) and second circumferential modes (Figure 2.5b) are paired and rotated relative to one another (Scholl et al., 1998). In a real combustion chamber the location of the nodal lines will be determined by asymmetries in the chamber shape (Hickling et al., 1983).

Several researchers have studied the phenomenon of ringing in HCCI engines in more depth. Vressner et al. (2003) mounted eight distributed pressure transducers in the combustion chamber of a large Diesel HCCI engine and

found that the directions of the pressure waves were random, and thus concluded that the auto-ignition events causing them differed in number, location and timing from cycle to cycle. Yelvington and Green (2003) proposed that the ringing is due to local parcels of fuel/air mixture that burn too fast, so the required expansion rates for the parcels exceed the speed of sound. These local overpressures then lead to resonant pressure waves. Eng (2002) compared knock in SI combustion with ringing in HCCI combustion in the same engine and found that much larger in-cylinder oscillations could be withstood without increases in audible noise in HCCI combustion. This is because the acoustic energy is concentrated to lower frequencies in HCCI combustion and pressure oscillations at these frequencies are not as effectively transmitted through the engine structure as those at higher frequencies. Andreae et al. (2007) found that the higher frequencies contained a larger fraction of the total power in microphone signals outside the engine than the in-cylinder pressure signal, but it was still the first order mode power that dominated and was the most significant contributor to noise. Further, they concluded that it was not transmission of cylinder pressure waves through the engine that caused the acoustic radiation from the engine, but vibration of the engine structure excited by the first few in-cylinder waves.

Ringing phenomena have been much less extensively researched than knock, which has been a limitation for high compression ratios in gasoline engines from the beginning. Since both phenomena are manifested in fluctuations of pressure traces, and the resulting noise emitted from the engine are very similar, a brief discussion of the knock phenomenon is justified. Grandin (2001) presented an extensive historical overview of research concerning knock phenomena in his thesis. During the last century there were two main explanatory theories, the detonation theory and the auto-ignition theory, but eventually the latter prevailed. An explanation of detonation is provided by Glassman and Yetter (2008): if the volume behind a deflagration wave is closed, the wave can undergo transition to supersonic speeds. This is what is called *detonation*. The pressure and temperature of the shock wave increase, causing further reactions that in turn enhance the wave. However, detonation is unlikely to occur in internal combustion engines since the transition length from deflagration to detonation is more than a meter for most fuels; much longer than normal combustion chambers. Grandin concluded that early researchers failed to see knock as an acoustic phenomenon and thus proposed detonation to explain the wave-like phenomena. Knock is now regarded as arising from auto-ignition of the end-gas ahead of the propagating flame, causing substantial local pressure rises sending out shock waves that can put the combustion chamber into resonance as explained above (Heywood, 1988). This was already observed more than 70 years ago, by Withrow and Rassweiler (1936), who captured auto-ignition ahead of the flame front using high-speed photography at rates

of 5000 pictures per second.

Besides the similarities in the noise resulting from ringing in high load HCCI combustion and knock in SI combustion, HCCI combustion is very similar to auto-ignition of the end-gas in SI combustion. The reader might then wonder how we can deliberately use such auto-ignition, and the answer once again lies in dilution, which is used in HCCI combustion to slow down the combustion speed to acceptable levels.

2.5 Methods for increasing the HCCI high load limit

2.5.1 Stratified Charge Compression Ignition - SCCI

Charge inhomogeneity and its effects on combustion and emissions in HCCI engines have been examined in numerous studies published in the last ten years. A literature review is provided here focusing on how an inhomogeneous charge (mainly delivered using DI) can be used to extend the upper load limit (although most published investigations have focused on combustion phasing control).

Calculations of fluid mechanics and chemical kinetics in HCCI combustion described by Aceves et al. (2000) showed that several zones are needed to accurately predict the burn duration. Using only one zone (implying that conditions in the cylinder are completely homogeneous) leads to major over-prediction of the burn rate. In a multi-zone model "the hottest part of the mixture ignites first and compresses the rest of the charge, which ignites after a short time lag". Amano et al. (2001) proposed that charge inhomogeneity (fuel and temperature) can be used to reduce the maximum pressure rise rate and ringing intensity; a hypothesis they verified in simulations with natural gas as the fuel. However, in early optical measurements of the effect of fuel inhomogeneity on combustion, Richter et al. (2000) compared the combustion of poorly mixed fuel delivered by port fuel injection and well-mixed fuel, prepared in a mixing tank, and while they observed differences in the fuel distribution prior to combustion, they detected no significant differences in the combustion. Increasing the stratification level using a late direct injection (SOI up to 60 CAD bTDC) of gasoline Sjöberg et al. (2002) found that a late injection caused intense ringing behaviour, together with earlier combustion phasing. Similarly, Marriott and Reitz (2002) also found that a late direct injection of gasoline required a lower intake temperature to compensate for the earlier combustion phasing, and very late DI was limited by ringing. Both Sjöberg et al. (2002) and Marriott and Reitz (2002) used high compression ratio engines operating with very lean mixtures ($\lambda \approx 3$). Kumano and Iida (2004) reported experi-

mental indications that a more inhomogeneous charge (created in the intake port) of DME reduces the rate of heat release and provides a longer emission of chemiluminescence compared to a more homogeneous charge. With late DI of PRF50 fuel in the compression stroke, Berntsson and Denbratt (2007b) found that both the lateness and the amount of fuel injected in the late injection cause a reduced and prolonged rate of heat release and using optical measurements they observed that ignition occurs first in richer zones. Importantly, in the two last cited studies, the authors used fuels which displayed two-stage ignition, which are further discussed shortly. More recently, Brewster et al. (2008) found that a late direct injection of gasoline under stoichiometric conditions could be used to increase the load substantially (from 3.5 bar to 7 bar $IMEP_n$), although this was with substantially later combustion phasing and it is unclear what would have happened if they had allowed the combustion to be as late in the homogeneous case (they used fixed NVO cam timings). In a study by Dongbo et al. (2009) it is shown that in an engine operating on gasoline with NVO at λ=1.56, charge stratification can effectively reduce pressure rise rates if the stratification is sufficient to create fuel rich zones, otherwise it increases the pressure rise rate. This finding is very interesting since it agrees with the finding presented in Chapter 4.

The most comprehensive studies on charge stratification and its possibilities for load extension have been performed at Sandia National Laboratories. Dec and Sjöberg (2004) managed to isolate the fuel chemistry effects from other effects, such as those of wall temperature and residuals, on auto-ignition at different fuelling rates using a so-called "fire 19/1 mode" in which 19 cycles fire under the same conditions and the 20th cycle is used for measurements with varying parameter settings. They concluded that auto-ignition of iso-octane and gasoline has little sensitivity to the fuel concentration while that of PRF80 is highly sensitive to it, a higher fuel concentration requiring a lower intake temperature for constant combustion phasing. This is because PRF80 includes N-heptane, a two-stage ignition fuel under the conditions studied. The heat released from the low temperature reactions increases with fuel concentration and thus advances the phasing of the main combustion. Based on these observations, they also showed that fuel stratification using late DI of PRF80 (but not iso-octane) effectively advances the combustion phasing. They applied this knowledge in a following investigation, (Sjöberg and Dec, 2006) in which they managed to increase the load, with fuel stratification by late DI, from 5.37 to 5.97 bar $IMEP_g$ under constant combustion phasing with acceptable ringing and NO_X levels due to the smoothing effect on the heat release. Following this work, they compared effects of charge stratification when using PRF73 and pure iso-octane (Yang et al., 2011). For PRF73 the conclusions were the same, but for iso-octane they found that even though combustion phasing remained constant, the pressure rise rates increased with increased stratification; similar

to the results reported by Sjöberg et al. (2002) and Marriott and Reitz (2002). Importantly, in all three cited studies (Dec and Sjöberg, 2004; Sjöberg and Dec, 2006; Yang et al., 2011) high compression ratios were used to achieve HCCI combustion and operation was far from stoichiometric ($\lambda > 2$). When applying boosted intake air (thus increasing the cylinder pressure), Dec and Yang (2010) found that gasoline shows what they call intermediate-temperature heat release (ITHR), between low temperature heat release and main combustion, and in a subsequent study (Dec et al., 2011) they used this in a partial fuel stratification strategy that was also effective for gasoline.

A combustion concept worth mentioning here is partially premixed compression ignition (PPCI). The purpose of PPCI is to avoid diffusion combustion in Diesel engines were fuel injection and combustion occur simultaneously which leads to high NO_X and soot emissions. To separate these events Kalghatgi et al. (2006) showed that gasoline is a much more suitable fuel than Diesel because of its lower cetane number (higher octane number). By injecting gasoline instead of Diesel in a heavy duty Diesel engine they showed that the increased ignition delay provided by gasoline separated the injection and combustion events providing significantly lower smoke and NO_X levels and thus loads could be increased (up to 14.86 bar IMEP at 200 kPa intake pressure) while maintaining low levels of these emissions (although higher than the limits used in this project). Also, it is stated that HCCI would not be possible at the same loads due to failure of auto-ignition or excessive combustion speed. This type of combustion is thus the most stratified type of combustion before diffusion combustion where injection and combustion occur simultaneously. For more information on this type of combustion in Diesel engines see for example (Kalghatgi et al., 2007; Manente et al., 2009; Hanson et al., 2009; Manente et al., 2011).

As can be seen from this literature review, the results of using charge stratification seem to be dependent on several factors, for example the fuel used, the air dilution ratio, the type of engine and boosting. The main objectives of the studies this thesis is based upon was to investigate ways in which charge stratification (created by using a late direct injection) could be used to increase the upper load limit of HCCI combustion with fuels normally exhibiting single-stage ignition in a gasoline type engine controlled using NVO (thus with low in-cylinder pressures and close to stoichiometric operation). Further, efforts were made to explain why charge stratification works under these conditions.

2.5.2 Boosting

It is widely accepted that boosting the intake air allows the load to be increased in HCCI engines. When increasing the intake pressure more air is inducted into the cylinder and thus more diluent gases are available to damp

the combustion. This was demonstrated by Christensen et al. (1998) in experiments with a single-cylinder, large displacement Diesel engine where loads up to 14 bar $IMEP_n$ (1000 rpm) at an intake pressure of 300 kPa (obtained with an external compressor) were achieved, compared to 3.8 bar $IMEP_n$ under naturally aspirated conditions using natural gas as fuel. However, at the boosted high load case, the cylinder pressure reached 250 bar and the pressure-rise rate reached 34.4 bar/CAD which are values much higher than what can be tolerated in gasoline engines. In early experiments using a gasoline NVO-operated engine, Cairns and Blaxill (2005a) fitted a small turbocharger to a four-cylinder 2.0 litre engine and investigated the operating range. As an example, they managed to extend the high load limit at 3000 rpm from 2.5 bar in naturally aspirated operation to 4.6 bar BMEP with an intake pressure of 230 kPa. Johansson et al. (2009) investigated the operating range of a similar engine and at 3000 rpm they increased the load from 3 bar to 4.25 bar $IMEP_n$ which is a smaller increase. However, they only reached an intake pressure of $\approx$170 kPa. This indicates the difficulty of finding a suitable turbocharger for the low flow rates normally encountered in HCCI (with NVO). Further, if one uses a suitable turbocharger for HCCI operation it will be too small for use in SI operation at higher loads, thus another, larger turbocharger will also have to be used for that purpose. Such issues of turbocharger matching are discussed in Shingne et al. (2010).

In recent work, Kuboyama et al. (2009) have demonstrated something they call blow-down super charging. This is based on using the re-breathing strategy (instead of NVO) where the exhaust valve is reopened late in the intake stroke to get the residuals back into the combustion chamber. With a combination of increased back-pressure (controlled with an exhaust throttle) and the blow-down pressure wave from another cylinder they managed to reach 5.75 bar $IMEP_n$ (6.5 bar in combination with stratification of EGR). Relying of pressure pulses is however speed dependent unless variable pipe lengths are used.

2.5.3 EGR

The use of external exhaust gas recirculation (EGR) is not a load increasing strategy in it self. But at high loads, NO_X emission levels can often be excessively high also for HCCI combustion and if these are to be taken care of by the three-way catalyst, EGR can be used to reach stoichiometric conditions. This was demonstrated by Cairns and Blaxill (2005b) where it was shown that using only trapped residuals to maintain stoichiometric conditions was not possible at higher loads due to excessive combustion rates (because of the high temperature leading to overly advanced combustion phasing) and thus cooled EGR was used in combination with trapped residuals. In order to cope with excessive NO_X emissions at high loads Johansson et al. (2009) also utilized EGR

for stoichiometric operation in combination with intake air boosting. General (chemical and thermodynamical) effects that EGR has on the auto-ignition in HCCI combustion for different fuels can be found in (Sjöberg et al., 2007).

2.5.4 Two-stroke operation

As already mentioned in Section 2.2.3, most of the early research on HCCI combustion focused on two-stroke engines, see for example Onishi et al. (1979) and Noguchi et al. (1979). In two-stroke operation there is a power-stroke in every revolution, in contrast to four-stroke operation where there is a power stroke every other revolution. This implies that there is greater potential for higher engine power using a two-stroke strategy.

Asai et al. (1995) describe the development of the Honda EXP-2 motorcycle that participated in the Grenada-Dakar rally in 1995. This was a two-stroke engine that used HCCI combustion at low loads, controlled using a special exhaust port timing valve. As they could use a smaller engine than their competitors (who used four-stroke SI engines) and utilized HCCI combustion they obtained superior fuel economy. Similarly, Duret and Venturi (1996) describe a two-stroke engine developed for automotive applications which used direct injection and HCCI. They report fuel economy improvements of 20% compared to a four-stroke (SI) engine of equivalent power.

If both four-stroke and two-stroke strategies are to be applied in the same engine, the switching between the two modes will require greater flexibility in valve timings, using for example electro-magnetic valves (Kojic et al., 2007). Further, to induct air into traditional two-stroke engines the piston is used to build up pressure in the crankcase, which is then released to the cylinder for scavenging. For an engine with overhead valves a turbocharger can be used, but since a higher pressure is required in the intake than in the exhaust it is difficult to cope with only a turbocharger, but a compressor can be used for additional boost (Osborne et al., 2005).

Finally, note that the major parameter for controlling two-stroke HCCI combustion is the amount of residuals retained in the combustion chamber (Duret, 2007), which makes it very similar to four-stroke HCCI using the NVO strategy for combustion control.

Chapter 3

Experimental equipment and methods

A variety of engine configurations, instruments and methods have been used in the project. Those applied in experiments yielding the results presented in Chapter 4 are described here.

3.1 Multi-cylinder engine

Two versions of the multi-cylinder engine were used in the project. The one used in the study reported in Paper III is described here, but it had only minor differences to the one used in the study described in Paper I. The engine used for the experiments was a Volvo Car short in-line six-cylinder (SI6) engine of 3.2 litre displaced volume. A photograph of the engine is shown in Figure 3.1a, a schematic of the engine is shown in Figure 3.1b and some specifications of the engine are presented in Table 3.1.

This engine differed from the production version in that it was equipped with

Table 3.1 – Multi-cylinder engine parameters

Parameter	Value
Bore	84 mm
Stroke	96 mm
Compression ratio	11.4
Valve lift	≈3 mm (HCCI); ≈10 mm (SI)
Fuel	Gasoline (101 RON, 88 MON)
	E85 (104 RON, 92 MON)
Fuel pressure	15 MPa
Water / oil temperature	90 / 97 °C

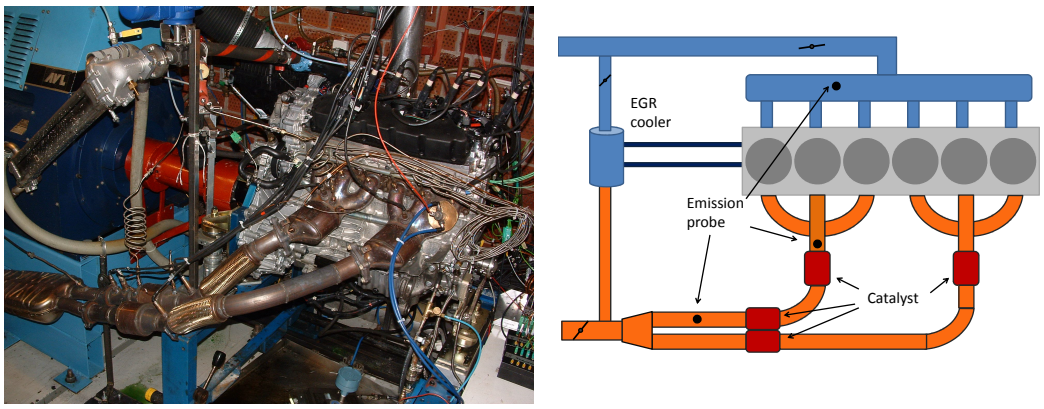

(a) Photograph. **(b)** Schematic diagram.

Figure 3.1 – Volvo Car multi-cylinder, multi-mode combustion engine used to explore the upper load limits of HCCI/SCCI operation

cam profile switching (CPS) and variable cam timing (VCT) on both the intake and the exhaust side. The CPS system allows the engine to be operated with two different cam profiles on each side: one with low lift and short duration for HCCI/SCCI operation and one with high lift and long duration for SI operation. The VCT system allows the phasing of both intake and exhaust valve events to be adjusted across 60 CAD ranges. A schematic of the CPS-VVT hardware is displayed in Figure 3.2a and the system's possible valve profiles are displayed in Figure 3.2b.

The combustion chamber geometry was of pent-roof type with a flat piston. A spray-guided direct injection system, with a centrally placed multi-hole injector delivering a horseshoe-shaped spray pattern, was used to supply the fuel (another modification compared to the production version), see Figure 3.3.

For emission after-treatment, the engine was equipped with four three-way production catalysts designed to meet ultra-low emission vehicle (ULEV) emission limits for SSI combustion. The exhaust system was of the 6-2-1 type with one pair of closed coupled catalysts and one pair of under-floor catalysts. The engine was modified to accommodate an external EGR system for stoichiometric operation, which added exhaust gas directly after the air cleaner in the first parts of the intake system to ensure satisfactory mixing of the intake air and EGR. A valve was mounted in the exhaust pipe to maintain a constant absolute back-pressure of 105 kPa. The EGR was cooled to approximately 100 °C using the engine coolant. Downstream of the cooler, an EGR valve was mounted to regulate the amounts of EGR. Once the EGR entered the intake system it had been further cooled to about 60 °C. However, varying the EGR levels never caused more than 5 °C variations in the temperature at the intake port.

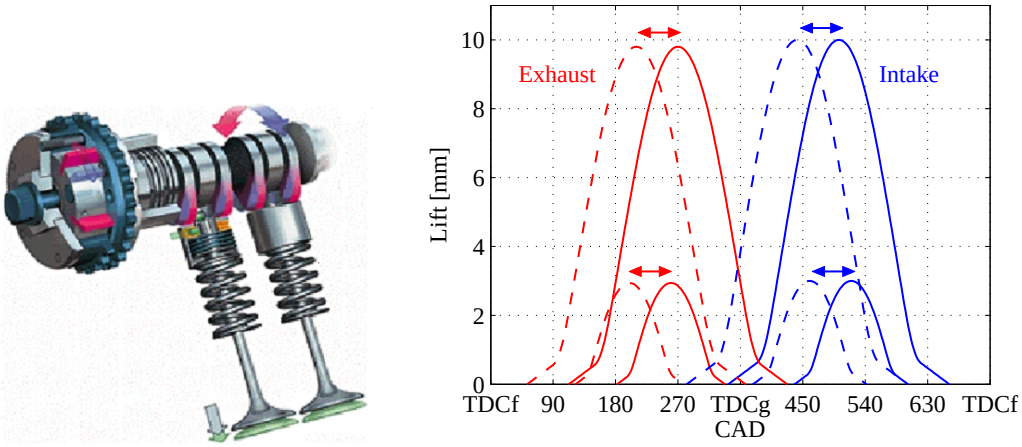

(a) Hardware. **(b)** Possible valve lift profiles.

Figure 3.2 – CPS-VVT system of the multi-cylinder engine.

Figure 3.3 – Spray-guided direct injection system used in the multi- & single-cylinder engines.

Together, the engine features made it possible to run all the combustion strategies described in this thesis (homogeneous SI, stratified charge SI, HCCI and SCCI). In order to handle these strategies, and the mode-switches between them, the production engine control unit (ECU) was changed to a development ECU. Since HCCI combustion phasing is affected by many variables, among others the wall temperature, compression ratio and fuel loading, all of which vary somewhat between the cylinders, cylinder balancing is used. Generally, the control system in this engine reads the location of peak pressure (LPP) and then tunes the combustion phasing to a required set point using the VCT system for "bulk" tuning and a pilot injection at the beginning of the NVO for tuning individual cylinders. However, during experiments, only individual cylinder tuning was used (cam timing was manually set). Further, preliminary tests showed that using a pilot injection was unfavourable for extending the

high load limit, thus the cylinder balancing control was applied to the main injection instead. This works well for HCCI operation when a negative valve overlap is used since more fuel, in addition to increasing the load, also provides hotter residuals, and thus earlier phasing of the coming cycle. The result is constant combustion phasing with the same phasing in all cylinders, but somewhat different loads for each cylinder ($\leq \pm 0.2$ bar $IMEP_n$). Using the control loop in this manner increased the load range somewhat, but only when operation was on the lean side of stoichiometric. The same approach was used for SCCI combustion, in which the control system was used for the main injection while the late injection was manually set.

3.2 Single cylinder engine

The AVL 5411 gasoline single-cylinder rig at Chalmers was used for metal engine experiments and optical experiments.

3.2.1 Metal (thermodynamic) configuration

Two different metal engine setups have been used in the project. Engine parameters of both are presented in Table 3.2. Both setups had similar combustion chambers to the multi-cylinder engine and used centrally placed direct injectors. The first setup was used in initial tests on SCCI where the possibility of reducing ringing at fixed loads was evaluated. A photograph of the engine in the first setup is shown in Figure 3.4a. Fixed low-lift camshafts (similar to those of the multi-cylinder engine) were used and the engine was naturally aspirated. To maintain constant combustion timing, an electrical heater was used in the intake as the engine lacked VCT capabilities.

The second setup, which was more complex, was used to evaluate the high load limit of HCCI/SCCI with fully flexible valves, boosting and EGR. A

Table 3.2 – Single-cylinder metal engine parameters.

Parameter	Setup 1	Setup 2
Bore	84 mm	84 mm
Stroke	90 mm	90 mm
Compression ratio	11.3	11.4
Valve lift	3 mm	varying
Fuel	Gasoline (99.5 RON)	Gasoline (101 RON, 88 MON)
Fuel pressure	15 MPa	15 MPa
Water / oil temperature	90 / 90 °C	90 / 90 °C

schematic diagram of the setup is presented in Figure 3.4b. The active valve train (AVT) system, manufactured by Lotus Engineering, is an electronically controlled, hydraulically operated system that provides complete flexibility in valve profile design of each valve individually and can switch between different profiles in real time. The control software is designed for 4-stroke operation with two revolutions in each cycle. However, it provides the possibility to use double lift profiles and can thus be "tricked" into operating in two-stroke mode. A similar EGR system to the one used in the multi-cylinder engine was mounted on the engine for stoichiometric operation. A Roots blower type compressor was used to increase intake pressures, and an electrical heater was used after the compressor to maintain a constant intake temperature of 50 °C in order to level out the changes in temperature with varying boost pressures.

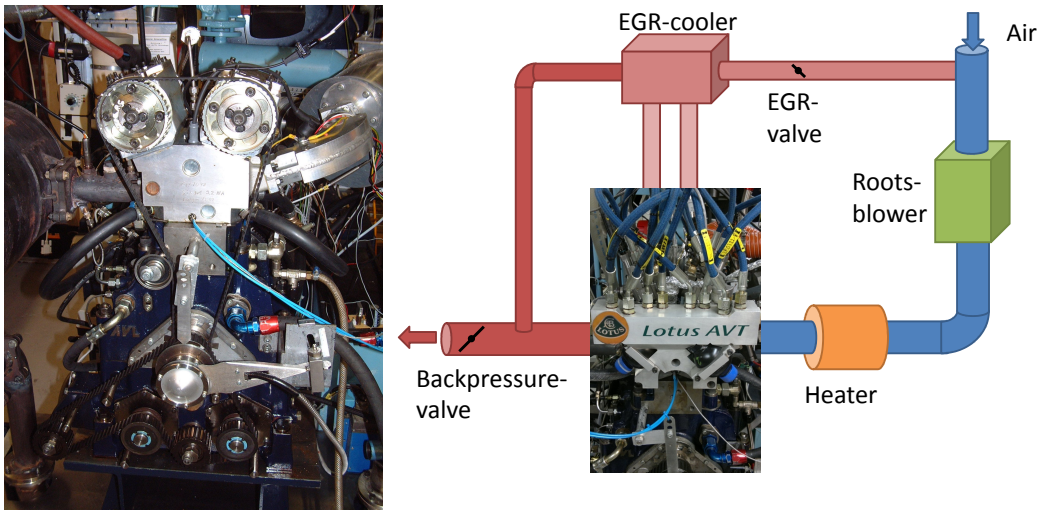

(a) Photograph of the engine in setup 1.

(b) Schematic diagram of the engine in setup 2.

Figure 3.4 – Single-cylinder metal engine.

3.2.2 Optical configuration

Three optical setup configurations have been used in the project. The setup used in the study presented in Papers IV & VI is described here.

In the optical engine, light is collected from the combustion chamber through the piston, which incorporates a quartz window of 74 mm diameter. The piston is extended with openings on two sides so that a 45° mirror can be inserted. The bore and stroke are 83 and 90 mm, respectively, thus the optical engine has a slightly smaller displaced volume than the metal engine. The combustion chamber differs from that of the metal engine in that it has two pent-roof

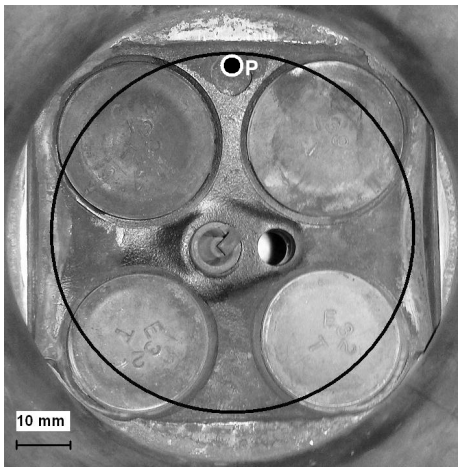

Figure 3.5 – Photograph of the combustion chamber in the single-cylinder optical engine taken from below through the cylinder. The black circle shows the field of view provided by the optical access through the piston. The white circle, labelled P, shows the location of the pressure transducer. The injector is positioned in the centre, next to the spark plug, but was not mounted when this photograph was taken.

quartz windows to allow laser light to enter at one side and exit at the other. Figure 3.5 shows a photograph of the combustion chamber taken from below, through the cylinder. The black circle indicates the optical access imposed by the piston window edges. The pent-roof windows are to the left and right, and the pressure transducer is located between the two intake valves (as in the multi-cylinder engine, but not the single-cylinder metal engine, where it is located at the position of the right pent-roof window). The valve system is the same as in metal engine setup 1, with fixed low lift short duration camshafts, thus to fine tune the combustion phasing, heated intake air was used. The injection system used was of the same type as in the multi-cylinder and single-cylinder metal engine, with a centrally placed injector providing 15 MPa fuel pressure. Figure 3.6 shows a photograph of the optical setup used in the study described in Paper VI to measure in-cylinder temperature.

3.3 Standard measuring equipment

In-cylinder pressure measurements are essential for acquiring knowledge of engine performance. Based on the pressure measurements, parameters such as load (IMEP), heat release characteristics and ringing can be calculated. The accuracy of estimates of such parameters therefore depends on the quality of the pressure measurements, which are taken using pressure transducers. Two kinds of pressure transducers were used in the project. In the single-cylinder

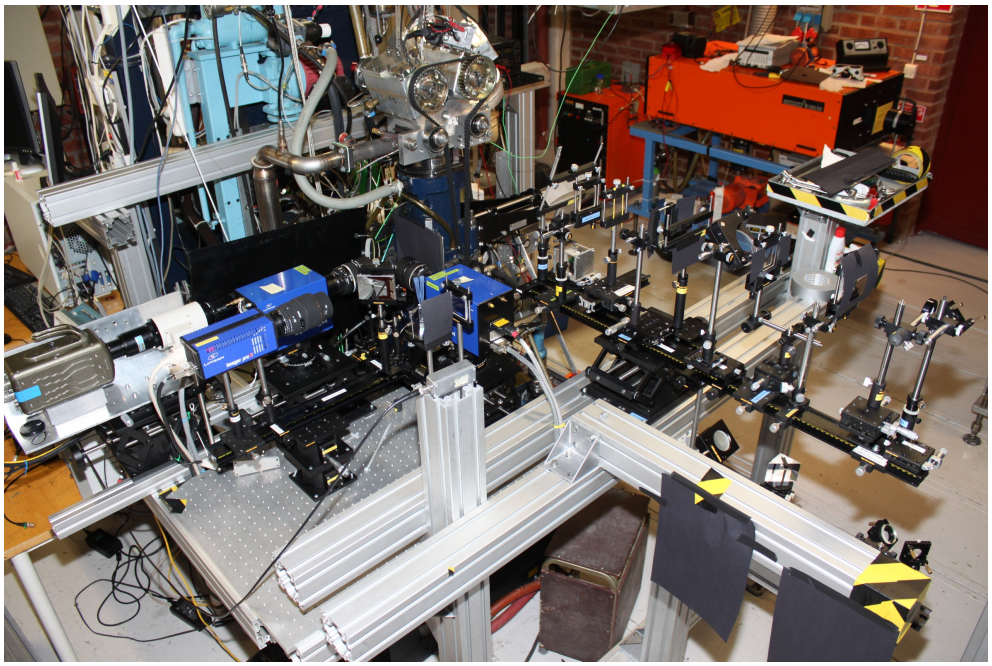

Figure 3.6 – Photograph of the optical engine setup.

metal engine measurements, a Kistler 6061b cooled pressure transducer was used. Unfortunately, this transducer is too large for convenient installation in the optical engine (because of the pent-roof windows) and multi-cylinder engine (because of neighbouring cylinders). Thus, smaller uncooled Kistler 6053 transducers, which are less accurate because of their sensitivity to thermal shock, were used for those applications instead. To minimize interference from thermal shock, the 6053 transducers were mounted with a small recess designed to minimize internally imposed pressure oscillations. The pressure signals were amplified with Kistler 5011 or 5044 charge amplifiers and acquired using an AVL Indimaster 670 system. For real-time combustion analysis, AVL IndiCom software was used. However, all data presented in this thesis were evaluated using Matlab and Excel (heat release calculations can be found in Appendix C).

The emission measuring instruments consisted of a flame ionization detector for HC, non-dispersive infra-red radiation detectors for CO and CO_2, a chemiluminescence analyser for NO_X, and a paramagnetic susceptibility analyser for O_2. Soot was measured using an AVL 415 smoke meter or an AVL Micro Soot sensor. The fuel flow was measured using both an AVL fuel balance, which measures changes in fuel weight over a certain period, and a Micro Motion meter, which is a Coriolis flow measurement device. The Micro Motion meter gave more accurate, repeatable and instantaneous readings, so the fuel balance was used as a secondary backup system. In the multi-cylinder engine

AFR values were measured using LA4 lambda meters from ETAS and a binary Lambda Sond was used for tuning towards stoichiometric mixtures, while in the single-cylinder engine a lambda meter from Horiba was used. In both cases, calculations using the exhaust gas concentrations taken from Brettschneider (1979) were used to verify lambda readings. Temperatures were measured using type K thermocouples.

3.4 Optical measuring equipment

The high-speed video (HSV) camera used for the experiments was a Vision Research Phantom v7, which was connected to a Hamamatsu C9548-03 high-speed gated image intensifier equipped with a quartz lens. The frame rate used for solely HSV experiments was 111111 fps, which corresponds to 12.35 frames per CAD (at 1500 rpm) and an exposure time of $\approx$9 μs, with a resolution of 64×64 pixels. Alternatively, an imaging grating spectrograph was placed in front of the image intensifier, and the camera was operated at a resolution of 256 pixels along the spectral dimension and 64 pixels along the spatial dimension at a rate of 75000 fps. When used along with other cameras the frame rate and resolution were set at 66666 fps (corresponding to 7.41 frames per crank angle degree) and 128×128 pixels, respectively.

Three CCD-cameras were used for temperature measurements: a LaVision Imager Pro X double-frame camera originally intended for PIV measurements and two image-intensified LaVision Dynamight cameras, in each case at a resolution of 1024×1024 pixels. The cameras were used to capture laser-induced fluorescence from the 4^{th} harmonic of an Nd:YAG-laser (266 nm) and an excimer laser operating with XeCl (308 nm) as the excitation sources.

3.5 General measurement proceedure

3.5.1 Metal engine

Each morning during the experimental campaigns the engine coolant (and oil in single-cylinder experiments) was heated up and then kept at a constant temperature of 90°C, with a conditioning system. During this time, the emission measurement equipment was heated up and calibrated (and recalibrated in the afternoon). A reference point was used to check for deviations in the engine's behaviour by comparing IMEP, the location of 50% heat release (CA50), temperatures, emission levels etc. to those obtained in an earlier reference test. Most measurements were repeated to obtain indications of the spread/deviation in measurements and parameter sweeps were run in random order to eliminate time trends. Logging was started once all parameters

(IMEP, CA50, emissions, temperatures etc.) had stabilized. Fast data, such as in-cylinder pressure, were logged for 300 cycles while slow data, such as temperatures and emissions, were averaged over 100 seconds. All parameters from the cylinder pressure measurements were calculated for individual cycles, then average values of the parameters were calculated.

3.5.2 Optical engine

The engine was heated to a normal operating temperature of 90°C before starting the experiments. It was then motored and the intake heaters were activated. When an appropriate intake temperature for satisfactory combustion phasing and ringing intensity was reached the combustion was started directly in HCCI/SCCI mode, with the aid of a spark, by turning on the fuel supply. After a few seconds, when the combustion had stabilised, the spark was turned off. After a few more seconds measurements commenced. As the cylinder head was uncooled and operation was at relatively high loads the operating time with combustion was only about 30 seconds. Measurements were taken during 100 cycles for in-cylinder pressure. In solely HSV experiments 65 repeated cycles were recorded with the camera while in temperature measurements five cycles were recorded with high speed video and LIF images (due to limitations imposed by the read-out time of the Dynamight cameras).

3.6 Identifying the high load limit

As noted in Paper I, and observed in later studies, when the load is increased in HCCI combustion the range of possible combustion phasing timings is narrowed. Early combustion is limited by fast combustion and ringing. To calculate the ringing intensity (Section 2.4), a cut-off frequency of 4000 Hz was found to be appropriate for the engines used in this work, since it captured all the pressure fluctuations while retaining all other combustion information (IMEP, heat release, pressure rise rate etc.). The limit for RI was set to 1 bar, at which a clearly audible "knocking" sound appears. Too late combustion, in contrast, leads to unstable combustion. The high load limit is thus set by the point at which the region between the ringing (early combustion) and unstable (late combustion) thresholds becomes too narrow for viable operation. For combustion stability, limits based on the coefficient of variation (CV) of $IMEP_n$ were used. However, since this measure of deviation is normalized to the load it is not applicable when loads approach zero, thus the standard deviation (σ) of $IMEP_n$ was used instead. For operation at $IMEP_n \geq 3.3$ bar a limit of 3% CV was applied, while for lower loads a limit of 0.1 bar σ was applied. In addition, no misfires were allowed.

The third load constraint, which was most important in the charge stratification experiments, related to the quantity of soot emitted. The Euro VI standards for passenger cars stipulate that soot emissions must not exceed 0.005 g/km, which translates to approximately 35 mg/kWh in the NEDC (New European Drive Cycle) for a medium-sized passenger car (requiring an average power of 4.8 kW). In the single-cylinder rig, soot was measured using the Micro Soot sensor, for which an upper limit of 20 mg/kWh in net indicated specific soot (ISSoot) was set. In the multi-cylinder engine, a load constraint for soot emissions of 0.1 FSN (Filter Smoke Number, as measured by the AVL 415 smoke meter) was employed (which approximately equals 1.35 mg/m^3), the minimum level that the smoke meter can measure accurately. To get an estimation on how this relates to the legislative limit, let us assume that we have a 3.2 litre engine operating at 1500 rpm throughout the cycle with 100% volumetric efficiency, thus consuming ≈47 m^3 of air (in worst case) which results in ≈0.006 g/km (if exhaust gases are approximated as air at ambient conditions). A summary of the general load limiters is presented in Table 3.3.

Apart from these general load limiters, a limit on NO_X of 10 ppm was employed in some cases. If using the same worst case scenario on air flow as for soot, this limit would correspond to ≈0.08 g/km to be compared to the Euro VI standard of 0.06 g/km.

Table 3.3 – Load limiters.

Parameter	Limit
Ringing intensity	1 bar
$\sigma(IMEP_n)$ for $IMEP_n \leq 3.3$ bar	0.1 bar
$CV(IMEP_n)$ for $IMEP_n \geq 3.3$ bar	3 %
ISSoot (single-cylinder)	20 mg/kWh
FSN (multi-cylinder)	0.1

3.7 Capturing pressure oscillations optically

The methodology used to capture pressure oscillations optically is briefly presented here (a more detailed explanation is provided in Paper IV).

During the main heat release period, intense chemiluminescence is emitted from species such as electronically excited OH and CO_2, but hot residuals, mainly H_2O, also emit radiation in the red and near infra-red parts of the spectrum (Gaydon, 1974; Hwang et al., 2008; Iijima and Shoji, 2007). Therefore, when capturing images inside the combustion chamber, not only will the chemiluminescence from the combustion reactions be detected but also emissions from the resultant hot gases. Emission spectra from 270 to 690 nm

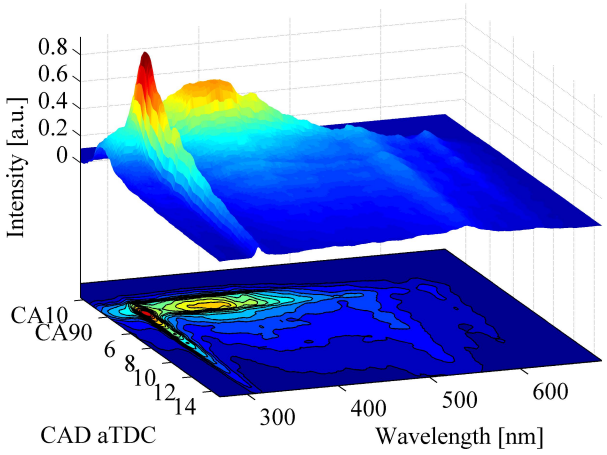

Figure 3.7 – Crank angle-resolved light emission spectra, recorded using an HSV camera coupled to a spectrometer, during a typical cycle covering the main combustion event and the subsequent 10 CAD.

recorded during one HCCI cycle with the HSV camera and image-intensifier connected to the spectrograph are shown in Figure 3.7. In this wavelength range, the primary emission peaks are a relatively narrow peak around 306 nm due to OH and a broad peak centred at approximately 400 nm attributed to CO_2 formation. The luminescence intensity was highest during the main heat release period, but late reactions resulted in the light emission extending well beyond 90% heat release (CA90). Unfortunately, the signal detected for hot H_2O was rather weak because the image intensifier used had low sensitivity to infrared light. Therefore, a large proportion of the light detected after the main heat release was chemiluminescence from late reactions. The intensity of light emitted by hot residuals should theoretically be proportional to their molecular density and enhanced by the higher local temperatures associated with high pressure areas. Both increased pressure and temperature should also increase the rate of late reactions and hence further increase the light emitted. Thus, the light intensity should vary with variations in pressure.

Light (pressure) oscillations were filtered out using a high-pass filter with a cut-off frequency of 5000 Hz (which for consistency was also used in pressure transducer measurements in these experiments) in each pixel. In order to spatially correlate the pressure oscillations with the intensity of the preceding combustion, the combustion chamber was divided into 16 zones, as shown in Figure 3.8. In each of these zones, the maximum derivative of the light emission intensity (which was found to be a robust measure of the combustion intensity, see Appendix B) was averaged over all the pixels contained within the zone. One problem encountered using these 16 zones was that a large derivative in one zone would typically be associated with a small derivative in the opposite

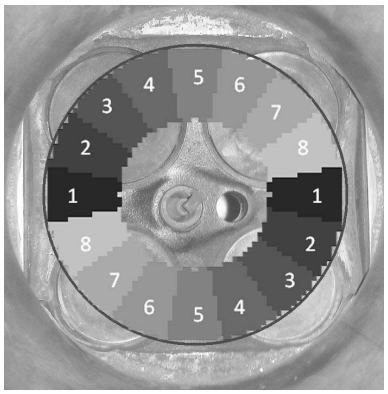

Figure 3.8 – Diagram of the zones used to correlate the amplitude of oscillation modes with the light intensity derivative. The labels show pairs of opposite zones.

zone, whereas fast combustion in opposite zones generally gave rise to the same oscillation modes, thereby reducing any correlations. Therefore, from the 16 zones, eight values were extracted, each defined as the highest value of the average maximum derivative obtained from opposite zones. The zones in Figure 3.8 are labelled to illustrate the eight pairs of opposite zones. The magnitude of the derivative in such a zone should be related to the magnitude of the derivative in its pixels and the number of pixels with a large derivative within it.

3.8 2D temperature measurements

To explore phenomena associated with charge stratification and its ringing inhibition, in-cylinder temperature and fuel concentration measurements were acquired and correlated to characteristics of the following combustion captured by monitoring chemiluminescence. The aim was not to resolve absolute values of temperature perfectly, rather identifying zones of hotter and colder mixtures.

Two-wavelength planar laser-induced fluorescence (PLIF) was used in this work to obtain estimates of in-cylinder temperature distributions before combustion. The technique exploits changes in the fluorescence spectrum of a tracer (in this case 3-pentanone) that occur with changes in temperature, and their dependence on the excitation wavelength (Figure 3.9), which are due to shifts in both the absorption spectrum (relative numbers of photons with different wavelengths in the exciting laser light absorbed by the tracer) and the fluorescence quantum yield (ratio of the number of photons emitted to the number of photons absorbed). For homogeneous mixtures (of known concentration) it would be sufficient to use a single excitation wavelength to measure the temperature, but to measure temperatures of an inhomogeneous mixture

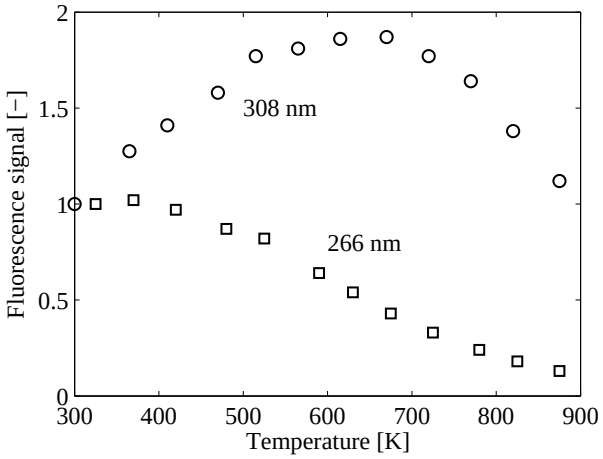

Figure 3.9 – Changes with temperature in relative fluorescence signals from 3-pentanone (per molecule) excited by light at 266 and 308 nm wavelengths, normalized to the values at 300 K. Data from Koch (2005).

the fluorescence signal is also dependent on the fuel concentration. For such measurements the ratio of signals emitted from excitation using two different wavelengths, in this case 266 nm and 308 nm, can be used.

Interested readers can find a more thorough description of the technique and data on different fuel tracers in the thesis by Koch (2005). Examples of previous applications include analyses of temperature distributions in unburnt gases in a two-stroke SI engine by Einecke et al. (2000), the mixing of hot exhaust gas residuals with fresh intake charge in HCCI combustion by Rothamer et al. (2008) and naturally occurring thermal stratification in HCCI combustion by Snyder et al. (2011).

A photograph of the optical setup has already been shown in Figure 3.6, but since this is somewhat cluttered, a simplified schematic diagram of the optical setup is presented in Figure 3.10. Note that this schematic is not in scale. Two laser beams, one from the excimer laser (308 nm) and the other from the Nd:YAG laser (266 nm), were spatially overlapped by dichroic mirrors and formed into horizontal laser sheets (42 mm wide) passing through the quartz windows and cylinder a few mm below the spark plug. The laser optics were carefully adjusted so that there was near perfect overlap of the two laser planes at both the incoming and outgoing pent-roof windows, since the same volume must be excited by both wavelengths. The two lasers were triggered 1 μs apart from each other to avoid interference. A small fraction ($\approx$10%) of the light was deflected before entering the cylinder by a tilted quartz plate and directed through a cuvette filled with a liquid mixture of isooctane and 3-pentanone. The resulting fluorescence signals were captured by the double-frame CCD-camera to measure the distribution of the laser intensity across the plane.

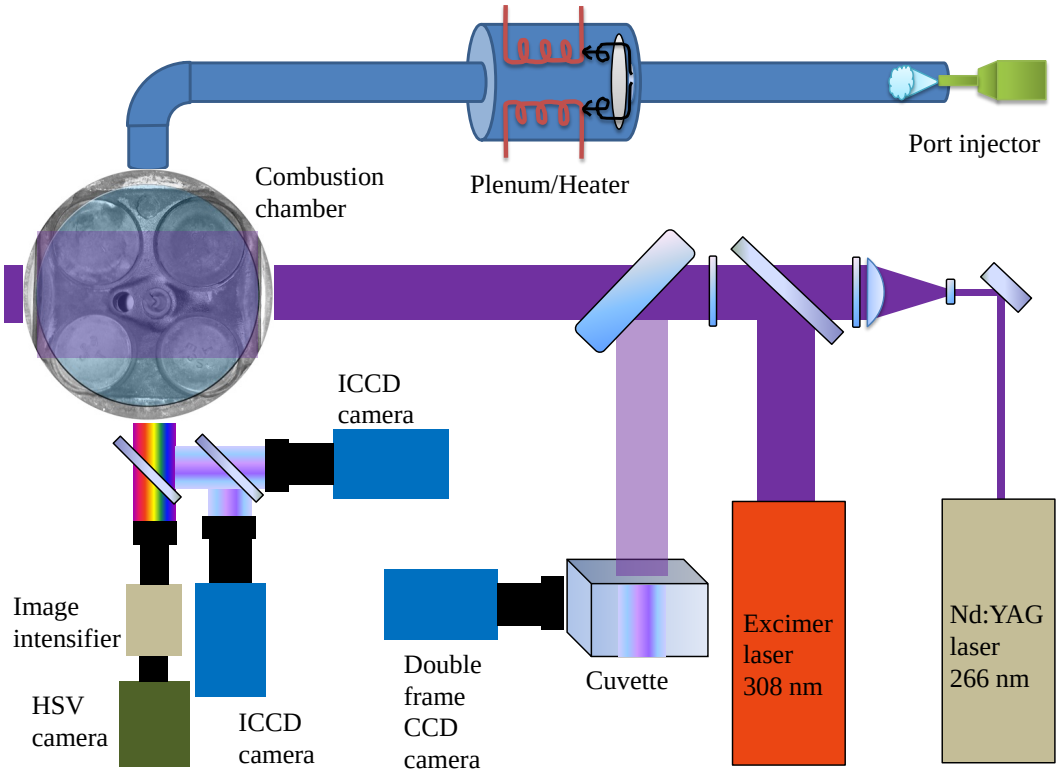

Figure 3.10 – Schematic of the optical setup and engine intake system used for in-cylinder temperature measurements.

Images of the in-cylinder laser-induced fluorescence light and light emissions from the following combustion were acquired through the piston window via the 45° mirror. A dichroic mirror was used to deflect the LIF signal, which was further split by a beamsplitter plate before entering the two carefully aligned Dynamight cameras, each gated to capture one of the LIF signals. The remaining light (most of the light emitted during combustion, including UV light) transmitted by the dichroic mirror was captured with the high speed video camera connected to the image intensifier.

After each measurement the fuel supply was turned off to let the engine cool under motored conditions until the next measurements could begin. During this time, images of background fluorescence (from windows and surfaces) were captured by keeping the lasers on but with no fuel or tracer supply. Further, a port injector was used to supply pure 3-pentanone in the intake before the plenum, and at the inlet of the plenum a plate was mounted to diverge the flow and improve mixing. The plenum also held the heaters for elevating the air temperature, which also further improved the mixing. This setup was considered to provide a homogeneous mixture in the cylinder and was used for light

collection efficiency (LCE) reference measurements. The port injector was also used for calibration measurements under motored conditions at different timings (CAD). Calibration temperatures for these measurements were obtained from GT-Power (1D engine simulation software). All measurements (except for calibration measurements) presented in this thesis were taken at 15 CAD bTDC since later measurements included fluorescence from other species than 3-pentanone.

Once the temperature is obtained it can be used to compensate the fluorescence signal so that the spatial fuel distribution can be accurately estimated, otherwise it will be overestimated in cold regions and underestimated in hot regions. More on how this and temperature calibration was performed can be found in paper VI and the steps for estimating the temperature based on the LIF measurements are presented in Appendix A.

Chapter 4

Results

In this chapter, selected results are presented to further explain the ringing phenomenon, and both how and why SCCI is an effective strategy for reducing it, even with fuels displaying single-stage ignition under the conditions studied. Effects of boosting the intake air to increase HCCI and SCCI loads are also discussed and finally some results of two-stroke operation are presented as an alternative strategy for extending the load.

4.1 Ringing phenomenon

The ringing phenomenon was studied in the optical engine under homogeneous operation (at 1500 rpm, 4.5 bar $IMEP_n$ and $\lambda = 1.2$ with iso-octane as fuel) using the HSV camera with image intensifier. Details of the procedures used to evaluate the data acquired from these measurements can be found in Paper IV and in Appendix B, here I will simply state that by applying frequency analysis to the high pass filtered (HPF) video sequences it was possible to extract the acoustic oscillation modes inside the combustion chamber that were induced by the rapid heat release. Illustrative results of such analysis, for a single cycle, are shown in Figure 4.1a and a schematic diagram of the modes is shown in Figure 4.1b. It was possible to identify four modes from the experiments and the cycle displayed has been chosen because it is one of the few cycles in which all four modes appeared simultaneously. However, as clearly apparent from this example, mode A1 clearly dominated, as was generally the case in all measurements but not often this strongly. This may be explained by the pent-roof windows forming two planar walls, one on the left and on the right of the combustion chamber, while in the orthogonal direction the walls where more wedge-formed (as can be seen in Figure 3.5).

In most experimental setups in-cylinder pressure oscillations can only be measured with the pressure transducer (if one is mounted). As a side issue to the main matter of ringing discussed in this section, it is interesting to compare

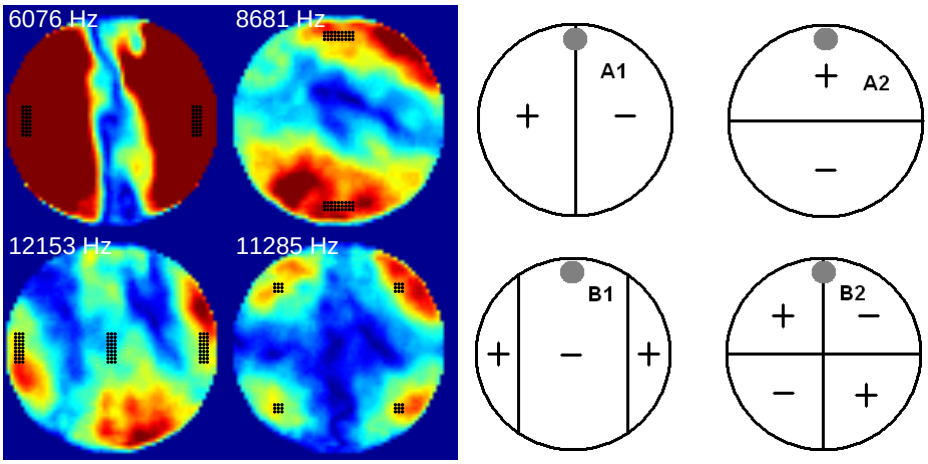

(a) Spatially resolved amplitudes at four different frequencies extracted from the HSV measurements. The amplitudes increase going from dark blue to dark red. Black dots indicate points where the amplitude was extracted from each mode.

(b) Corresponding schematic illustration. Lines indicate the nodes of constant pressure. Grey circles indicate the location of the pressure transducer.

Figure 4.1 – The four oscillation modes detected using the HSV camera in HCCI combustion.

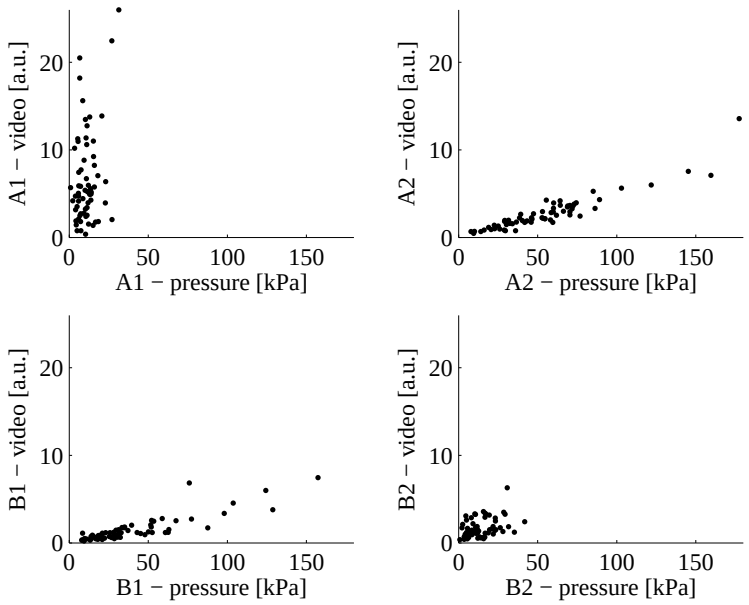

Figure 4.2 – Amplitudes captured by the HSV camera and the pressure transducer plotted against each other for 65 sequential cycles in each of the four modes.

the amplitudes of the different modes captured with the HSV camera to those captured with the pressure transducer and thus illustrate the importance of pressure transducer location, see Figure 4.2. Each amplitude from the HSV data are taken as the average from the zones (pixels) indicated in Figure 4.1a by black dots. These zones were chosen to minimize cross-talk between the different modes since some of them appear at almost the same frequency. The pressure transducer location is indicated in Figure 4.1b by the grey circles. Clearly, there is a correlation between the two different types of measurements for modes B1 and A2, but no correlation for modes A1 and B2. This is because the pressure transducer is located on the nodal lines of the A1 and B2 modes, where pressure is constant. In this engine, the most important mode (A1) was thus not detectable using the pressure transducer alone. Fortunately, this mode is probably not as dominant in the multi-cylinder engine (where the pressure transducer is located in the same place) since the walls are not as distinct as in the optical engine. In the single-cylinder metal engine, the pressure transducer is located at the position of one of the pent-roof glasses, and thus captures mode A1 more effectively.

It was possible to correlate the type and magnitude of acoustic modes with the location of zones with fast combustion (measured in terms of the maximum light intensity derivative, $\mathrm{LI}_{\mathrm{MaxDer}}$). Such correlations are displayed in Figure 4.3. The zone numbers correspond to the zones displayed in Figure

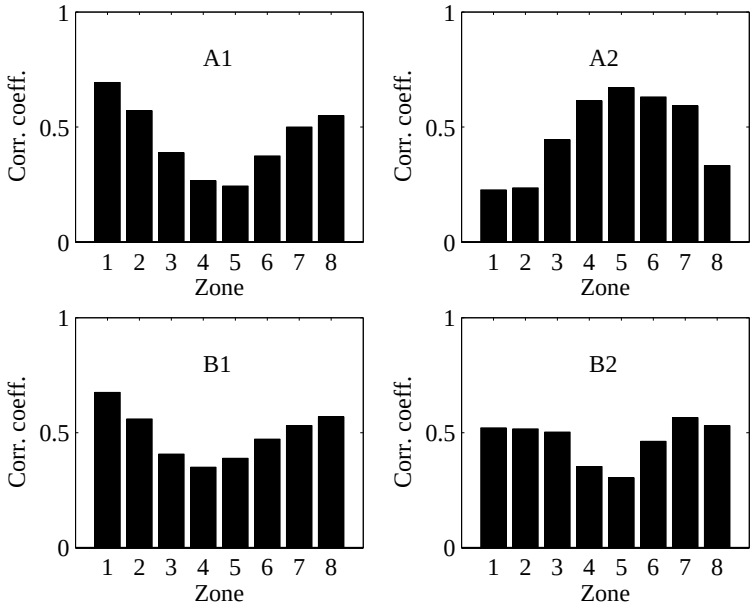

Figure 4.3 – Linear correlation coefficients between average values of the maximum light intensity derivative in each paired zone and amplitudes in the four different oscillation modes for 65 sequential cycles.

3.8. The correlation coefficient used in this thesis (Pearson's linear correlation coefficient) is a measure of the linearity between two variables. A perfect linear correlation (corr.=1) is unlikely here for two reasons. First, for small derivatives, meaning slow combustion, there will be no ringing at all and once ringing appears it may not increase linearly with the combustion intensity. The second reason can be illustrated by an example. Consider a case where high derivatives in both zones one and two give rise to high A1 amplitudes. Then, if one cycle has a high derivative in zone one and a low derivative in zone two, this would still produce a high amplitude in the acoustic mode A1, but it would also result in a lower correlation coefficient for zone two. Hence, Figure 4.3 should be interpreted by considering intermutual differences between the zones and their correlation coefficients. This said, it is now apparent that zones located to the left and right (near the pent-roof glasses) are mostly responsible for setting up oscillations in modes A1 and B1, while zones in the upper or lower part are mostly responsible for setting up oscillations in mode A2. These results are consistent with the hypothesis proposed by Yelvington and Green (2003) that ringing is caused by local parcels burning too rapidly. They also show that the location of these fast burning parcels influences the acoustic modes that form: one of two main findings from these investigations.

The second main finding concerned the location of the rapidly burning parcels. It was observed that mixtures igniting late generally burned rapidly,

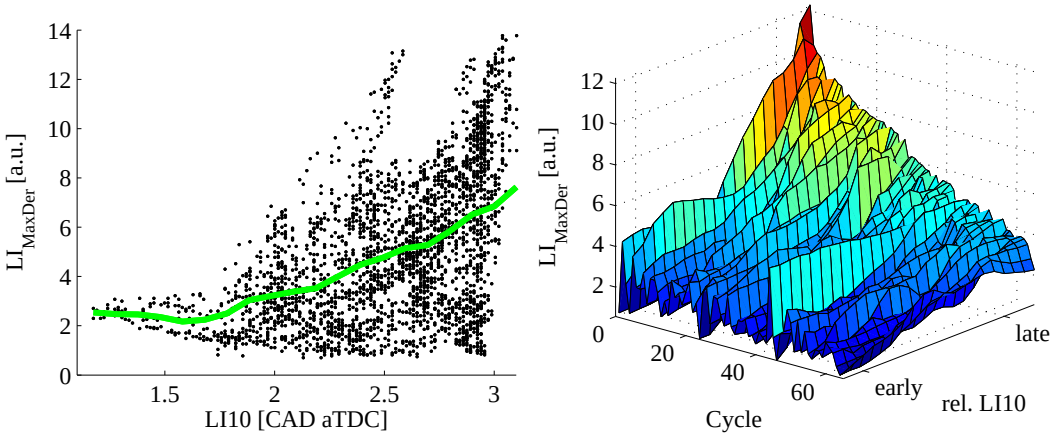

(a) Scatter points showing values for each pixel and curve showing average bahavior over each LI10 location.

(b) Average behaviour for 65 following cycles ordered in ascending derivative.

Figure 4.4 – Maximum light intensity derivative (LI_{MaxDer}) versus location of 10% light intensity (LI10) for the illustrative cycle.

while mixtures igniting early burned more slowly. To illustrate this, the maximum light intensity derivative is plotted against the timing of 10% light intensity (LI10) in Figure 4.4a for each pixel from one cycle. The green line shows the average intensity over each timing of LI10. Figure 4.4b shows this average curve, but for 65 following cycles ordered in maximum intensity for easier viewing. For motivation of LI10 as a measure of ignition timing, see Appendix B.

4.2 Stratified Charge Compression Ignition - SCCI

4.2.1 Effect on ringing

The single-cylinder metal engine (Setup 1) was used to investigate the potential of using charge stratification as a ringing inhibitor. Two injections were used, one in the intake stroke and one late in the compression stroke. In addition to testing the strategy with gasoline, it was also tested with the PRF mixed with 3-pentanone (50% N-heptane, 40% iso-octane and 10% 3-pentanone) that had been used in some early optical investigations and provided an excellent opportunity to compare fuels with single-stage ignition and two-stage ignition. Note that it is not correct to call this fuel mixture a PRF since it includes 3-pentanone but this notation is used here for simplicity. Two different end of

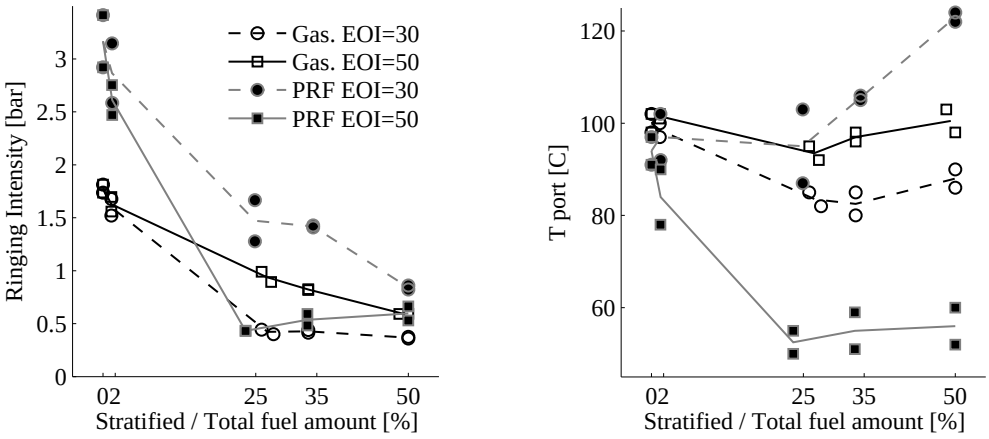

(a) Ringing intensity.

(b) Temperature at the intake port.

Figure 4.5 – Effect of variations in late injection timing and amount for gasoline (at 4 bar $IMEP_n$) and PRF with fuel tracer (50% N-heptane, 40% iso-octane & 10% 3-pentanone at 3.9 bar $IMEP_n$) at 1200 rpm and $\lambda \approx 1.4$.

injection (EOI) timings, with various proportions of fuel injected in the late injection were used in the tests, and the effects of these variations on ringing intensity are shown in Figure 4.5a. The intake air temperatures required to maintain constant combustion phasing (CA50=2 CAD aTDC) in these experiments are shown in Figure 4.5b. In tests with gasoline, ringing intensity declined linearly with the amount of the second injection when it was at 50 CAD bTDC. RI levels were only a third of the levels under homogenous conditions when 50% of the injection was late. When the second injection was at 30 CAD bTDC the reduction of RI was greater, but it levelled out with no additional benefit of injecting more than 25% late. In tests with PRF, the responses were different. Here, RI declined linearly with the amount of fuel injected in the second injection for EOI=30 CAD bTDC, with a third of the ringing levels when injecting 50% late compared to homogenous conditions. For injections at 50 CAD bTDC there was a huge reduction in ringing levels with only 25% fuel in the second injection, but increasing the amount of the late injection caused increases in ringing levels. The temperatures required for constant combustion phasing also substantially differed between the two fuels. For gasoline, only small changes in intake temperature were required, while for PRF, a reduction in intake temperature was required when the late injection was at 50 CAD bTDC, while an increase in temperature was required when the late injection was at 30 CAD bTDC.

The difference in responses when using the two fuels can be explained by examining heat release curves, which showed evidence of two-stage ignition

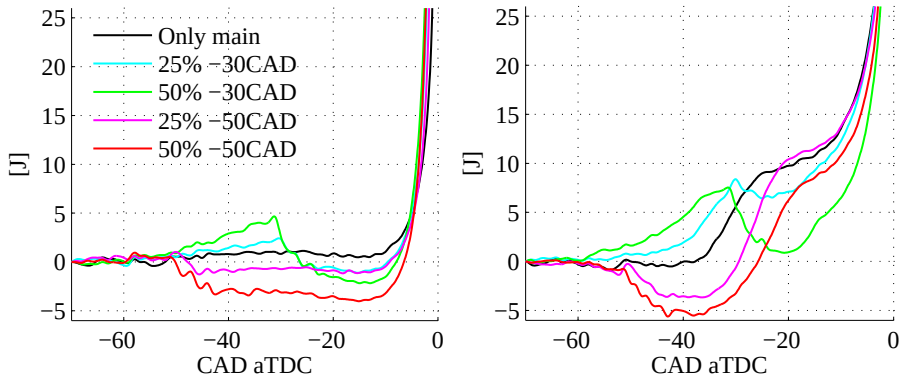

(a) Average cumulative heat release for gasoline.

(b) Average cumulative heat release for PRF.

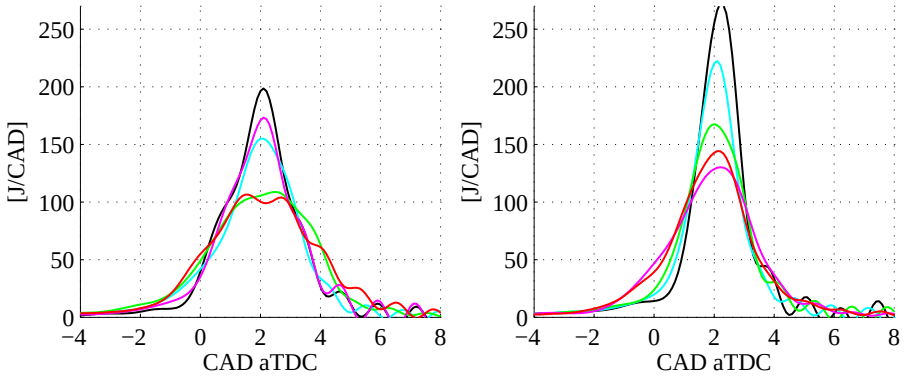

(c) Rate of heat release in single representative cycles for gasoline.

(d) Rate of heat release in single representative cycles for PRF.

Figure 4.6 – Heat release before main combustion (A & B) and during main combustion (C & D).

(or low temperature heat release) for PRF but not for gasoline. In Figure 4.6, gross heat release profiles are shown for 0%, 25% and 50% stratification at the two injection timings and for the two fuels. The average cumulative heat release profiles before the main combustion are displayed in Figure 4.6a for gasoline and in Figure 4.6b for PRF. Figure 4.6c shows the heat release rate during the main combustion for selected individual cycles with the same combustion phasing and with average behaviour in burn durations for gasoline and Figure 4.6d for PRF. Heat release calculations are described in Appendix C.

Since the low temperature heat release was relatively low in comparison to noise levels, it is easier to distinguish between the cases using average cumulative heat release traces. However, care must be taken when interpreting these plots. The γ values have been calculated for mixtures with all the fuel

injected. Before that, γ is underestimated, and the curve is shifted upwards, increasingly strongly as the proportion of fuel injected late increases. There is no evidence of low temperature heat release in the gasoline curves, which could explain the required reduction in intake temperature. However, the temperature drops caused by evaporation of the fuel are clearly visible. In contrast, the PRF curves display significant low temperature heat release. Let us take the homogeneous case where low temperature heat release appears after 40 CAD bTDC, as a reference. For the early injection cases, after the drop caused by fuel evaporation, the low temperature heat release seems to be larger than for the homogeneous case and, as explained by Dec and Sjöberg (2004) and Sjöberg and Dec (2006), this should be more concentrated in zones with more fuel and tends to advance the combustion phasing (indicated by the reduction in required intake temperature). Figure 4.6d also shows that the combustion is staged, with the main heat release starting earlier for these injection timings. However, injecting more fuel does not seem to cause any great changes, which might be due to increased charge cooling countering the effect of low temperature heat release. For the latest injection cases (EOI=30 CAD bTDC) low temperature heat release appeared to start before the second injection, earlier than in the homogeneous case, and after the injection there was no enhancement of low temperature heat release compared to that seen for the early injection. Too little time is probably available under these conditions for low temperature heat release in the fuel-rich (and cold) zones, and as can be seen in Figure 4.6d, the combustion event was less staged than when injection was 20 CAD earlier. At these late injections, the trends in ringing reduction and intake temperature requirements seem to be more similar to those for gasoline.

While there seems to be likely explanations for the mechanisms behind the ringing inhibiting effect of charge stratification for combustion with two-stage ignition (when injection is not too late), insufficient clues were found from these analyses to explain the mechanisms behind the effects for single-stage ignition. A hypothesis will be provided in Section 4.2.4, but additional results must be presented first.

4.2.2 Increasing naturally aspirated upper load limits

The potential for increasing load using SCCI was examined in experiments with the multi-cylinder engine, in which the timing of the late injection normally varied between 30 and 50 CAD bTDC (EOI), around 30% of the total fuel amount was injected in it, and two fuels were used: gasoline and E85. The resulting load limits and fuel saving relative to SSI combustion are shown in Figure 4.7. The blue curves are for lean operation, and starting at 1000 rpm it is notable that no significant load increase was obtained with SCCI, because generally the engine was not ringing-limited here, but instead air limited. For

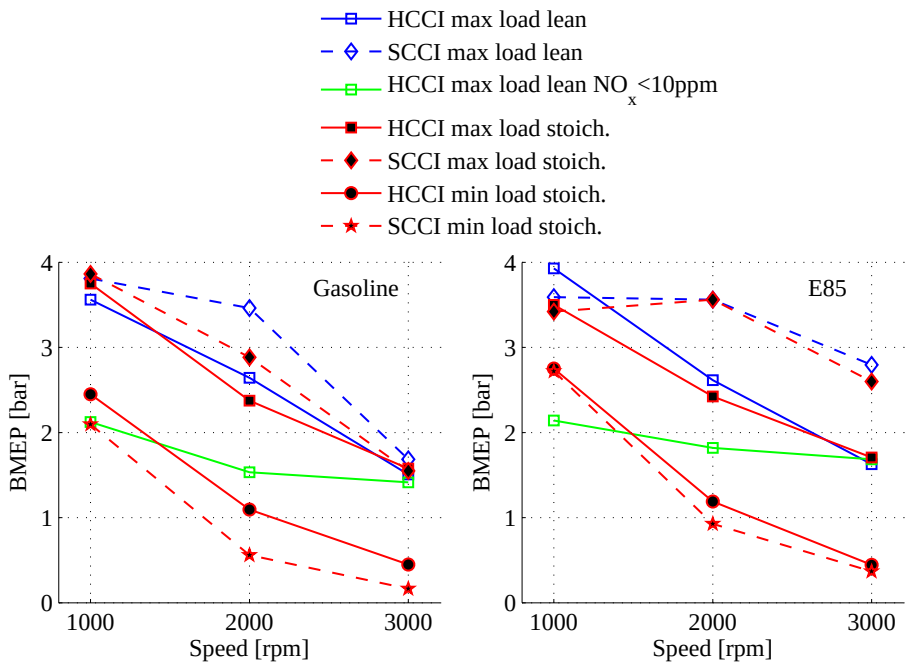

(a) Brake mean effective pressure (BMEP) using gasoline (left) and E85 (right).

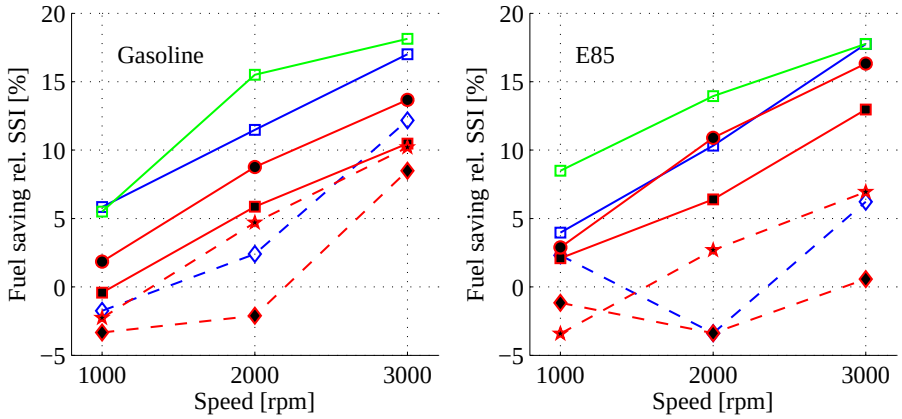

(b) Fuel saving relative to SSI operation, using gasoline (left) and E85 (right) at the load limits displayed in (a).

Figure 4.7 – SCCI and HCCI load limits in the multi-cylinder engine under naturally aspirated operation.

E85, comparisons are difficult since the engine was barely operable at 1000 rpm because generally E85 was more difficult to ignite requiring a much larger NVO. Whether this was a consecuence of the greater charge cooling of E85 or because E85 is harder to auto-ignite was not investigated since it was beyond the scope of the study. Even though E85 has a higher octane rating it must not mean that it is harder to auto-ignite in HCCI combustion as discussed by Kalghatgi and Head (2006). In order to obtain any data it was necessary to change the main injection to a pilot injection before the NVO. At 2000 rpm, on the other hand, the possible load increase was around 1 bar for both fuels, but soot was the limiting factor for gasoline and air the limiting factor for E85. At 3000 rpm, soot was even more limiting for gasoline, and only small load increases were possible since ringing could not be substantially reduced. On the other hand, for E85 which showed no soot problems because it is an oxygenated fuel (Cheng et al., 2002), the load could be increased by 1.1 bar until ringing limited any further increase.

At these upper load limits NO_X levels proved to be high (hundreds of ppm), even for HCCI. Without lean NO_X after-treatment these levels would be unacceptable, so a maximum load limit for lean HCCI with NO_X limited to 10 ppm was produced, indicated by the green curves in Figure 4.7a. With NO_X as an additional load limiter it is apparent that the maximum load was greatly restricted, except at 3000 rpm where ringing was still limiting. For this reason, an external EGR system was built and incorporated into the engine to allow stoichiometric operation. Maximum loads under stoichiometric HCCI and SCCI are also shown in Figure 4.7a. Generally, lower loads were achieved under stoichiometric conditions, in which the largest reduction was for SCCI with gasoline because of high soot levels. The results also showed that stoichiometric HCCI and SCCI could cover the range all the way down to lean NO_X limited HCCI, as shown in Figure 4.7a, except at 1000 rpm for E85.

The fuel saving observed under the test conditions, relative to SSI combustion, for each strategy and fuel at their respective load limits, are shown in Figure 4.7b. In general, fuel consumption reductions were larger at lower loads, because the efficiency of SI operation deteriorates rapidly at low loads. For lean operation at the maximum load limits, fuel consumption benefits were observed at all points except for SCCI at 1000 rpm with gasoline as fuel and at 2000 rpm with E85 as fuel, because at these two points the mixture was stoichiometric, resulting in poor combustion efficiency. With intended stoichiometric operation (and hence use of external EGR) at the high load limit the fuel consumption increased due to poor combustion efficiency and for SCCI it was often worse than in SSI combustion. However, it should be remembered that the goal was to maximize the load, and fuel consumption was not used as a parameter when deciding the settings. By compromising on maximum load, fuel consumption could probably be improved, as indicated by the stoichiomet-

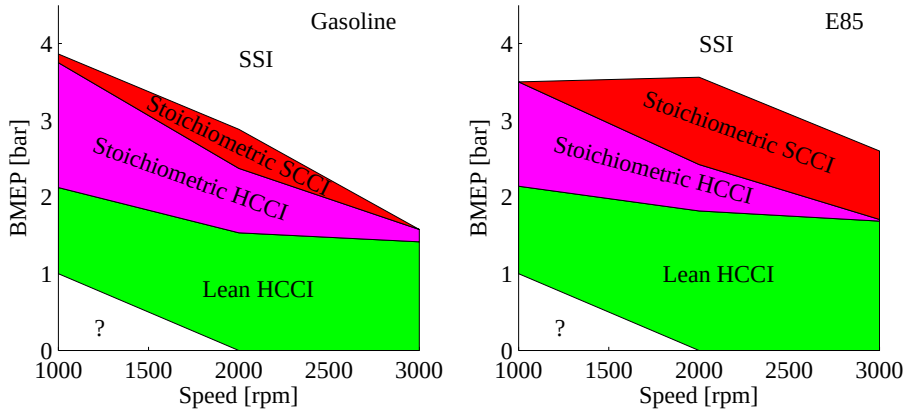

Figure 4.8 – Proposed operating strategy if no lean NO_X after-treatment is available for gasoline (left) and E85 (right).

ric low load limits, where HCCI still shows substantial (and SCCI moderate) fuel consumption reductions.

Based on the determined load limits and the objective of the project to extend the load of HCCI type combustion, preferably without extra lean NO_X after-treatment, a proposed operating strategy is illustrated in Figure 4.8. Lean HCCI, which is most beneficial in terms of fuel consumption, is used up to a load at which NO_X emissions exceed some defined limit (here 10 ppm). Above this limit external EGR is applied and the engine runs in stoichiometric HCCI to as high a load as possible until ringing becomes excessive. Here, the engine switches to stoichiometric SCCI, but the optimal range for this mode is uncertain, since at the maximum possible limit stoichiometric SCCI seldom provides fuel consumption benefits relative to standard SSI combustion. Once the engine has to switch to SSI combustion, the exhaust gases are already stoichiometric and a mode switch should not compromise the emission levels, since in all stoichiometric HCCI/SCCI cases examined in this study HC, CO, and NO_X were virtually fully converted in the three-way catalyst. The lower limit of lean HCCI was not examined, thus the minimum loads for the engine using this combustion strategy are uncertain. If lean NO_X after-treatment was used the engine could probably switch from lean HCCI to lean SCCI, which would apparently provide better fuel consumption reductions, but with fuel consumption punishments due to the after-treatment (rich operation using lean NO_X traps or urea using SCR catalysts).

Note that all experiments presented here were run without the use of a spark. However, it was shown that a spark can increase the load substantially. More on this and the effects of different levels of external EGR can be found in Paper III.

4.2.3 Boosting for additional load increase

The next step for increasing the load is to boost the intake air. This was investigated in the single-cylinder metal engine at 2000 rpm using gasoline as fuel. The purpose was to compare different strategies under boosted intake air and whether increased air pressure should be realized using a mechanically driven compressor or a turbocharger was beyond the scope of this investigation, thus a fixed back-pressure (of 105 kPa) was used for simplicity. In section 4.3 an estimation of the load and fuel consumption penalty from using a compressor is provided but here, no costs for boosting is taken into account.

Results of three different boost sweeps are displayed in Figure 4.9a for HCCI and 4.9b for SCCI. The first type of boost sweep was with a constant amount of injected fuel and, as can be seen, for HCCI the load increased slightly with increases in intake pressure, even though the amounts of fuel injected were the same. This was mainly a result of reductions in ringing intensity, which enabled closer to optimal combustion phasing and lower cooling losses due to reduced in-cylinder temperatures. However, the positive effects were partly offset by a reduction in combustion efficiency caused by the low temperatures. The low temperatures also caused NO_X levels to drop rapidly, and with intake pressures higher than 120 kPa they were below 10 ppm. For SCCI, the load increased more than for HCCI due to a smaller reduction in combustion efficiency. However, as the intake pressure increased, ringing also increased (contrary to HCCI) and at 140 kPa intake pressure ringing levels were too high. The NO_X level was not reduced as in HCCI but remained at a constant level owing to zones of higher fuel concentrations and higher temperatures.

The second and third types of boost sweep were under maximum load for lean and stoichiometric operation. When compensating for the higher intake pressure with more fuel to maximise load at all times, the load increased more than linearly for HCCI, with a lower increase under stoichiometric conditions. The fuel saving relative to SSI combustion was more than twice as high under lean conditions than under stoichiometric conditions due to better combustion efficiency, and as NO_X emissions dropped below 10 ppm above 140 kPa intake pressure it would be pointless to utilize stoichiometric operation above this pressure. At the highest intake pressure, the load was increased by 2.7 bar to 7.4 bar $IMEP_n$ for lean HCCI, which can be compared to Cairns and Blaxill (2005a) who reached 6 bar BMEP at the same speed and intake pressure.

Stoichiometric SCCI also increased linearly with increases in the intake pressure, and provided markedly higher loads than stoichiometric HCCI, but only slightly higher loads than lean HCCI. However there were no fuel consumption benefits relative to SSI combustion because of low combustion efficiencies ($\approx$93%). For lean SCCI at maximum load, problems with ringing once again appeared with boosting, and increased with increasing boost pressures, thus

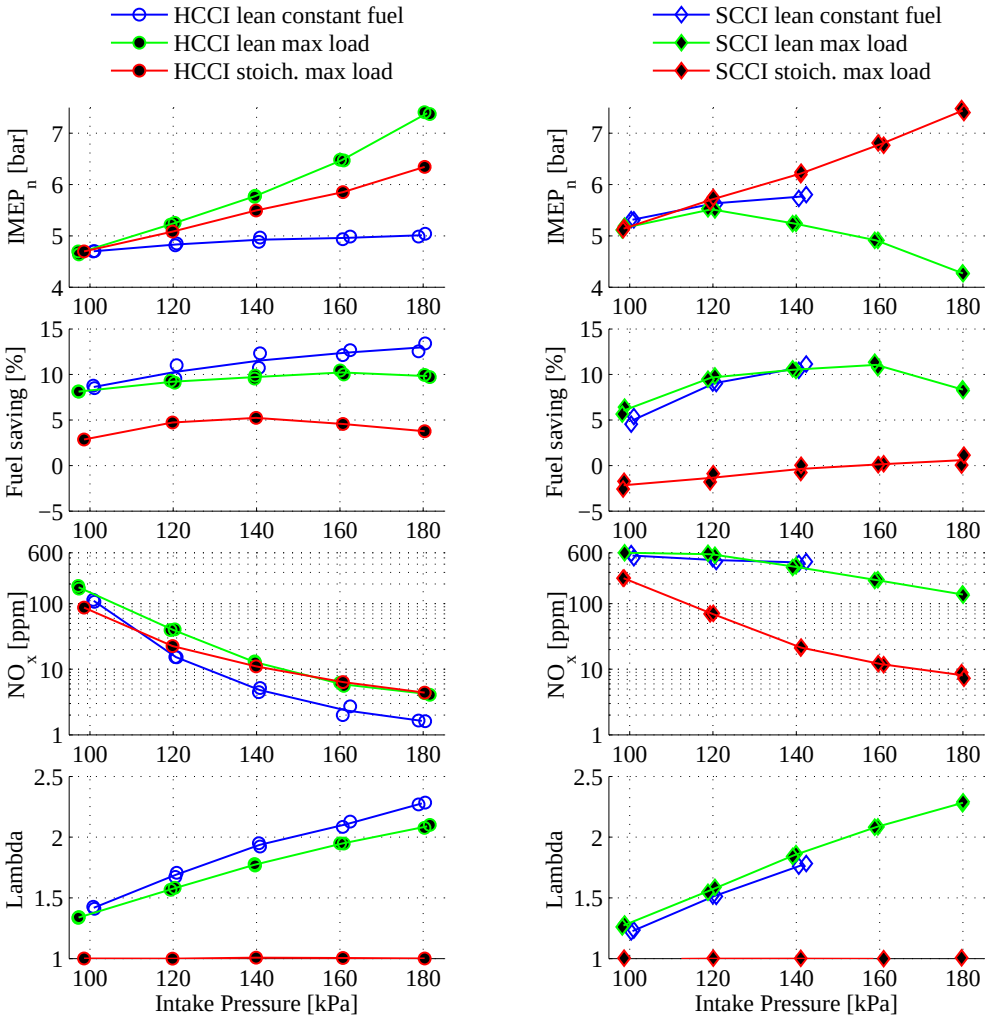

(a) HCCI **(b)** SCCI

Figure 4.9 – Results of boost sweeps at 2000 rpm under constant fuel amount, lean maximum load and stoichiometric maximum load, showing $IMEP_n$, fuel saving over SSI operation, NO_X levels and λ.

reducing the maximum loads at high intake pressures. The increased ringing associated with charge stratification is consistent with findings by Yang et al. (2011), and seems to occur when λ is increased beyond approximately 1.5.

4.2.4 Why SCCI reduces ringing under single-stage ignition conditions

To help elucidate why charge stratification using a late injection is effective for reducing ringing under near-stoichiometric conditions, in-cylinder fuel and temperature distributions were evaluated using the two-wavelength planar laser-induced fluorescence technique and correlated to the succeeding combustion captured with the HSV camera. Six different cases were compared at 1500 rpm, 4 bar $IMEP_n$, $\lambda = 1.2$ and CA50 = 8 CAD aTDC in the optical engine with varying timing and amount of the late injection, as described in Table 4.1. The fuel consisted of 85% iso-octane and 15% 3-pentanone.

Relative fuel concentrations (RFC) estimated from measurements with both 266 (RFC_{266}) and 308 nm (RFC_{308}) excitation, temperature compensated RFC ($RFC_{T.C.}$), temperatures, LI10 values and the maximum light intensity derivatives obtained for one cycle in each of the six cases are shown in Figure 4.10. RFC refers here to the fluorescence signal divided by the mean, hence RFC=1 corresponds to approximately $\lambda = 1.2$ or $\theta = 0.83$ (depending on whether the volume measured represented the entire combustion chamber). Going from case A to D - from injection in the intake stroke, to a split injection with later second injection - richer regions became richer and leaner regions leaner, clearly illustrating that a more fuel-stratified mixture was created. Comparing case B with case E and case C with case F, it is apparent that using a larger second injection also resulted in a more stratified charge. In cases C to F richer regions can be easily seen to be colder, perhaps most clearly in case D, were the measurement was closest to the injection. The timing of ignition, once again represented by LI10, seems to spread more in stratified cases than

Table 4.1 – Timings and amounts of fuel injected in late injections in the six test cases.

Case	EOI [CAD bTDC]	Amount [%]
A	homogeneous	
B	50	≈30
C	40	≈30
D	30	≈30
E	50	≈50
F	40	≈50

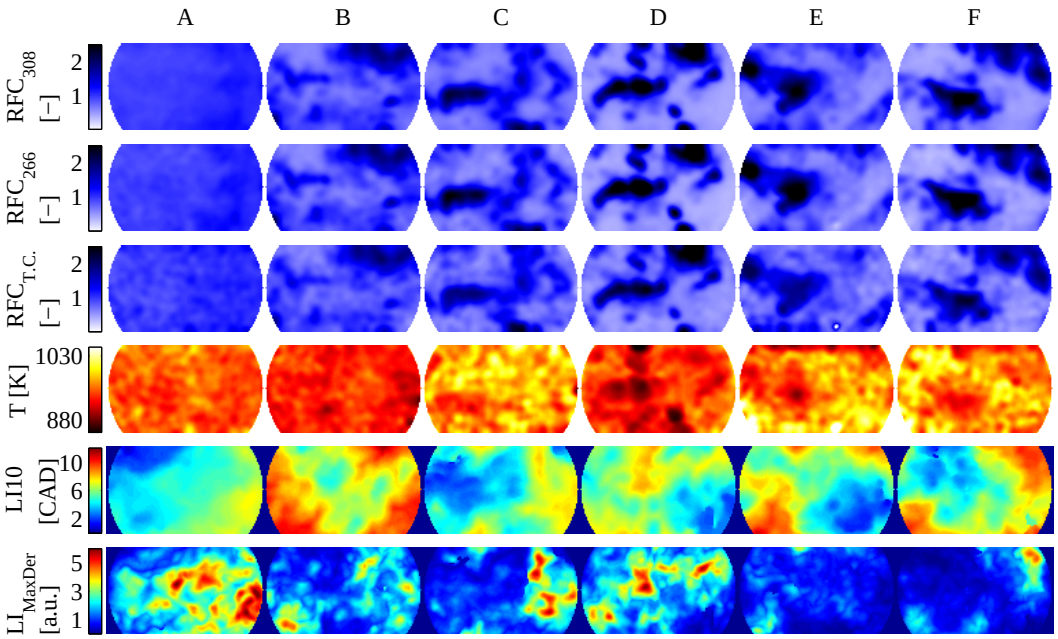

Figure 4.10 – Rows (top to bottom): RFC values from 308 nm and 266 nm excitation, temperature compensated RFC values, temperatures, LI10 values and maximum light intensity derivatives, in illustrative cycles for the six test cases (A-F, columns). RFC and temperature are measured 15 CAD bTDC.

in the homogeneous case. The maximum light intensity derivative seems to be higher in later burning regions, as also reported in Section 4.1. However, it was lower in the stratified cases than in the homogeneous case.

To better differentiate between cases and spatially correlate LI_{MaxDer} and LI10 values with temperature and fuel concentrations more objectively, it is important to use statistical methods, rather than simply trying to compare the images visually, which can be highly subjective. In paper VI this is done for all three RFC values and the differences are discussed but here only data for $RFC_{T.C.}$ is presented.

In Figure 4.11, spatial standard deviations (averaged over 10 cycles) of $RFC_{T.C.}$, temperature and LI10 within each measurement are plotted for each of the six test cases (with standard deviations around the means indicated by error bars). The first case (P) display the values in motored conditions, with 3-pentanone injected far upstream of the engine, which is considered to create a homogeneous mixture. Thus, the values indicate the levels of noise for RFC and temperature (but not perfectly because the signals were generally stronger under motored conditions, which reduced the effect of background noise). Also, for temperature there is an effect of natural stratification as discussed in paper VI. For the other cases it is apparent that using a second injection, delaying

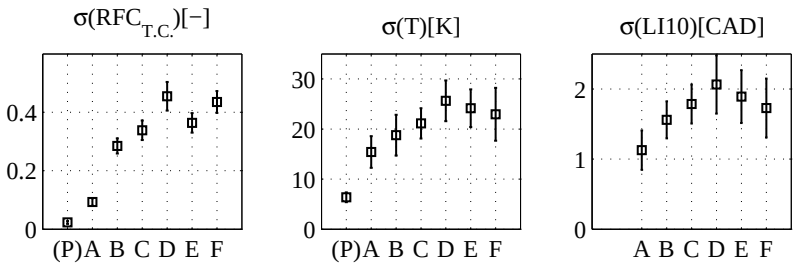

Figure 4.11 – Spatial distribution of $RFC_{T.C.}$, temperature and ignition timing within measurements for each of the six cases and motored operation with port injection of 3-pentanone (P), represented by squares as averages from 10 measurements (60 for P) and error bars indicating the spread between cycles.

the second injection and use of a larger second injection result in greater fuel stratification. The trends are similar for the temperature stratification, but with greater deviations between measurements. LI10 trends clearly follow the stratification level; more spatially distributed ignition being associated with greater stratification levels.

To spatially correlate different parameters with one another (pixel by pixel), Pearson's linear correlation coefficients were used once again. The left plot in Figure 4.12 show correlations between temperature and $RFC_{T.C.}$ which are negative in stratified cases, showing that relatively fuel-rich regions are colder than relatively lean regions in the considered cases, and that this is not solely due to fluorescence signals being weaker in hotter regions. Applying temperature compensation to the RFC values shifted the correlation from negative to strongly positive for the homogeneous cases (see paper VI), due to effects of structures on the temperature distribution and small scale noise being superimposed (pixel by pixel) on the RFC. However, the relative effect of this declines when the fuel stratification increases, hence temperature-$RFC_{T.C.}$ correlations are negative for stratified cases and increasing the delay of the later injection increases the strength of the negative correlation.

The plots to the right in Figure 4.12 display correlations between timing of ignition captured with the HSV camera and $RFC_{T.C.}$ (middle) and temperature (right). Generally, greater fuel concentrations seem to cause later ignition, and higher temperatures earlier ignition. The correlation between LI10 and $RFC_{T.C.}$ is higher in the homogeneous case (A) than in the stratified cases. This is attributed partly to weaker cylinder gas motion, due to the absence of a late injection, resulting in smaller changes in the fuel distribution between the LIF and chemiluminescence measurements. In addition, variations in fuel concentration are smoother, thus gas motions have less effect on the correlations in case A. In the stratified cases ignition occurs earlier in relatively lean, hot regions than in richer, colder regions, especially in cases B-D. In the other

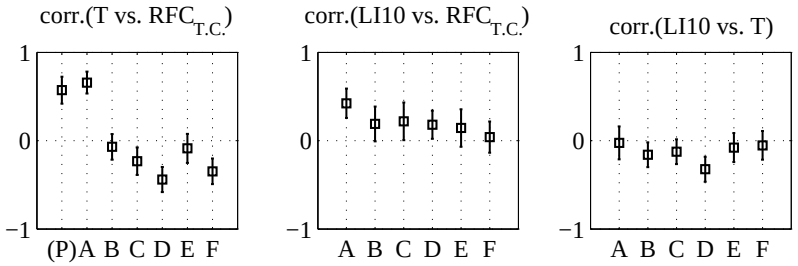

Figure 4.12 – Spatial correlations between temperature and $RFC_{T.C.}$, ignition timing and $RFC_{T.C.}$ and between LI10 and temperature presented as squares for the average from 10 measurements (60 for P) with error bars indicating the spread between cycles.

two cases (E and F) the correlations are weaker, even though 50% of the fuel is injected late in these cases, possibly because of the stronger motions in the time between LIF and chemiluminescence measurements created by the large late injection.

Generally, the correlations are rather weak, partly because of the difference in time between LIF and chemiluminescence measurements (restricted by fluorescence from other species than 3-pentanone at later LIF measurements) and partly because of the difference in volumes captured in the images (the LIF signals originate from a thin sheet, while chemiluminescence signals originate from a bigger volume). A further factor is that relationships between these parameters did not seem to be linear (see paper VI), and were not expected to be linear. However, it was more clear that early igniting zones had relatively low fuel concentrations and relatively high temperatures. This pattern is statistically evaluated in Figure 4.13. The upper left panel show the average values of $RFC_{T.C.}$ for the 20% of pixels showing the earliest ignition. Again, the average values of ten measurements are displayed, with errorbars indicating standard deviations. As can be seen, mixtures in zones (pixels) displaying early ignition are leaner than average. The lower left plot show the probabilities of this statement being true (determined using t-tests), and as can be seen they are high except for the last case, where increased gas motion changes the spatial distributions between LIF measurements and combustion most strongly.

The second top panel shows the average relative temperatures ($T\text{-}T_{mean}$) of the 20% of zones (pixels) showing the earliest ignition. While for all cases the values are shifted to higher temperatures, again indicating that pixels showing early ignition are hotter than average, the errorbars more often extend below zero, indicating that the significance of this observation is weaker (but still moderate) as also seen in the panel below.

Correspondingly, in the 20% of zones (pixels) showing the latest ignition the fuel concentration (third column in Figure 4.13) is richer than the average

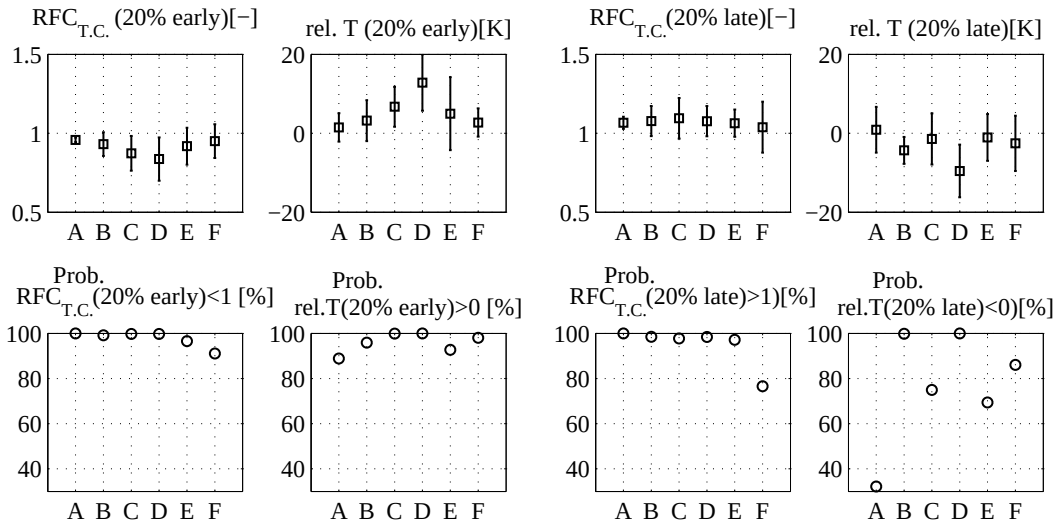

Figure 4.13 – Relative fuel concentration and temperature of the 20% of pixels showing earliest ignition and latest ignition together with significanse levels of observed trends.

and the temperature (fourth column) is lower than the average, although the trends are weaker and less significant for two reasons: the time between LIF and chemiluminescence measurements is longer for the late igniting zones, and the late igniting zones are displaced by previous combustion in the other zones. However, almost all of the statistics indicate that ignition does indeed occur first in relatively lean, hot regions and later in richer, colder regions.

As was shown in section 4.1 for homogeneous combustion, zones burning late also burned more rapidly and were interpreted as the cause of ringing. The left panel in Figure 4.14, in which the spatial correlation between the maximum light intensity derivative and ignition timing are plotted for each of

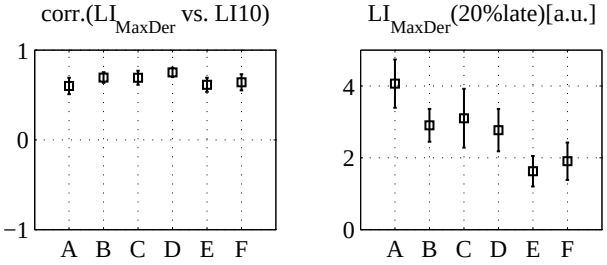

Figure 4.14 – Spatial correlations between combustion intensity (LI_{MaxDer}) and ignition timing (left panel) and combustion intensity in the 20% of latest burning pixels (right panel) presented as squares for the average from 10 measurements with error bars indicating the spread between cycles.

the cases, shows that this also holds for stratified combustion. However, the right panel shows that the amplitude of the derivative for the 20% of latest burning pixels was reduced in stratified cases, and most strongly when 50% of the fuel is injected late, in accordance with its effects on ringing intensities, shown in Figure 4.5a.

It is now possible to formulate a plausible explanation for the effect of charge stratification on ringing intensity in combustion with single-stage ignition, based on the following observations:

- Introducing a second injection in the compression stroke and both a larger amount and later timing of the second injection enhance the reduction in ringing levels.
- If the global air/fuel ratio is much leaner than stoichiometric ($\lambda >\approx 1.5$) charge stratification increases ringing instead of reducing it.
- Combustion efficiency often deteriorates under stratified conditions.
- Zones burning late normally burn rapidly and were seen as the cause of ringing.
- Ignition appears to occur first in leaner and hotter zones and late in rich and colder zones.
- Combustion speed is reduced in the late burning zones when stratification is applied.

Thus, when applying charge stratification in mixtures that are moderately globally lean ($1 \leq \lambda <\approx 1.5$), ignition occurs first in lean and hot zones. The late burning zones, which normally burn rapidly and cause ringing burn more slowly with charge stratification. This only works when these zones are rich (as also found by Dongbo et al. (2009)) so that combustion speed is reduced because of lack of oxygen and the extra fuel acting as a diluent in a similar way as air acts as a diluent on the lean side of stoichiometric but with higher specific heat capacity absorbing more heat from the reactions. Although no optical measurements were performed on very globally lean mixtures ($\lambda >\approx 1.5$) a possible explanation for the increased ringing in such cases is that while the ignition sequence is the same, the late burning regions are not rich, instead they are closer to stoichiometric with possibilities of burning very rapidly with high heat release.

The mechanisms underlying the effects of charge stratification when using fuels displaying single-stage ignition and two-stage ignition thus seem to be completely different, as richer zones burn earlier for two-stage ignition (Dec and Sjöberg, 2004; Sjöberg and Dec, 2006) the ringing reduction in those cases might be due to less fuel being present in later burning zones.

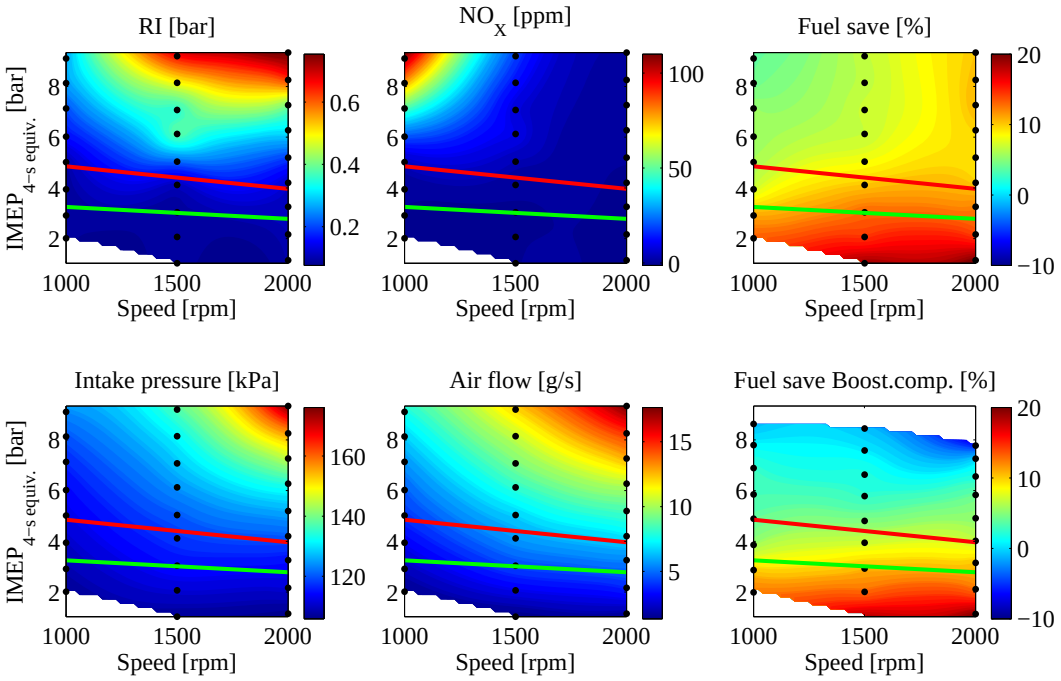

Figure 4.15 – Operating range investigated in two-stroke operation using constant combustion phasing and fixed valve profiles. The red line indicates the maximum load for stoichiometric four-stroke SCCI operation and the green line shows that for lean four-stroke HCCI operation with NO_X restriction. The load is shown as the four-stroke equivalent. In the lower right panel, the loads and fuel saving have been penalised to account for the work required by a compressor.

4.3 Two-stroke operation

Charge stratification proved to be an effective tool for reducing ringing and extending the high load limit. However, because of the poor combustion efficiency, it does not seem to provide great fuel consumption reductions. This section describes some preliminary experiments on a completely different way of extending the load, namely two-stroke operation. Brief tests were performed to find a set of suitable valve profiles and timings (see paper V) which were then used in speed/load sweeps. While the load was determined by the amount of fuel injected, the boost pressure was adjusted to maintain a constant combustion phasing (CA50=2 CAD aTDC) under atmospheric back pressure. As such, no optimisation for two-stroke operation was performed on individual points with regards to any parameter. Figure 4.15 shows the results from these speed/load sweeps and note that IMEP is presented as four-stroke equivalent values for comparison ($IMEP_{4\text{-s equiv.}} = 2 \times IMEP_{2\text{-s}}$). The black dots in each plot show the actual points tested; it is clear that the engine could

be operated in two-stroke HCCI mode from 9 bar $IMEP_{4\text{-s equiv.}}$ to idle (1 bar $IMEP_{4\text{-s equiv.}}$) at all speeds except 1000 rpm, where 2 bar was the lower limit. The green and red lines in the plots show the maximum load (in $IMEP_n$) from the multi-cylinder engine for NA four-stroke lean HCCI with a NO_X limit of 10 ppm and stoichiometric SCCI, respectively.

Ringing was not a problem for two-stroke HCCI over the entire range tested, and it should be noted that at loads corresponding to the SCCI load limit, the ringing levels were negligible under two-stroke operation. NO_X levels also proved to be very low over most of the operating range except at low speeds and high loads. Although the relevant data is not provided here, the combustion stability and soot emissions were both within the limits stipulated in the project. As such, all of the load limiters used in this work were satisfied over this large operating range (except NO_X at low speeds and high loads) even though no particular effort was made to ensure that this happened.

The main drawback encountered with two-stroke operation was the large amount of air required to push out the residuals. However, this engine was in no way designed for two-stroke operation and had significant short-circuiting (air moving directly from the intake to the exhaust) since it was designed for positive tumble motion. This is shown by the high intake air pressures and air flow in Figure 4.15. If boosting costs are not taken into account, the fuel saving over SSI combustion is high across the entire speed/load range. In order to get a feeling for the penalty incurred by using a mechanical compressor, the loads in the final plot of Figure 4.15 were adjusted to reflect the work required by a compressor with an efficiency of 70% (throughout). The fuel savings relative to SSI after imposing this penalty were then recalculated. Even though high boost pressures were required, the achieved loads remained considerably higher than those that were possible with NA four-stroke operation. Moreover, the fuel savings remained respectable at loads compatible with four-stroke NO_X-limited HCCI ($\approx$10%) and at four-stroke stoichiometric SCCI ($\approx$7%). However, the fuel savings are smaller above the SCCI limit; at the highest speeds and loads tested, the fuel economy becomes worse than that for SSI.

To compare two-stroke operation to boosted four-stroke operation, the boost sweep curve for lean four-stroke HCCI (from Figure 4.9a) is replotted in Figure 4.16 with the addition of two-stroke values at 2000 rpm (but with $IMEP_{4\text{-s equiv.}}$ on the x-axis). Values are provided with and without boosting penalties (from a mechanically driven compressor). It could be possible to achieve four-stroke operation with a turbocharger but for comparative purposes, a penalty was incorporated also for this mode. As can be seen, at intake pressures above 130 kPa, two-stroke operation provides higher loads than four-stroke operation but the boosting penalty reduce the maximum loads greatly at the highest boost pressures since the intake air pressures and mass flows increase. When comparing fuel consumption benefits over SSI combustion, we see that when

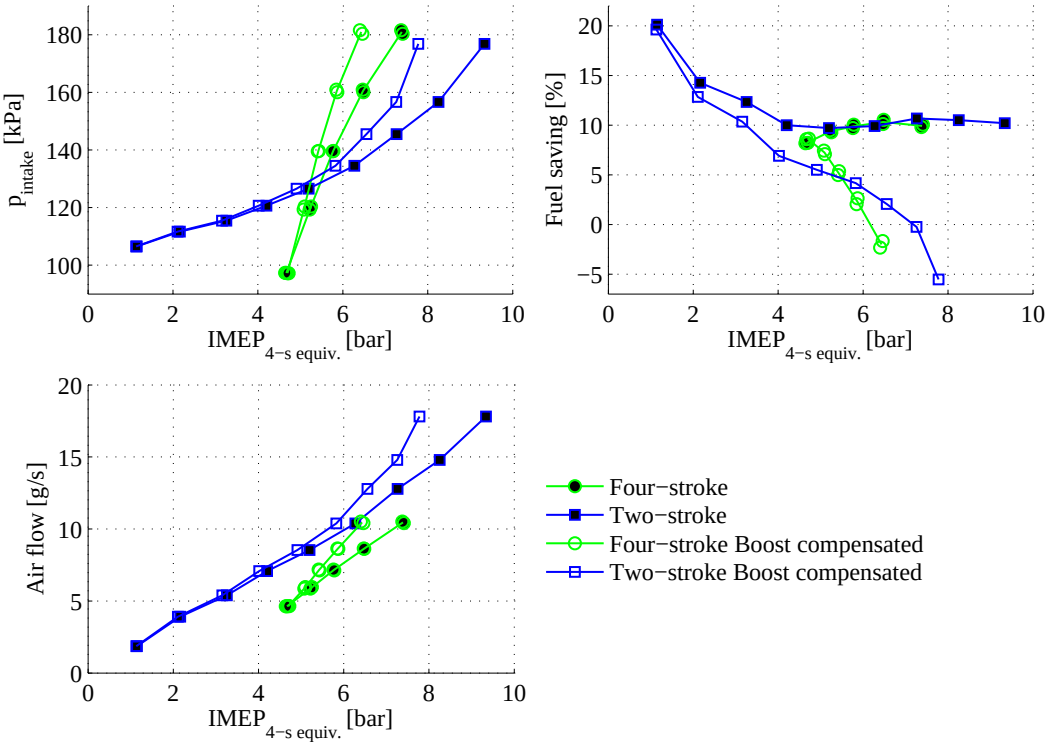

Figure 4.16 – Load/boost sweeps for two-stroke HCCI operation compared to four-stroke lean HCCI at 2000 rpm with and without boosting penalties. Loads are presented as four-stroke equivalent values.

both strategies are un-compensated, the fuel saving is 10% at the higher loads. However, with the penalties included, the fuel savings are greatly reduced. If the system was optimised for two-stroke operation, the fuel savings would probably end up somewhere in between the compensated and un-compensated values. However, it is likely that this would also increase the amount of ringing and NO_X emissions because the dilution level would be reduced but they should never reach four-stroke values since the load in each cycle is still much lower for the same power output.

Even though the system and the points tested were not optimized for two-stroke operation, the results suggest that this might be an alternative and better way to increase the upper load limit compared to using four-stroke operation with charge stratification, stoichiometric operation, boosting or some combination of those methods where operation are under load-limiting conditions. However, implementing two-stroke possibilities require substantial modifications of the engine.

Chapter 5

Discussion and conclusions

In accordance with the objectives of the project this thesis is based upon, the main focus was on possible strategies to overcome in-cylinder pressure oscillations (ringing) in order to extend the high load limit of HCCI combustion, preferably without using additional engine components. Using the direct injector to create a stratified charge was seen as one possibility. However, available literature gave conflicting indications of the utility of this strategy, reporting both positive and negative effects. Great potential has been reported for operation with fuels displaying two-stage ignition (see for example Kumano and Iida 2004; Sjöberg and Dec 2006; Berntsson and Denbratt 2007b) while adverse effects have been reported when the fuel display single-stage ignition (see for example Sjöberg et al. 2002; Marriott and Reitz 2002; Yang et al. 2011). Since the project dealt with gasoline engines intended to use SI combustion at high loads, the effects of charge stratification were investigated mainly with fuels displaying single-stage ignition under the conditions studied such as gasoline, E85 or pure iso-octane.

Results of the experiments summarised in the thesis, and appended papers, showed that the stratification strategy can indeed work, even under single-stage ignition conditions. However, the global air/fuel ratio must not be excessively lean, as was the case in most previously reported experiments. The fuel injected late in the compression stroke creates fuel-rich zones that are colder than the lean zones. Ignition was found to occur early in the lean zones and late in the rich zones. Late burning zones were also found to burn more rapidly than early igniting zones (in both homogeneous and stratified operation) and were identified as the main cause of acoustic oscillations. However, since the late-burning zones are rich when using charge stratification they burn more slowly, thus reducing the ringing intensity. A possible explanation for the increased ringing levels when using very lean mixtures is that the late burning zones are closer to stoichiometric, and thus have the potential to burn rapidly, with a concentrated high energy release (but this last hypothesis was not ver-

ified experimentally). Previous studies have attributed the ringing reduction of charge stratification for fuels displaying two-stage ignition to staged combustion, with longer combustion durations where ignition occurs first in rich zones because of greater low temperature heat release in those zones. This is then a completely different scenario, in which the late burning zones are leaner (rather than richer, as observed under the conditions applied here) than the global conditions. To further investigate these phenomenons, detailed chemical kinetic simulations should be performed.

It is interesting to note, based on explanations for knock and ringing, that both of them seem related in that the cause of the pressure fluctuations is a local volume that is auto-ignited with too rapid combustion. The difference lies in the preceding combustion, where in SI combustion there is flame propagation and in HCCI combustion there is auto-ignition.

Charge stratification was shown to provide the potential to extend the high load limit by up to around 1 bar BMEP, but since this was with near stoichiometric charges it yielded lower fuel economy improvements than pure HCCI operation. However, the results presented in this thesis are mostly from efforts to push the load as high as possible. In early investigations (described in Paper II, but not in Chapter 4) the fuel economy was virtually the same for HCCI and SCCI at the same load. However, this was under lean conditions and can only be applied if lean NO_X after-treatment is used, since charge stratification consistently increased NO_X emissions to unacceptable levels. Otherwise, EGR must be utilized to maintain global air/fuel ratios at stoichiometric conditions, thus allowing the three-way catalyst to reduce NO_X. Doing this has a direct negative effect on the fuel economy improvements. Thus, the results imply that in practice charge stratification cannot be used without additional engine features; either a lean NO_X after-treatment device or an EGR system is required to deal with the extra NO_X. Nevertheless, even if fuel economy benefits relative to SI combustion may seem disappointing at the high load limit, the ability to delay mode-shifts is highly welcome.

To further investigate the potential utility of the SCCI strategy, more attention should be paid to the region between the high load limits for SCCI and HCCI under lean and stoichiometric conditions. Further, the impact of gas motion on SCCI combustion should be investigated. Increasing the gas motion should help to improve mixing during late combustion, which could increase the combustion efficiency by bringing oxygen and fuel together more effectively to oxidise the last remaining fuel. However, this would probably also result in a need for later injections to maintain the stratification level at ignition and it would also increase the heat losses.

If boosting is applied, the scope for SCCI is reduced since SCCI would have to be maintained at stoichiometric conditions to make it effective and to cope with the increased NO_X emissions associated with the strategy, while lean

HCCI can reach almost the same loads with greatly reduced NO_X emissions. To extend the load while maintaining fuel economy improvements, lean HCCI with boosted air intake thus seems to be a better alternative. However, this also requires additional equipment; either a turbocharger (which would require careful matching to the low flow-rates in HCCI operation and thus could not be used for SI operation), or a compressor (which would require either electrical energy or mechanical energy, both of which have to be taken from the engine, thus reducing the gains in fuel consumption). An alternative may be to use a combination of a turbocharger and compressor.

A more fundamental option to increase the load is to implement the possibility of operating the engine in two-stroke HCCI mode. For an engine that is also capable of operating in four-stroke mode, this would require a valve train that can shift between the two modes. To operate such a two-stroke engine, the intake pressure would have to exceed the exhaust pressure. A turbocharger system capable of delivering a higher intake pressure than exhaust pressure over a large operating range is difficult to design. Therefore, a compressor solution might be better, or a combination of the two. The penalty of using a compressor was briefly investigated and although substantial power was required by the compressor, due to the high flow-rates and pressures, there were still significant gains in fuel economy at loads corresponding to the high load limits of four-stroke NA HCCI/SCCI operation. For better efficiency, the combustion system (including the combustion chamber, intake and exhaust ports) would have to be re-designed to improve scavenging in two-stroke operation in order to remove more residuals with lower intake pressures, possibly by using reversed tumble. Further, if an engine is modified for two-stroke HCCI operation it could also be made capable of operating in two-stroke SI mode. The engine could then be downsized, relative to four-stroke counterparts, which would reduce friction and allow weight reductions, further reducing fuel consumption and CO_2 emissions.

It is impossible to tell what the transport sector will look like in the far future, but a variety of technologies and fuels will probably co-exist. Those chosen are likely to depend on the geographic location and available natural resources. In cities, where journeys are usually short, electrification seems promising, while for longer journeys the internal combustion engine is still an attractive solution, and if the engines to be used are large, HCCI combustion will offer great fuel economy improvements with the possibility of maintaining cost-effective emission after-treatment. Even in electrical vehicles it seems that range extenders (small internal combustion engines) will be common. These small engines and other highly downsized engines reduce the scope for HCCI combustion. In any case, wherever a gasoline engine is used and operated in a low load regime, HCCI combustion should reduce fuel consumption and CO_2 emissions. This thesis has demonstrated ways of increasing the opera-

tional range of HCCI while facilitating emission after-treatment, thus making it more attractive even for small engines. Practical implementation by car manufacturers will depend on the incentives for them to reduce CO_2 emissions in the future.

Chapter 6

Summary of appended papers

Paper I

An Evaluation of Different Combustion Strategies for SI Engines in a Multi-Mode Combustion Engine

by: Daniel Dahl, Ingemar Denbratt and Lucien Koopmans

Written for and presented at the *SAE World Congress*, Detroit, Michigan, April 14, 2008. Published in *SAE International Journal of Engines*, April 1, 2009.

This paper presents results from the first experiments conducted using the multi-cylinder engine. The engine's capabilities of running four different combustion strategies made it ideal for comparing them in the same engine.

Homogeneous lean SI, spray-guided lean SI and HCCI were compared to stoichiometric homogeneous SI in the low load/speed region. The variable valve timing made it possible to run the engine with large amounts of residuals using a large valve overlap, which is beneficial for fuel consumption in homogeneous stoichiometric SI operation. This resulted in quite low improvements in homogeneously lean operation. Spray-guided SI and HCCI gave comparable fuel consumption benefits: ≈8-24% improvements for spray-guided SI and ≈15-22% improvements for HCCI. However, spray-guided SI combustion performance was not optimal in the engine because the spray-spark-piston geometry was not optimized, which made it difficult to run the engine without misfires at ideal combustion phasing. The results showed that neither homogeneous nor stratified lean SI can suffice without lean NO_X after-treatment, while HCCI might. Engine-out temperatures were also higher for HCCI than spray-guided SI, which is beneficial for after-treatment of CO and HC.

This initial study clearly showed that the range of possible combustion phasings in HCCI combustion narrows at higher loads, limited by ringing at one end and unstable combustion at the other.

The author planned, set up and performed the experiments. He also post-processed the data, wrote the paper and presented it, supported throughout by Lucien Koopmans and Ingemar Denbratt.

Paper II

Reducing Pressure Fluctuations at High Loads by Means of Charge Stratification in HCCI Combustion with Negative Valve Overlap

by: Daniel Dahl, Mats Andersson, Andreas Berntsson, Ingemar Denbratt and Lucien Koopmans

Written for and presented at the *SAE Powertrains, Fuels and Lubricants Meeting*, Florence, Italy, June 15, 2009.

In the study reported in this paper, the focus was turned towards HCCI, more precisely the high load limit of HCCI. It began with investigations of the effects of late injection on fuel distribution and combustion when running the optical engine in SCCI mode, using LIF to monitor a fuel-tracer, formaldehyde and OH, complemented by high speed video to capture chemiluminescence from the combustion. A PRF fuel with two-stage ignition was used in the experiments, which showed that formaldehyde concentrations were higher in fuel-rich regions and that chemiluminescence from the combustion was more intense and less homogeneous when using charge stratification compared to homogeneous operation.

To obtain further insight into the strategies' capability to reduce pressure fluctuations, experiments were also conducted using the single-cylinder metal-engine. In addition to the PRF-fuel used in the optical experiments, gasoline was also used in the tests. In operation with both fuels, the SCCI strategy effectively reduced both ringing and the maximum pressure rise rate under constant load, and these effects increased with increasing stratification. However, two different mechanisms appeared to be involved in the ringing inhibition: it was probably due to observed low temperature chemistry in operation with PRF fuel, but not gasoline (for which no explanation was found).

The author performed the optical experiments in collaboration with Mats Andersson, who together with Andreas Berntsson had constructed the original optical setup (which was slightly modified for these experiments). Mats Andersson was responsible for the optical techniques, i.e. deciding which techniques to use and how they function. The author was further responsible for setting up and performing the metal-engine experiments, all the data evaluation and writing the paper, with support of the co-authors.

Paper III

HCCI/SCCI Load Limits and Stoichiometric Operation in a Multi-Cylinder Naturally Aspirated Spark Ignition Engine Operated on Gasoline and E85

by: Daniel Dahl and Ingemar Denbratt

Published in *International Journal of Engine Research*, February 1, 2011.

In this paper, the SCCI strategy was tested in the multi-cylinder engine to evaluate the extent to which the load could be increased while keeping ringing intensities, combustion instability and emissions below certain limits. As the project involved utilization of alternative fuels, both gasoline and ethanol (E85) were tested. The results showed that at 1000 rpm SCCI did not allow load extension, mainly because air supply limited operation of the engine at this speed rather than ringing. At 2000 rpm it was possible to increase the load by approximately one bar for both fuels, while at 3000 rpm only SCCI with ethanol provided a load increase. The main difference between the fuels was that soot levels limited stratification for gasoline, but no soot problems were observed for ethanol. It was soon realized that NO_X emissions were too high, using not only the SCCI strategy but also HCCI. The strategies were therefore tested in combination with EGR to run the engine under stoichiometric conditions. This approach was highly successful, since all main emissions (CO, HC and NO_X) were efficiently converted in the catalyst. However, stoichiometric operation reduced the maximum load and increased the fuel consumption.

Based on the results, an engine operating strategy was proposed with the prerequisite that no lean NO_X after-treatment should be used. Further, the paper provides information on the engine's behaviour under varying λ levels, achieved by varying the EGR amounts, and when the proportions of internal

and external residuals are altered under stoichiometric conditions.

The author planned, set up, performed and evaluated the experiments and wrote the paper under supervision of Ingemar Denbratt.

Paper IV

The Origin of Pressure Waves in High Load HCCI Combustion: A High-Speed Video Analysis

by: Daniel Dahl, Mats Andersson and Ingemar Denbratt

Published in *Combustion Science and Technology*, October 3, 2011.

This paper presents a deeper investigation of the nature of ringing, and how it arises in HCCI combustion. Using image-intensified high-speed video it was possible to capture the rapid combustion, and more importantly, the in-cylinder pressure oscillations that arise. Using image/video -analysis it was also possible to filter out the acoustic modes that were set up by the intense combustion. The type and magnitude of these oscillations could also be correlated to locations in the combustion chamber where rapid combustion occurred. The most rapid combustion, responsible for the oscillations, occurred in regions that ignited last.

The author planned, set up and performed the experiments together with Mats Andersson. The author also performed the data evaluation and wrote the paper with the support of Mats Andersson and under supervision of Ingemar Denbratt.

Paper V

Valve Profile Adaptation, Stratification, Boosting and 2-stroke Strategies for Raising Loads of Gasoline HCCI Engines.

by: Daniel Dahl and Ingemar Denbratt

Written for and presented at the *SAE World Congress & Exhibition*, Detroit, Michigan, April 24, 2012. Published in *SAE International Journal of Engines*, August, 2012.

This paper continues from the point Paper III ended, presenting an investigation of the maximum load limits of HCCI and SCCI when boosting the intake air. A fully flexible hydraulically actuated valve system was used in the study, in which optimal cam timings for increasing the high load limit were initially determined. Based on the results, valve timings adapted for high loads were applied and boost sweeps were carried out for HCCI and SCCI under lean and stoichiometric conditions. Boosting proved to be very effective for increasing the load, for all strategies except lean SCCI, in which charge stratification reduced the load instead of increasing it. Boosted lean HCCI proved to be the best strategy, according to these experiments, since it provided almost as high loads as stoichiometric SCCI while providing low fuel consumption and low NO_X emissions.

The flexibility of the valve system also made it possible to perform some preliminary tests on two-stroke operation, which showed great potential since it allowed operation at higher loads with less ringing, greater stability and lower fuel consumption and emissions than when using the other strategies.

The author planned, set up, performed and evaluated the experiments and wrote the paper under supervision of Ingemar Denbratt.

Paper VI

The Role of Charge Stratification for Reducing Ringing in Gasoline Engine HCCI Combustion

by: Daniel Dahl, Mats Andersson and Ingemar Denbratt

Submitted for publication

In the study reported in this paper, optical methods were used to characterise the phenomenon of charge stratification and its ringing inhibiting properties for fuels that display single-stage ignition. A method called two-wavelength planar laser-induced fluorescence was used to obtain in-cylinder images of the temperature and fuel distributions before combustion in HCCI/SCCI operation. These measurements were correlated with the subsequent combustion captured using high-speed video. It was found that the extent of fuel and temperature stratification correlated well with the spatial distribution of combustion timing. Further, regions igniting early had leaner and hotter gas than other regions. The latest burning regions, which normally burn most intensively and cause the ringing, were fuel-rich in SCCI operation, which may explain the reduction in combustion speed in these zones and the inhibiting effect of charge stratification on pressure oscillations under these conditions.

The author planned, set up and performed the experiments together with Mats Andersson. Mats Andersson was responsible for the optical techniques, i.e. deciding which techniques to use and how they function. The author also evaluated the data and wrote the paper with support of Mats Andersson and under supervision of Ingemar Denbratt.

Appendix A

2D temperature estimation

The steps in the procedure used for estimating the two-dimensional temperature distribution based on the LIF measurements are explained here. The results of each step are displayed in Figure A.1 (the first row shows unprocessed images). The procedure was applied first to the measurements of background fluorescence (BF), then to the measurements of light collection efficiency (LCE), and finally to the actual measurements obtained during a combustion cycle. These procedures were applied to each individual image from both wavelengths. They were also applied to calibration measurements, but in those cases the LCE images and actual measurements were the same.

1. Subtract the background noise level, obtained from a reference area outside the cylinder and the cuvette. Extract region of interest.

2. Extract the spatially resolved laser plane intensity from the cuvette images. Normalize with a reference intensity (taken from one reference file) and filter.

3. *Normalize BF-images with respect to the average absolute laser intensities and save an average image of the five images, denoted "BF" (this step is only performed for BF-images and for those images the sequence ends here).*

4. Subtract the BF image multiplied by the average absolute laser intensity. The subtracted information is then related to the current laser intensity.

5. Normalize images with normalized laser plane intensity vectors. In this way the total signal will also be adjusted for the total laser intensity.

6. Filter images with a circular averaging filter, radius 5 pixels.

7. *Normalize each image with respect to its mean value, and save an average image of the five images, denoted "LCE" (this step is only performed for LCE-images and for those images the sequence ends here).*

8. Normalize images with respect to the LCE.

9. Calculate the ratio between 308 nm and 266 nm images in each pixel and translate to temperature using calibration data.

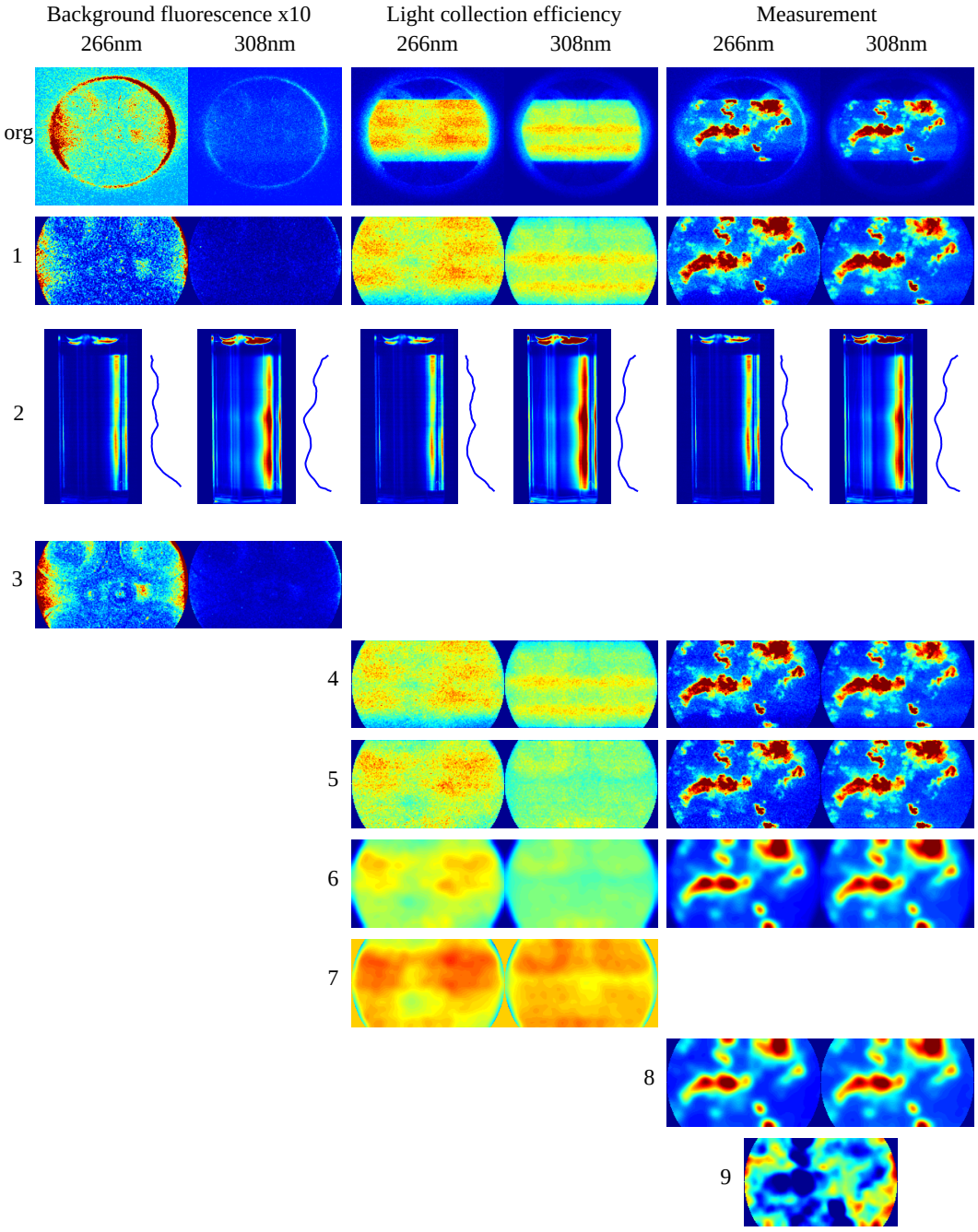

Figure A.1 – An example of results from each step in the evaluation procedure for estimating the temperature.

Appendix B

HSV analysis

The purpose of this appendix is to explain and justify why the timing of 10% light intensity (LI10) was used to spatially resolve ignition timing and why the maximum light intensity derivative (LI_{MaxDer}) was used to spatially resolve the magnitude of the heat release. Some practical considerations are also discussed.

Figure B.1 shows a plot of the light intensity (LI) and cumulative light intensity (CULI) (captured with the HSV camera), averaged over the whole field of view, against CAD for a single representative cycle. Also included in the figure are the rate of heat release (ROHR) and the cumulative heat release (CUHR) based on pressure measurements (the ill-looking heat release profile is due to the rather heavy ringing and excessive blow-by observed in the optical engine). If all we could see were chemiluminescence from the main reactions,

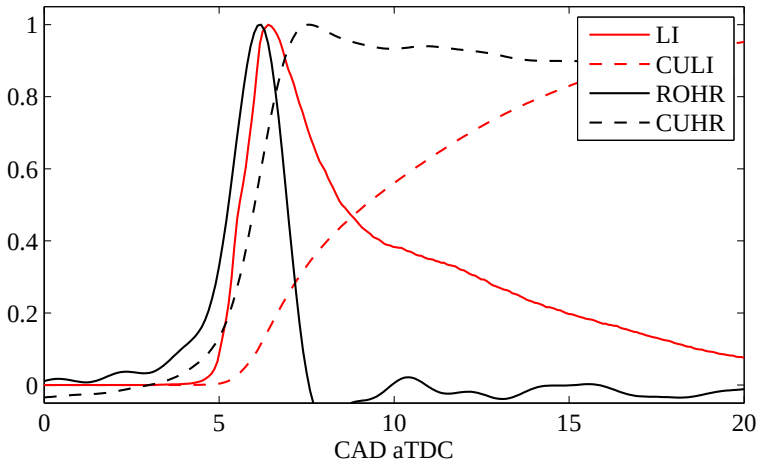

Figure B.1 – The light intensity and cumulative light intensity averaged over the field of view in an representative cycle together with a plot of the rate of heat release and cumulative heat release against CAD. All curves are normalized to their maximum values.

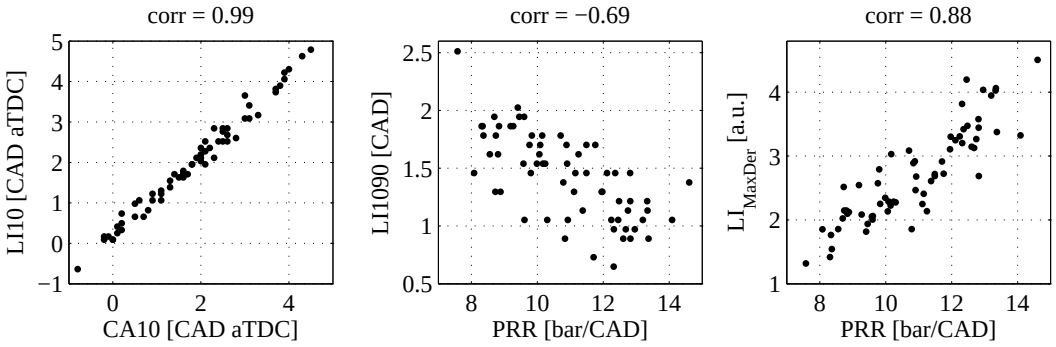

Figure B.2 – LI10 vs. CA10, LI1090 vs. PRR and LI_{MaxDer} vs. PRR for 65 repeated cycles, and the linear correlations between them.

one might expect that the ROHR and the LI would coincide. Unfortunately, as demonstrated in section 3.7, this is not the case. The result is that the CULI is not a good representation of the CUHR in any way, and so the timing of 10% of the maximum CULI can not be used as a measure of ignition timing. However, we see that the LI curve starts to increase at the upswing of the CUHR curve. This suggests that 10% of the maximum LI intensity would be a better threshold value. This supposition is verified in the left-hand panel of Figure B.2, in which LI10 is plotted against CA10 for 65 repeated HCCI cycles; it is clear that the two values correlate very well.

A high LI level should correspond to intense heat release and thus also to a rapid pressure increase, which causes pressure oscillations. However, under stratified conditions, rich zones that contain soot can produce very high LI levels that are not representative of the heat release. One possible approach would be to use the time between 10% and 90% LI (LI1090) as a measure of the local combustion intensity and thus also the pressure-rise rate (PRR). This is displayed in the middle panel of Figure B.2; although there is correlation, it is not very good. The parameter providing the best correlation to the pressure-rise rate (PRR) globally and most robust approach in spatial terms was the maximum light intensity derivative as shown in the right panel of Figure B.2.

It is necessary to apply some processing during single-pixel analysis to avoid erroneous results. In Figure B.3, the LI is plotted against CAD for two pixels that are 4 mm apart. The grey curves show the values after spatial filtering, and the black curves show the values after applying a moving average time-wise filter. In order to find LI10 and the appropriate region from which to extract LI_{MaxDer}, the timing of maximum LI is required. As can be seen in the second plot, it is not possible to simply find the absolute maximum LI since in this case we would find that for a highly luminous "particle", which could be material from the piston rings or soot. Consequently, the first peak needs to be identified. However, as can be seen in the first plot of Figure B.3, noise

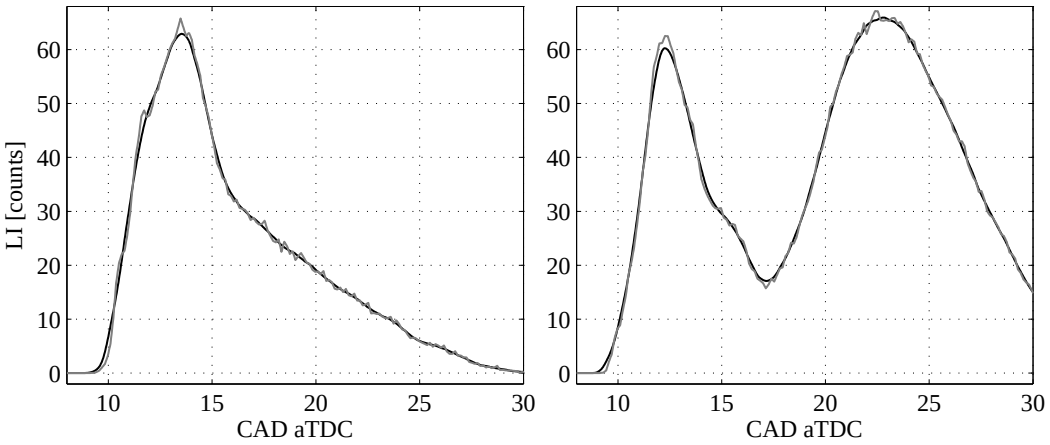

Figure B.3 – LI from two pixels (one in each panel) 4 mm apart plotted as a function of CAD. The black curves show the LI after a moving average filter had been applied to the grey curves.

can cause small peaks and so a moving average filter was applied to the curve. Calculation of $\mathrm{LI}_{\mathrm{MaxDer}}$ was performed on the filtered curve using the central difference method.

Appendix C

Pressure trace analysis

This section discusses the procedures in the heat release calculations performed in this project along with the author's own experiences on the subject. All heat release calculations on in-cylinder pressure data were performed using Matlab.

By applying the first law of thermodynamics to the combustion chamber, assuming that the gas is ideal and by neglecting any mass transfer over the boundaries, the chemical or gross heat release can be expressed as follows:

$$\frac{dQ_{ch}}{d\theta} = \frac{\gamma}{\gamma - 1} P \frac{dV}{d\theta} + \frac{1}{\gamma - 1} V \frac{dP}{d\theta} + \frac{dQ_{ht}}{d\theta} \tag{C.1}$$

where Q_{ch} is the heat released during combustion, θ is the crank-angle, γ is the ratio of specific heats, P is the cylinder pressure, V is the volume and Q_{ht} is the heat transfer to the combustion chamber walls. If the heat transfer term is neglected we obtain the net heat release, which corresponds to the work transferred to the piston. For details on how this equation is derived, see Heywood (1988).

Extensive tuning is required to obtain a properly representative heat release curve. Various methods for estimating the heat release exist but regardless of which method is used, a number of parameters must be tuned since they have a large impact on the resulting heat release:

- Correct phasing of pressure with θ. This only changes if the crank angle encoder is repositioned and should thus be constant throughout a measurement series.

- The change in geometry of the combustion chamber as function of θ should be known. It is more difficult to know the exact clearance volume which therefore requires tuning, but once performed it should remain constant throughout the measurement series if the geometry is not changed.

- The measured pressure must be "pegged" to a reference level and how this reference level is chosen has a great impact on the results. If the crank-angle resolved absolute intake pressure is measured, the pegging can be performed at an appropriate region around BDC before IVC where pressure is fairly constant. It will still require some tuning but less than would be the case if only the average intake pressure were known.

Motored pressure traces are useful for tuning these parameters (where the aim is to obtain zero gross heat release).

It then remains to be determined how γ and heat transfer should be treated. Different approaches were employed in this project and the following discussion explains them all in brief and then compares them with reference to an illustrative cycle.

Method 1 - full approach

Gross heat release is calculated with heat transfer being:

$$\frac{dQ_{ht}}{d\theta} = Ah_c \left(T - T_{wall}\right) \tag{C.2}$$

where the heat transfer coefficient (h_c) was calculated using the Woschni approximation (Woschni, 1967), which can be found in Heywood (1988). This approximation requires the tuning of some constants. However, in this work, a single factor was used for heat transfer rather than tuning all the constants. It also requires a motored pressure trace taken under the same circumstances as the actual measurement. In some cases, a representative motored pressure trace did not exist and was instead approximated using the polytropic expression:

$$P_m = P_{IVC} \left(\frac{V_{IVC}}{V}\right)^{\kappa} \tag{C.3}$$

where the polytropic coefficient κ was set to γ for air at relevant temperatures.

The ratio of specific heats was calculated using NASA polynomials (Burcat and Ruscic, 2005), where the specific heats are functions of temperature and composition. The temperature was approximated using the ideal gas law, with the mass estimated at IVC and the gas constant R was taken for air. To get the instantaneous gas composition, a temporary heat release was calculated with constant γ to approximate how much of the fuel had burned. In this way, the instantaneous concentrations of the major species O_2, N_2, CO_2, H_2O and fuel (approximated as iso-octane) can be estimated if one also knows λ and the residual amounts, which were taken from Ricardo Wave or GT-Power simulations.

While this method provides a good estimation of the heat release, it requires careful tuning. During tuning, the aim is to obtain a gross heat release that is approximately equal to the chemical energy released. Under motored conditions, a flat zero-level heat release should be obtained. An additional bonus of using this method for HCCI combustion is that the temperature before ignition should be around 1000 K, which can be used as an extra clue in the tuning procedure.

This method was used in paper V and in Figure 4.6 of this thesis.

Method 2 - simplest approach

The most simple method is to overlook heat transfer entirely and calculate the net heat release. Gamma can be taken as a fixed value (as done in Paper I) or it can be approximated according to Christensen (2000) as being linearly dependent on the temperature:

$$\gamma = \gamma_0 - \frac{0.08\,(T - 300)}{1000} \tag{C.4}$$

where γ_0 is the ratio of specific heats for the gas mixture at 300 K (used in Paper II). This can of course also be combined with heat transfer to obtain the gross heat release. The difficulty in only calculating net heat release is that there is no specific quantity to tune against.

Method 3 - the 'adequate' approach?

The polytropic approach (similar to Tunestål (2009)) provides a robust way of estimating the heat release under several different operating conditions without having to tune for each individual case. For the compression and expansion strokes, κ can be calculated between two points in each stroke using the polytropic relationship $P_1 V_1^{\kappa} = P_2 V_2^{\kappa}$ as:

$$\kappa = \frac{ln\frac{P_1}{P_2}}{ln\frac{V_2}{V_1}} \tag{C.5}$$

and linear interpolation can be applied between the chosen intervals. From own experience, if only the two end-points in each interval are used, noise can have a significant influence on the obtained κ. A better way is to find the κ that is most valid across the entire range using the following approach:

$$PV^{\kappa} = C \tag{C.6}$$

$$ln(P) + \kappa ln(V) = ln(C) \tag{C.7}$$

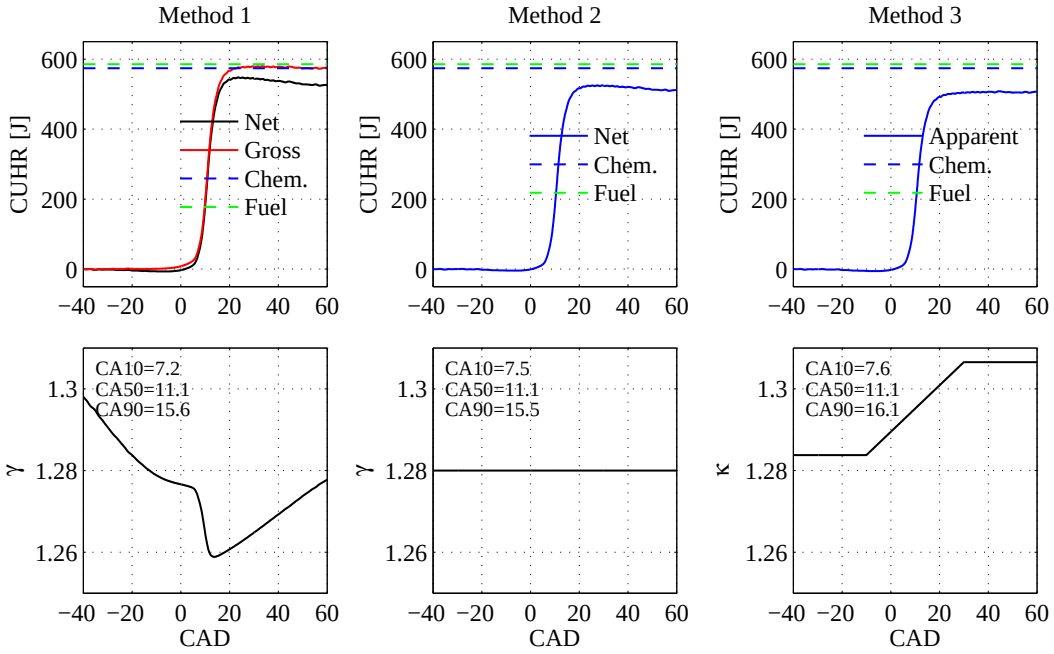

Figure C.1 – Cumulative heat release and γ/κ for the three methods described.

$$ln(P) = ln(C) - \kappa ln(V) \tag{C.8}$$

We have this relationship for all the points in the interval:

$$ln(\mathbf{P}) = \begin{bmatrix} 1 & -ln(\mathbf{V}) \end{bmatrix} \begin{bmatrix} ln(C) \\ \kappa \end{bmatrix} \tag{C.9}$$

and the trick is to find a value for C and κ that is most suitable, which we do by minimizing the least square error. In Matlab this is solved as:

$$\begin{bmatrix} ln(C) \\ \kappa \end{bmatrix} = \begin{bmatrix} 1 & -ln(\mathbf{V}) \end{bmatrix} \backslash ln(\mathbf{P}) \tag{C.10}$$

If we do this in appropriate intervals, the resulting heat release will be flat before and after combustion without using a heat transfer term, which makes it easy to identify CA10, CA50 and CA90. However, care must be taken to ensure that the intervals chosen do not contain combustion or any other repeated disturbance on the pressure trace. Let us call the result from this approach the "apparent" heat release, since it is neither the net nor the gross heat release. This method was used in Papers III, IV and VI.

Examples of the three methods are provided in Figure C.1 (in which a fixed γ was used for method 2). The same cycle is shown for all methods

and all that differs between them is the way γ and heat transfer are treated. For comparative purposes, the fuel energy and the chemical energy released (based on the measured amount of fuel injected and the combustion efficiency calculated from measured exhaust emissions) are also included. In method 2, γ was taken as the average from method 1. As can be seen for method 1, γ is lower after combustion than before because of the higher temperature, which has a greater impact than the composition effect (which would make γ higher for the residuals than for the unburnt mixture at equal temperatures). In contrast, for method 3, κ is higher after combustion then before because heat transfer is incorporated into κ.

If the aim is to compare the heat release profiles under different operating conditions, it is obvious that method one is the most appropriate. However, if we are only interested in combustion phasing, all methods provide equally good answers, as demonstrated by the CA50 values shown in the plots; this parameter is fairly robust. However, CA10 and CA90 are more sensitive (and therefore so too is the combustion duration, i.e. the period between CA10 and CA90). To conclude, this means that if one only wants the combustion phasing, relatively little effort is required as long as one makes sure that the estimated heat release before and after combustion is fairly flat.

Bibliography

S. M. Aceves, D. L. Flowers, C. K. Westbrook, J. R. Smith, W. Pitz, R. Dibble, M. Christensen, and B. Johansson. A Multi-Zone Model for Prediction of HCCI Combustion and Emissions. *SAE Technical Paper 2000-01-0327*, 2000.

T. Amano, S. Morimoto, and Y. Kawabata. Modeling of the Effect of Air/Fuel Ratio and Temperature Distribution on HCCI Engines. *SAE Technical Paper 2001-01-1024*, 2001.

M. Andreae, W. Cheng, T. Kenney, and J. Yang. On HCCI Engine Knock. *SAE Technical paper 2007-01-1858*, 2007.

M. Asai, T. Kurosaki, and K. Okada. Analysis on Fuel Economy Improvement and Exhaust Emission Reduction in a Two-Stroke Engine by Using an Exhaust Valve. *SAE Technical paper 951764*, 1995.

A. Berntsson and I. Denbratt. Optical Study of HCCI Combustion using NVO and SI Stratified Charge. *SAE Technical paper 2007-24-0012*, 2007a.

A. Berntsson and I. Denbratt. HCCI Combustion Using Charge Stratification for Combustion Control. *SAE Technical paper 2007-01-0210*, 2007b.

J. Brettschneider. Berechnung des Luftverhältnisses λ von Luft-Kraftstoff-Gemischen und des Einflusses von Meßfehlern auf λ. *Bosch Technische Berichte*, 6(4):177–186, 1979.

S. Brewster, G. Cathcart, and C. Zavier. The Potential of Enhanced HCCI / CAI Control Through the Application of Spray Guided Direct Injection. *SAE Technical paper 2008-01-0035*, 2008.

A. Burcat and B. Ruscic. Third Millennium Ideal Gas and Condensed Phase Thermochemical Database for Combustion with updates from Active Thermochemical Tables. Technical Report ANL-05/20 and TAE 960, Technion-IIT, Aerospace Engineering and Argonne National Laboratory, Chemistry Division, 2005.

K. Burgdorf and I. Denbratt. Cylinder Pressure Based Knock Detection Methods. *SAE Technical paper 972932*, 1997.

A. Cairns and H. Blaxill. Lean Boost and External Exhaust Gas Recirculation for High Load Controlled Auto-Ignition. *SAE Technical paper 2005-01-3744*, 2005a.

A. Cairns and H. Blaxill. The Effects of Combined Internal and External Exhaust Gas Recirculation on Gasoline Controlled Auto-Ignition. *SAE Technical paper 2005-01-0133*, 2005b.

A. Cheng, R. Dibble, and B. Buchholz. The Effect of Oxygenates on Diesel Engine Particulate Matter. *SAE Technical paper 2002-01-1705*, 2002.

M. Christensen. Homogeneous Charge Compression Ignition (HCCI) Engine. Licentiate Thesis, Lund Institute of Technology, 2000.

M. Christensen, B. Johansson, P. Amnéus, and F. Mauss. Supercharged Homogeneous Charge Compression Ignition. *SAE Technical paper 980787*, 1998.

J. Dec and M. Sjöberg. Isolating the Effects of Fuel Chemistry on Combustion Phasing in an HCCI Engine and the Potential of Fuel Stratification for Ignition Control. *SAE Technical paper 2004-01-0557*, 2004.

J. Dec and Y. Yang. Boosted HCCI for High Power without Engine Knock and with Ultra-Low NOx Emissions - using Conventional Gasoline. *SAE Int. J. Engines*, 3:750–767, 2010.

J. Dec, Y. Yang, and N. Dronniou. Boosted HCCI - Controlling Pressure-Rise Rates for Performance Improvements using Partial Fuel Stratification with Conventional Gasoline. *SAE Int. J. Engines*, 4:1169–1189, 2011.

I. Denbratt. Method of Controlling the Process of Combustion in an Internal Combustion Engine with Means for Controlling the Engine Valves. *Swedish Patent SE521782*, 1998.

Y. Dongbo, X. Fan, W. Zhi, and W. Jianxin. Limitation of Charge Stratification for High Load Extension of HCCI Combustion in a GDI Engine with NVO. *SAE Technical paper 2009-01-1343*, 2009.

C. Draper. The physical effects of detonation in a closed cylindrical chamber. *NACA Report No. 493*, pages 361–379, 1935.

P Duret. Two-stroke CAI engines. In H. Zhao, editor, *HCCI and CAI engines for the automotive industry*, pages 43–76. England: Woodhead Publishing Limited, 2007.

P. Duret and S. Venturi. Automotive Calibration of the IAPAC Fluid Dynamically Controlled Two-Stroke Combustion Process. *SAE Technical paper 960363*, 1996.

EEA. Evolution of CO2 emissions from new passenger cars by fuel type , November 2011. URL `http://www.eea.europa.eu/data-and-maps/figures/evolution-of-co2-emissions-from`.

S. Einecke, C. Schulz, and V. Sick. Measurement of temperature, fuel concentration and equivalence ratio fields using tracer LIF in IC engine combustion. *Applied Physics B: Lasers and Optics*, 71:717–723, 2000.

J Eng. Characterization of Pressure Waves in HCCI Combustion. *SAE Technical paper 2002-01-2859*, 2002.

EPA. EPA and NHTSA Propose to Extend the National Program to Reduce Greenhouse Gases and Improve Fuel Economy for Cars and Trucks, November 2011. URL `http://www.epa.gov/otaq/climate/documents/420f11038.pdf`.

O. Erlandsson. Early Swedish Hot-Bulb Engines - Efficiency and Performance Compared to Contemporary Gasoline and Diesel Engines. *SAE Technical paper 2002-01-0115*, 2002.

EU. REGULATION (EC) No 443/2009 OF THE EUROPEAN PARLIAMENT AND OF THE COUNCIL: setting emission performance standards for new passenger cars as part of the Communitys integrated approach to reduce CO2 emissions from light-duty vehicles. *Official Journal of the European Union*, L140:1–15, 2009.

A. Gaydon. *The Spectroscopy of Flames, 2nd ed.* England: Chapman and Hall, 1974.

J. Geiger, M. Grigo, O. Lang, P. Wolters, and P Hupperich. Direct Injection Gasoline Engines - Combustion and Design. *SAE Technical paper 1999-01-0170*, 1999.

I. Glassman and R. Yetter. *Combustion*. USA: Academic Press, 2008.

B. Grandin. *Knock in Gasoline Engines - the effects of mixture composition on knock onset and heat transfer*. PhD thesis, Chalmers University of technology, 2001.

R. Hanson, D. Splitter, and R. Reitz. Operating a Heavy-Duty Direct-Injection Compression-Ignition Engine with Gasoline for Low Emissions. *SAE Technical paper 2009-01-1442*, 2009.

J. Heywood. *Internal Combustion engine fundamentals*. Singapore: Macgraw-Hill Book Company, 1988.

R. Hickling, D. Feldmaier, F. Chen, and J. Morel. Cavity resonances in engine combustion chambers and some applications. *J. Acoust. Soc. Am.*, 73(4): 1170–1178, 1983.

W. Hwang, J. Dec, and M. Sjöberg. Spectroscopic and chemical-kinetic analysis of the phases of HCCI autoignition and combustion for single- and two-stage ignition fuels. *Combust. Flame*, 154:387–409, 2008.

A. Iijima and H. Shoji. A Study of HCCI Combustion Characteristics Using Spectroscopic Techniques. *SAE Technical paper 2007-01-1886*, 2007.

Y. Iwamoto, K. Noma, O. Nakayama, T. Yamauchi, and H. Ando. Development of Gasoline Direct Injection Engine. *SAE Technical paper 970541*, 1997.

T. Johansson, B. Johansson, P. Tunestål, and H. Aulin. HCCI Operating Range in a Turbo-charged Multi Cylinder Engine with VVT and Spray-Guided DI. *SAE Technical paper 2009-01-0494*, 2009.

G. Kalghatgi and R. Head. Combustion Limits and Efficiency in a Homogeneous Charge Compression Ignition Engine. *Int. J. Engine Res.*, 7:215–236, 2006.

G. Kalghatgi, P. Risberg, and H. Ångström. A Method of Defining Ignition Quality of Fuels in HCCI Engines. *SAE Technical paper 2003-01-1816*, 2003.

G. Kalghatgi, P. Risberg, and H. Ångström. Advantages of Fuels with High Resistance to Auto-ignition in Late-injection, Low-temperature, Compression Ignition Combustion. *SAE Technical paper 2006-01-3385*, 2006.

G. Kalghatgi, P. Risberg, and H. Ångström. Partially Pre-Mixed Auto-Ignition of Gasoline to Attain Low Smoke and Low NOx at High Load in a Compression Ignition Engine and Comparison with a Diesel Fuel. *SAE Technical paper 2007-01-0006*, 2007.

A. Kanury. *Introduction to Combustion Phenomena*. USA: Gordon and Breach, 1982.

J. Koch. *Fuel tracer photophysics for quantitative planar laser-induced fluorescence*. PhD thesis, Stanford University, Stanford, USA, 2005.

A. Kojic, J. Hathout, and A. Jasim. Method for extending HCCI load range using a two-stroke cycle and variable valve operation. *US Patent 7.231.892*, 2007.

L. Koopmans. *HCCI Combustion by Retaining Residuals.* PhD thesis, Chalmers University of technology, 2005.

L. Koopmans and I. Denbratt. A Four Stroke Camless Engine, Operated in Homogeneous Charge Compression Ignition Mode with Commercial Gasoline. *SAE Technical Paper 2001-01-3610*, 2001.

L. Koopmans, R. Ogink, and I. Denbratt. Direct Gasoline Injection in the Negative Valve Overlap of a Homogeneous Charge Compression Ignition Engine. *SAE Technical paper 2003-01-1854*, 2003.

T. Kuboyama, Y. Moriyoshi, K. Hatamura, T. Yamada, and J. Takanash. An Experimental Study of a Gasoline HCCI Engine Using the Blow-Down Super Charge System. *SAE Technical Paper 2009-01-0496*, 2009.

K. Kumano and N. Iida. Analysis of the Effect of Charge Inhomogeneity on HCCI Combustion by Chemiluminescence Measurement. *SAE Technical Paper 2004-01-1902*, 2004.

J. Lumley. *Engines - An Introduction.* USA: Cambridge University Press, 1999.

V. Manente, B. Johansson, and P. Tunestål. Partially Premixed Combustion at High Load using Gasoline and Ethanol, a Comparison with Diesel. *SAE Technical Paper 2009-01-0944*, 2009.

V. Manente, B. Johansson, and W. Cannella. Gasoline partially premixed combustion, the future of internal combustion engines? *Int. J. Engine Res.*, 12:194–208, 2011.

C. Marriott and R. Reitz. Experimental Investigation of Direct Injection-Gasoline for Premixed Compression Ignited Combustion Phasing Control. *SAE Technical Paper 2002-01-0418*, 2002.

NHTSA. Light-Duty Vehicle Greenhouse Gas Emission Standards and Corporate Average Fuel Economy Standards; Final Rule. *Federal Register*, 75 (88), 2010.

NHTSA. Summary of Fuel Economy Performance, October 2011. URL `http://www.nhtsa.gov/staticfiles/rulemaking/pdf/cafe/October_2011_Public.pdf`.

M. Noguchi, Y. Tanaka, T. Tanaka, and Y. Takeuchi. A Study on Gasoline Engine Combustion by Observation of Intermediate Reactive Products during Combustion. *SAE Technical paper 790840*, 1979.

C. Olsson. *Volvo: Lastbilarna igår och idag (Swedish)*. Sweden: Förlagshuset Norden AB, 1990.

S. Onishi, S. Jo, K. Shoda, P. Jo, and S. Kato. Active Thermo-Atmosphere Combustion (ATAC) - A New Combustion Process for Internal Combustion Engines. *SAE Technical paper 790501*, 1979.

R. Osborne, J. Stokes, T. Lake, P. Carden, J. Mullineux, R. Helle-Lorentzen, J. Evans, M. Heikal, Y. Zhu, H. Zhao, and T. Ma. Development of a Two-Stroke/Four-Stroke Switching Gasoline Engine - The 2/4SIGHT Concept. *SAE Technical Paper 2005-01-1137*, 2005.

M. Richter, J. Engström, A. Franke, M. Aldén, A. Hultqvist, and B. Johansson. The Influence of Charge Inhomogeneity on the HCCI Combustion Process. *SAE Technical Paper 2000-01-2868*, 2000.

D. Rothamer, J. Snyder, R. Hanson, and R. Steeper. Two-Wavelength PLIF Diagnostic for Temperature and Composition. *SAE Technical Paper 2008-01-1067*, 2008.

D. Scholl, C. Davis, S. Russ, and T. Barash. The Volume Acoustic Modes of Spark-Ignited Internal Combustion Chambers. *SAE Technical paper 980893*, 1998.

C. Schwartz, E. Schünemann, B. Durst, J. Fisher, and A. Witt. Potentials of the Spray-Guided BMW DI Combustion System. *SAE Technical paper 2006-01-1265*, 2006.

P. Shingne, D. Assanis, A. Babajimopoulos, P. Keller, D. Roth, and M. Becker. Turbocharger Matching for a 4-Cylinder Gasoline HCCI Engine Using a 1D Engine Simulation. *SAE Technical Paper 2010-01-2143*, 2010.

M. Sjöberg and J. Dec. Smoothing HCCI Heat-Release Rates Using Partial Fuel Stratification with Two-Stage Ignition Fuels. *SAE Technical Paper 2006-01-0629*, 2006.

M. Sjöberg, L. Edling, T. Eliassen, L. Magnusson, and H. Ångstrm. GDI HCCI: Effects of Injection Timing and Air Swirl on Fuel Stratification, Combustion and Emissions Formation. *SAE Technical Paper 2002-01-0106*, 2002.

M. Sjöberg, J. Dec, and W. Hwang. Thermodynamic and Chemical Effects of EGR and Its Constituents on HCCI Autoignition. *SAE Technical Paper 2007-01-0207*, 2007.

J. Snyder, N. Dronniou, J. Dec, and R. Hanson. PLIF Measurements of Thermal Stratification in an HCCI Engine under Fired Operation. *SAE Technical Paper 2011-01-1291*, 2011.

U. Spicher, J. Reissing, J. M. Kech, and J. Gindele. Gasoline Direct Injection (GDI) Engines - Development Potentials. *SAE Technical paper 1999-01-2938*, 1999.

R. Stone. *Introduction to Internal Combustion Engines*. China: Macmillan Press LTD, 1999.

TFA. Lohman - ettrig diesel (*Swedish*). *Teknik för alla*, 16:9 and 24, 1952.

R. Thring. Homogeneous-Charge Compression-Ignition (HCCI) Engines. *SAE Technical paper 892068*, 1989.

P. Tunestål. Self-tuning gross heat release computation for internal combustion engines. *Control Engineering Practice*, 17:518–524, 2009.

T. Urushihara, K. Hiraya, A. Kakuhou, and T. Itoh. Expansion of HCCI Operating Region by the Combination of Direct Fuel Injection, Negative Valve Overlap and Internal Fuel Reformation. *SAE Technical paper 2003-01-0749*, 2003.

A. Vressner, A. Lundin, M. Christensen, P. Tunestål, and B. Johansson. Pressure Oscillations During Rapid HCCI Combustion. *SAE Technical paper 2003-01-3217*, 2003.

J. Warnatz, U. Maas, and R. Dibble. *Combustion*. Germany: Springer, 2010.

C. Westbrook. Chemical kinetics of hydrocarbon ignition in practical combustion systems. *Proceedings of the Combustion Institute*, 28(2):1563 – 1577, 2000.

J. Willand, R. Nieberding, G. Vent, and C. Enderle. The Knocking Syndrome - Its Cure and Its Potential. *SAE Technical Paper 982483*, 1998.

L. Withrow and G. Rassweiler. Slow motion shows knocking and non-knocking explosions. *SAE Transactions*, 39(2):297–303,312, 1936.

G. Woschni. A Universally Applicable Equation for the Instantaneous Heat Transfer Coefficient in the Internal Combustion Engine. *SAE Technical Paper 670931*, 1967.

Y. Yang, J. Dec, N. Dronniou, and M. Sjöberg. Tailoring HCCI heat-release rates with partial fuel stratification: Comparison of two-stage and single-stage-ignition fuels. *Proceedings of the Combustion Institute*, 33(2):3047 – 3055, 2011.

P. Yelvington and W. Green. Prediction of the Knock Limit and Viable Operating Range for a Homogeneous-Charge Compression-Ignition (HCCI) Engine. *SAE Technical paper 2003-01-1092*, 2003.

H. Zhao. *HCCI and CAI engines for the automotive industry*. England: Woodhead Publishing Limited, 2007.